Methods for improving the precision of proton beam radiation therapy of cancer

George Dedes

Department of Medical Physics

LMU Munich

8th Loma Linda Workshop, Tuesday July 19th 2022

LMU LUDWIG-MAXIMILIANS-UNIVERSITÄT MÜNCHEN

Contents

Part I

Cancer statistics

- Leading causes of death:
  - US: 23% heart disease (700k), 21% cancer (600k) – total $8 \cdot 10^{-3}$ deaths/million
  - Germany: 35% heart disease (340k), 24% cancer (240k) – total $1.1 \cdot 10^{-2}$ deaths/million

Cancer statistics

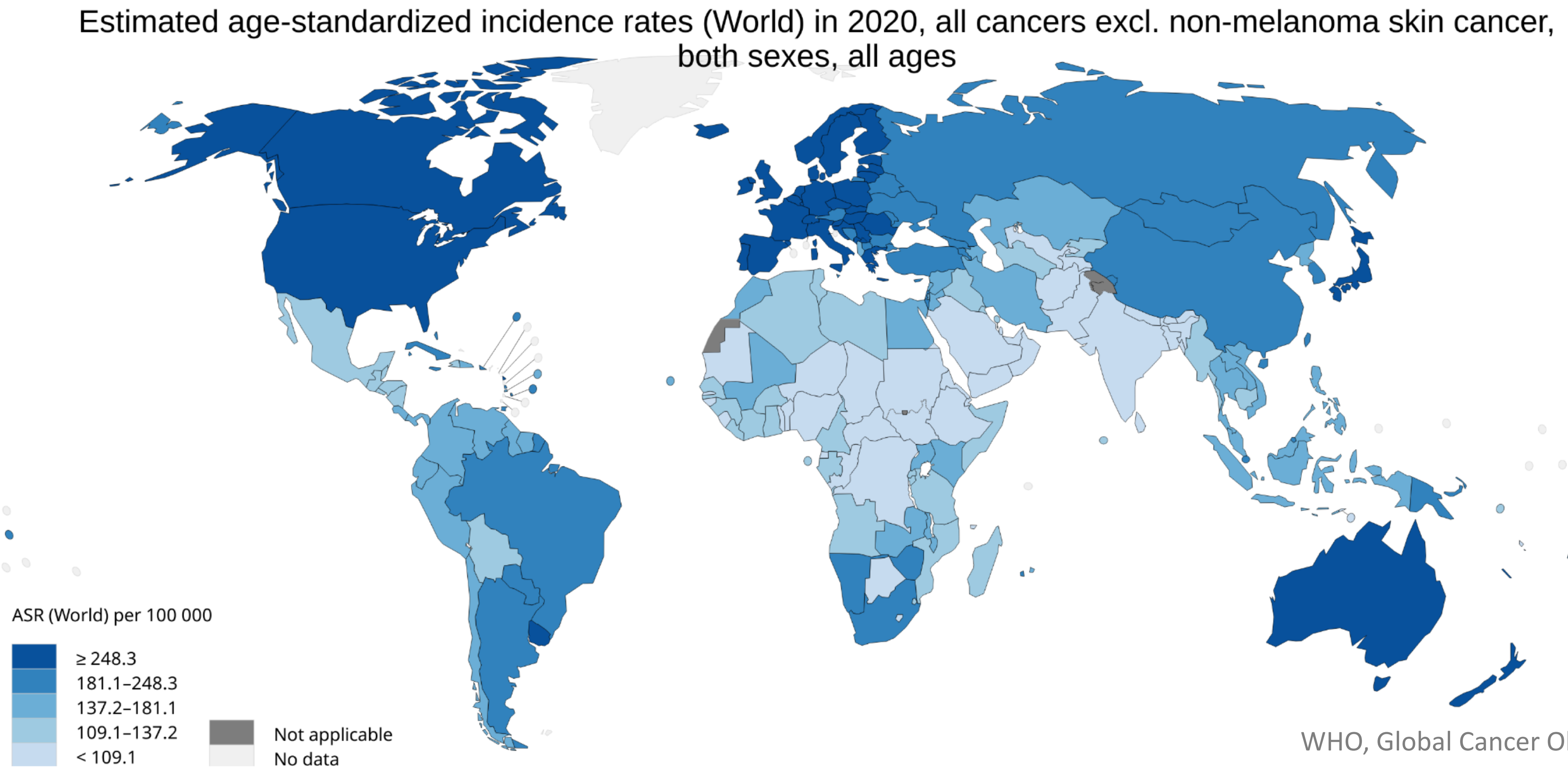

WHO, Global Cancer Observatory

- For a city like Munich (1.472M) approximately 3680 new cases every year

Treatment modalities

- Many and in most cases synergistic treatment modalities

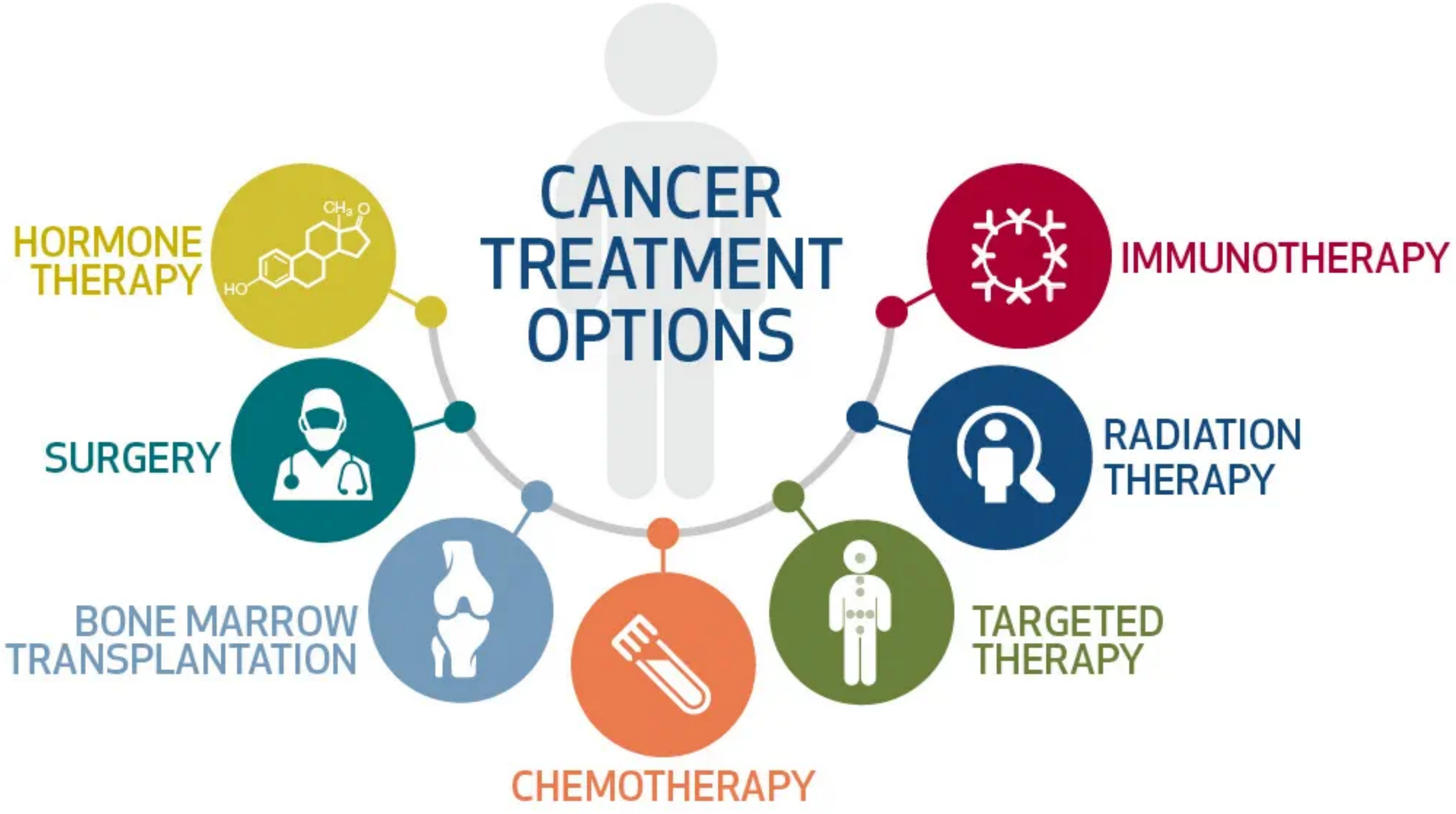

- Radiation therapy will be the conceptual basis of this talk

Radiation therapy – photons

- Ionizing radiation -> DNA damage -> cell death

- Photons attenuate in matter and indirectly ionize: $I = I_0 \cdot e^{-\mu x}$

- Dose maximum at shallow depths

- A single photon beam: no clinically useful dose distribution

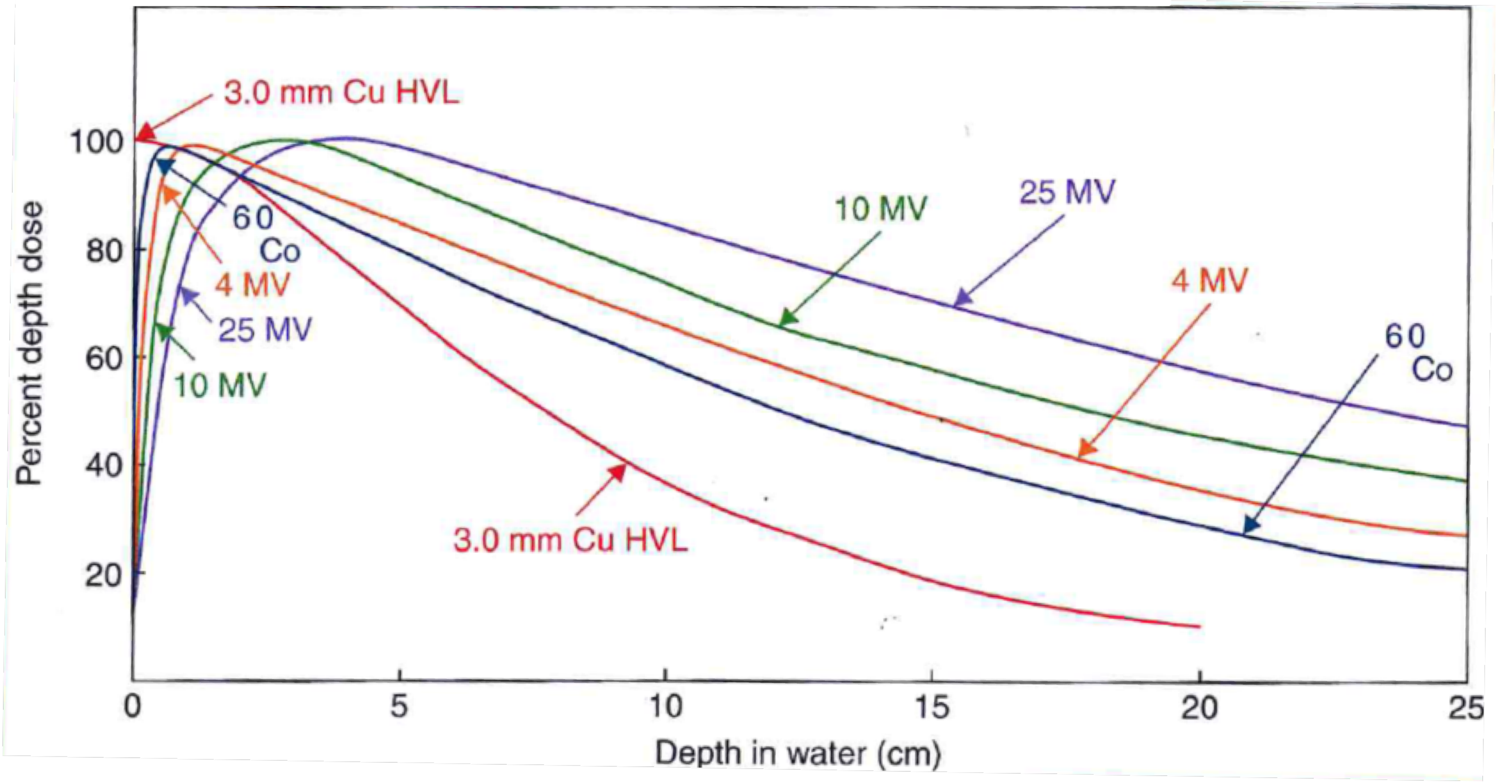

Br J Radiol. 1978;(suppl 11);

Radiation therapy – photons

Nat. Rev. Cancer 16(4): 234{249

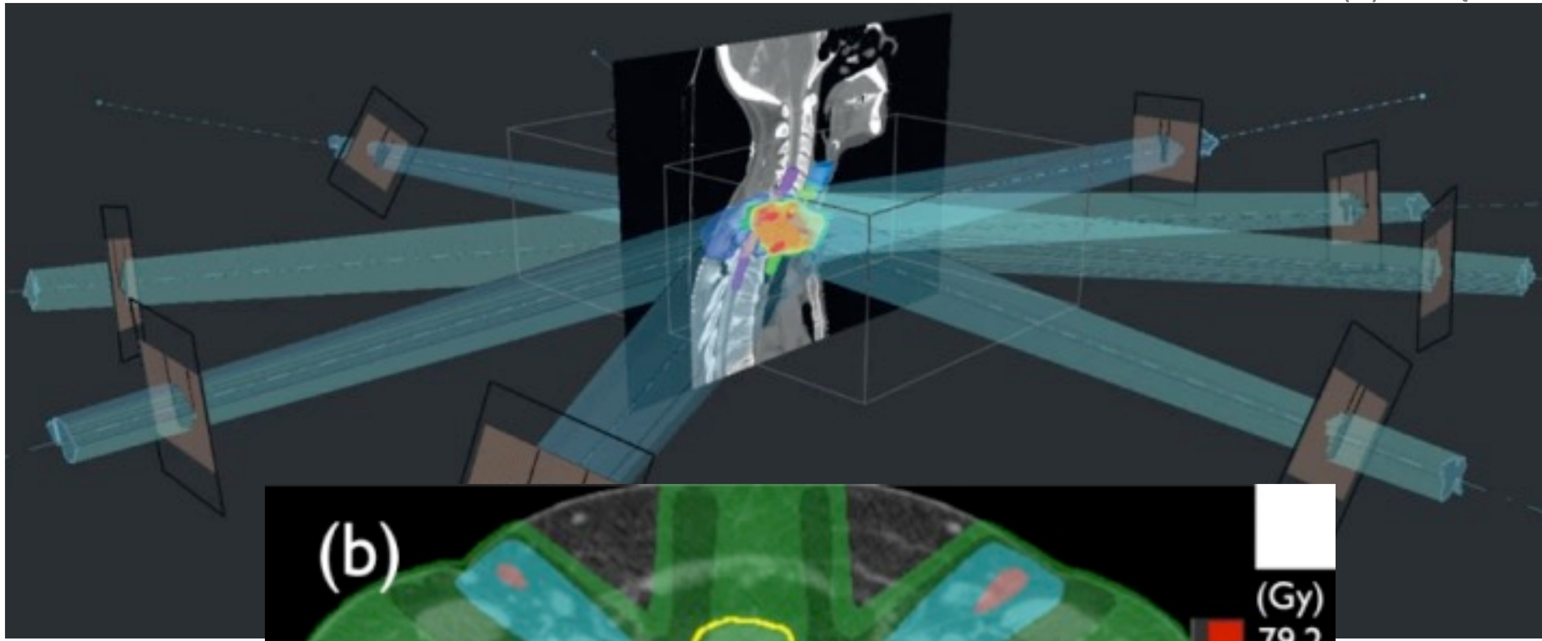

- Multiple fields superimposed
- High dose to the tumor
- Low dose bath around it
- Clinical dose distribution example:

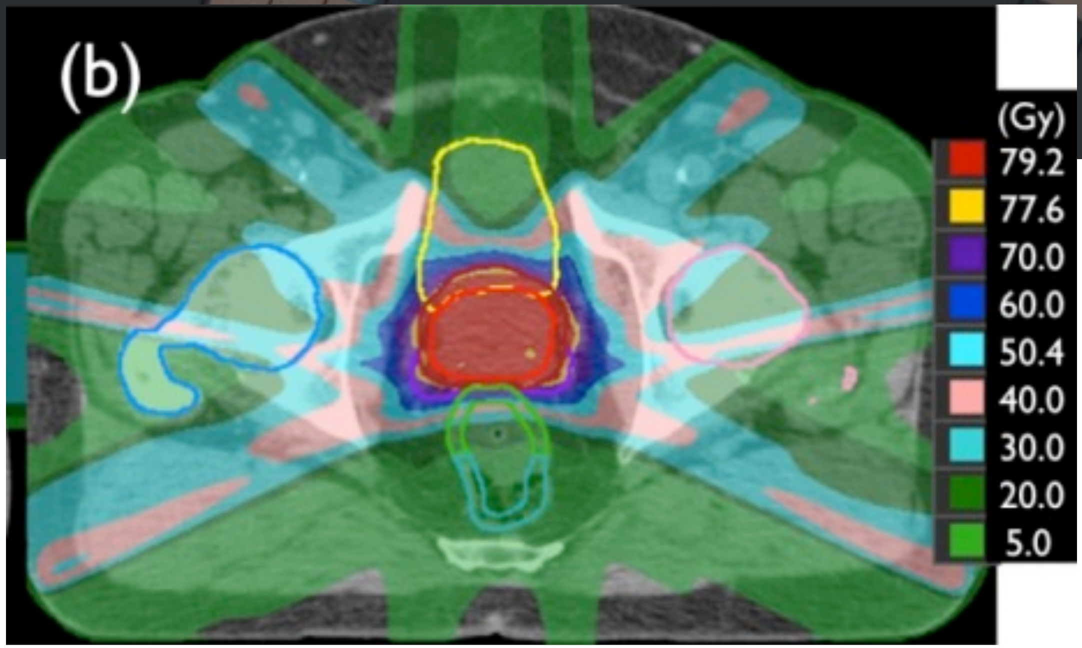

Prostate Cancer Prostatic Dis 22, 509–521 (2019)

Radiation therapy – ions

- More favorable depth-dose shape
- Maximum dose Bragg peak (BP) near end-of-range
- Low entrance and almost no exit dose
- Position of maximum regulated by particle energy
- Bragg curve: named after WH Bragg (1903)

J. Visualized Exp. (144)

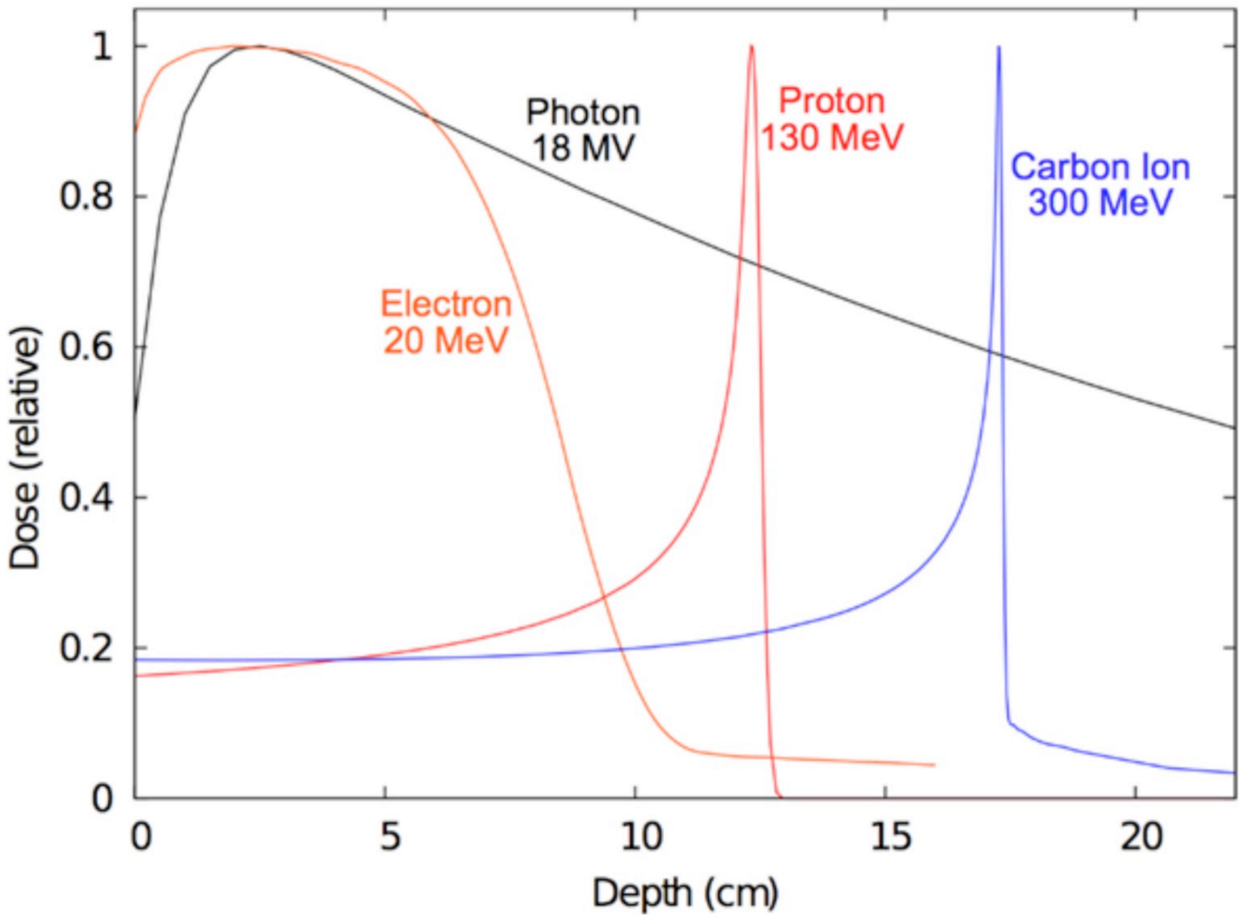

Radiation therapy – ions

- Spread-out BP (SOBP) for extended tumors
- Reduced peak to plateau dose ratio
- Fewer fields required - Reduced low dose bath

BioMed Research International, 2014, 389048

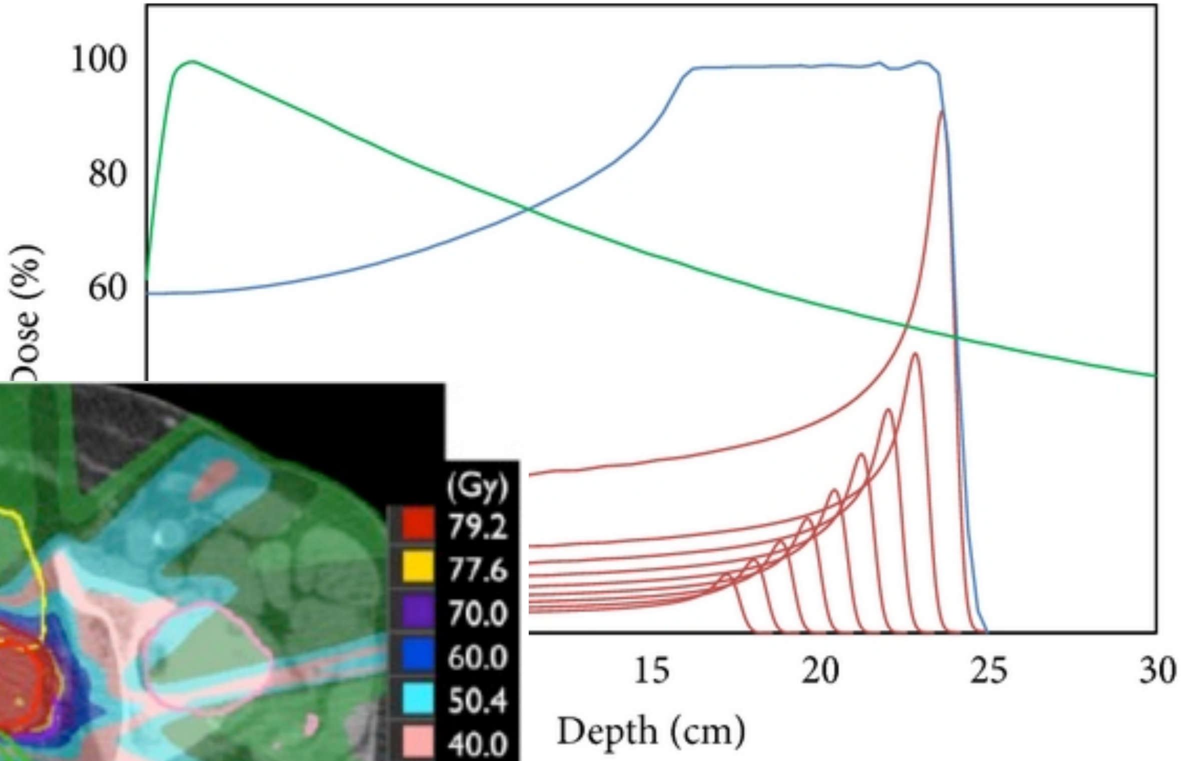

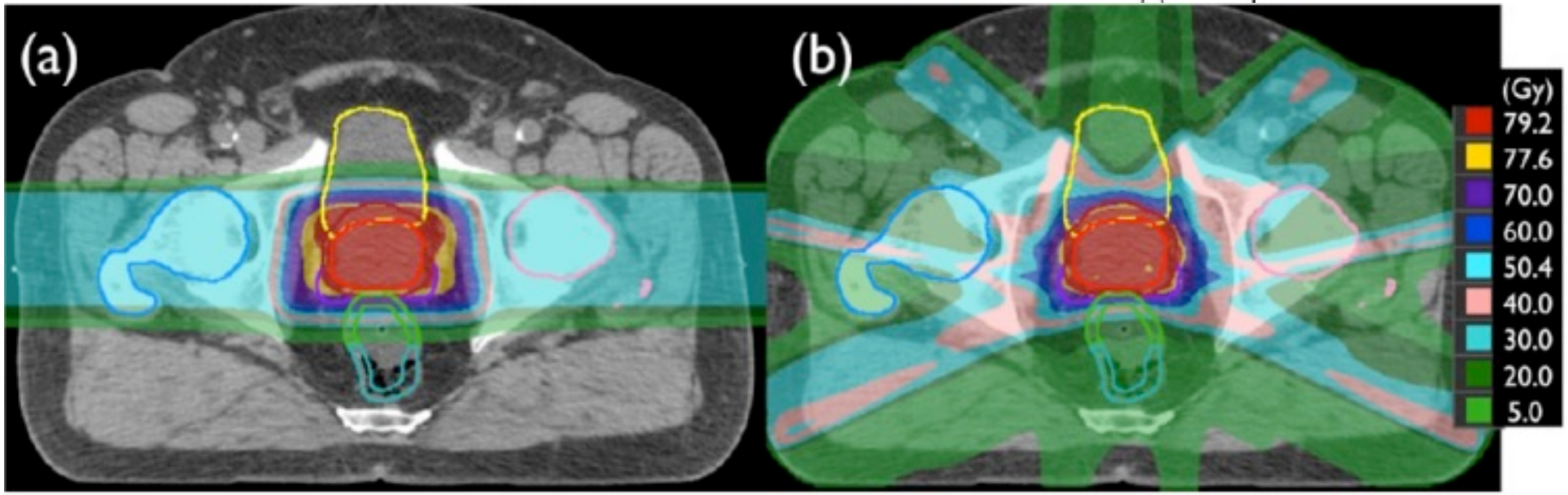

Prostate Cancer Prostatic Dis 22, 509–521 (2019)

Physics of proton therapy

- Brief reminder

- Main mechanisms

  - Ionizations/excitations (a)

  - Elastic scattering with nucleus (b)

  - Non-elastic interactions with nucleus (c)

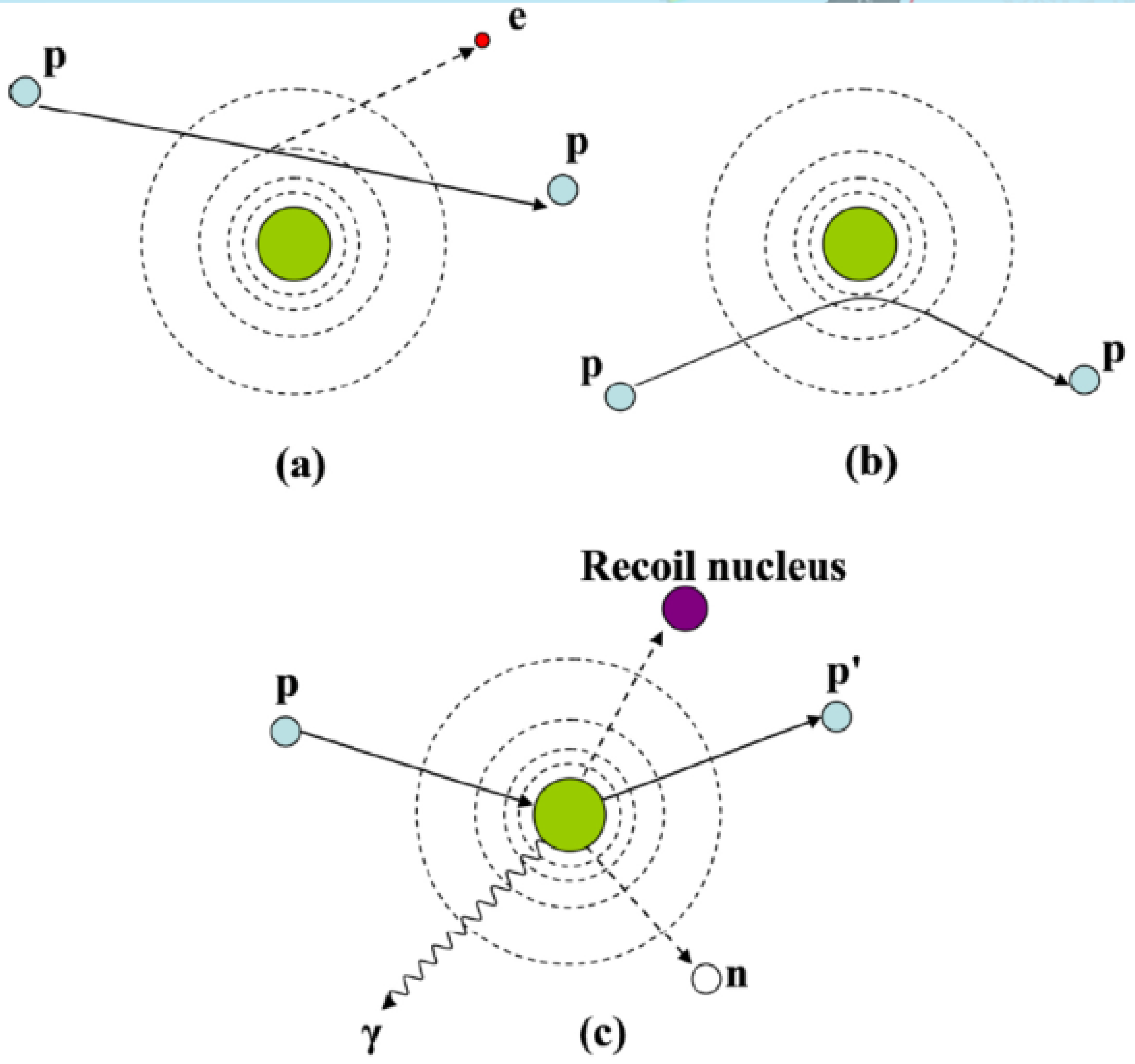

Phys. Med. Biol. 60(8): R155{R209

Physics of proton therapy

- Ion stopping power: $$\frac{S}{\rho} = -\frac{\mathrm{d}E}{\rho \mathrm{d}x} = 4\pi N_\mathrm{A} r_\mathrm{e}^2 m_\mathrm{e} c^2 \frac{Z}{A} \frac{z^2}{\beta^2} \left[\ln \frac{2 m_\mathrm{e} c^2 \gamma^2 \beta^2}{I} - \beta^2 - \frac{\delta}{2} - \frac{C}{Z} \right]$$

- Energy loss fluctuations: Gaussian (~1% for 200 MeV protons in water)

- To factor out energy dependence: $\mathrm{RSP} = \frac{S_{mat}}{S_{water}}$

Physics of proton therapy

- Coulomb scattering on nuclei

- Angular distribution approximately Gaussian:

$$\sigma_\theta = \frac{E_0}{\beta p c} z \sqrt{\frac{x}{X_0}} \left[1 + 0.038 \ln \left(\frac{x}{X_0} \right) \right]$$

- For ions of the same speed: $\frac{\sigma_{\theta 1}}{\sigma_{\theta 2}} = \frac{M_2}{M_1} \frac{z_1}{z_2}$ (6 times lower for ^{12}C wrt protons)

Physics of proton therapy

- Nuclear interactions: $\sigma_{\mathrm{R}}(E) = \sigma_0 \cdot f(E, Z_{\mathrm{T}})$

- Strong energy dependence at low energy

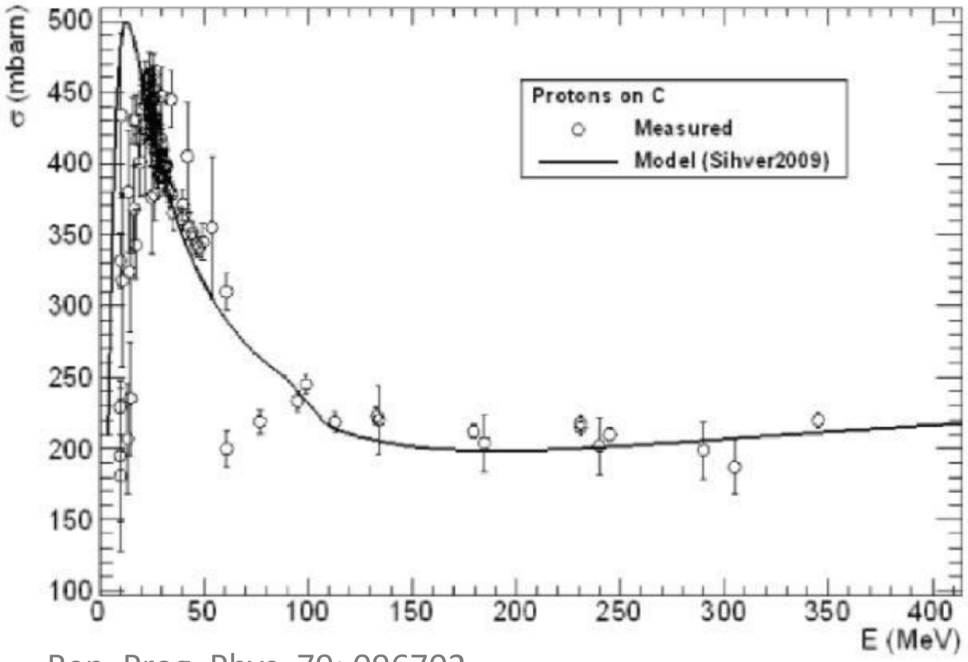

Rep. Prog. Phys. 79: 096702

Part II

Ion beam therapy workflow

- Several steps leading to treatment delivery

- Numerous imaging modalities involved

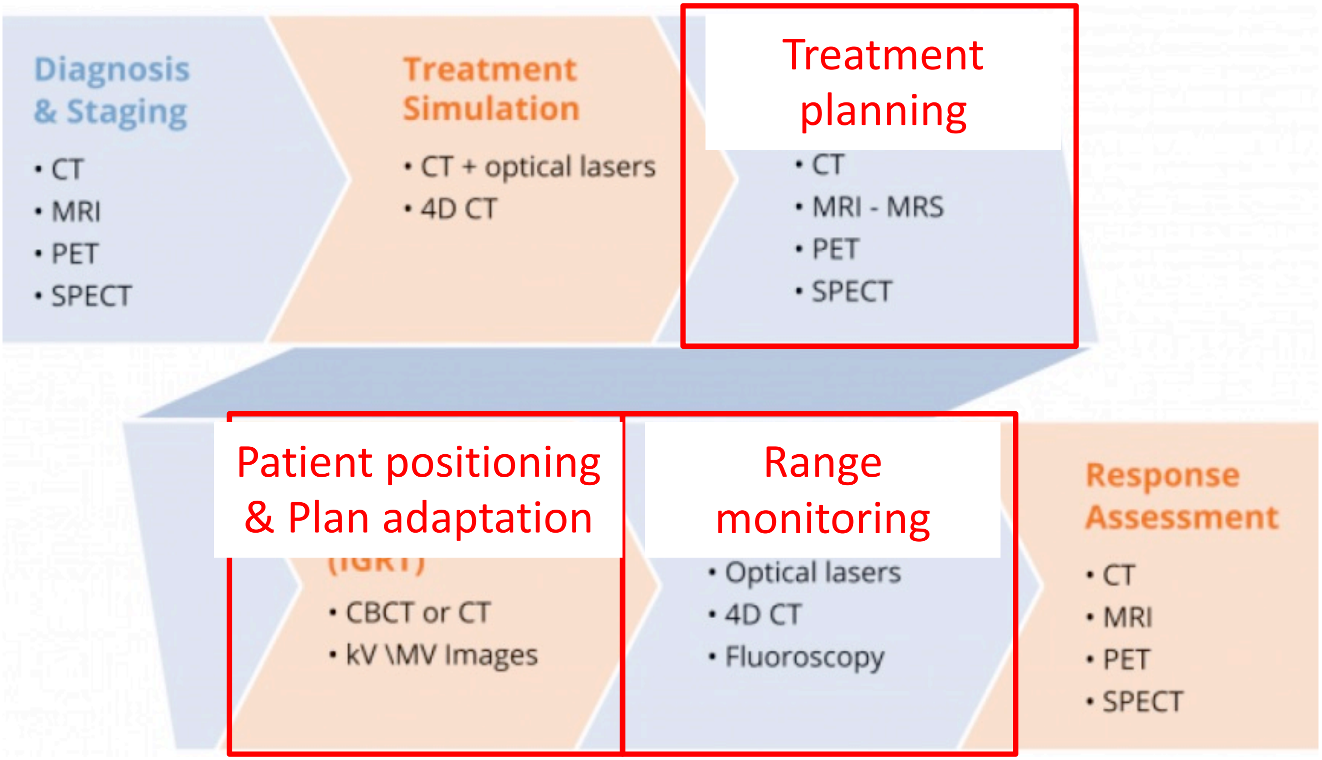

www.radiationoncology.com.au/

Ion beam therapy uncertainties

Phys Med Biol. 2013 Aug 7;58(15):R131-60

- Treatment planning (TP):
  - ➢ Need the exact ion range in the patient
  - ➢ 3D RSP map of the patient via imaging
  - ➢ RSP uncertainties -> range uncertainty
  - ➢ Biological rather than absorbed dose is prescribed
  - ➢ Biological uncertainties -> range uncertainty
    -> over/under dosage

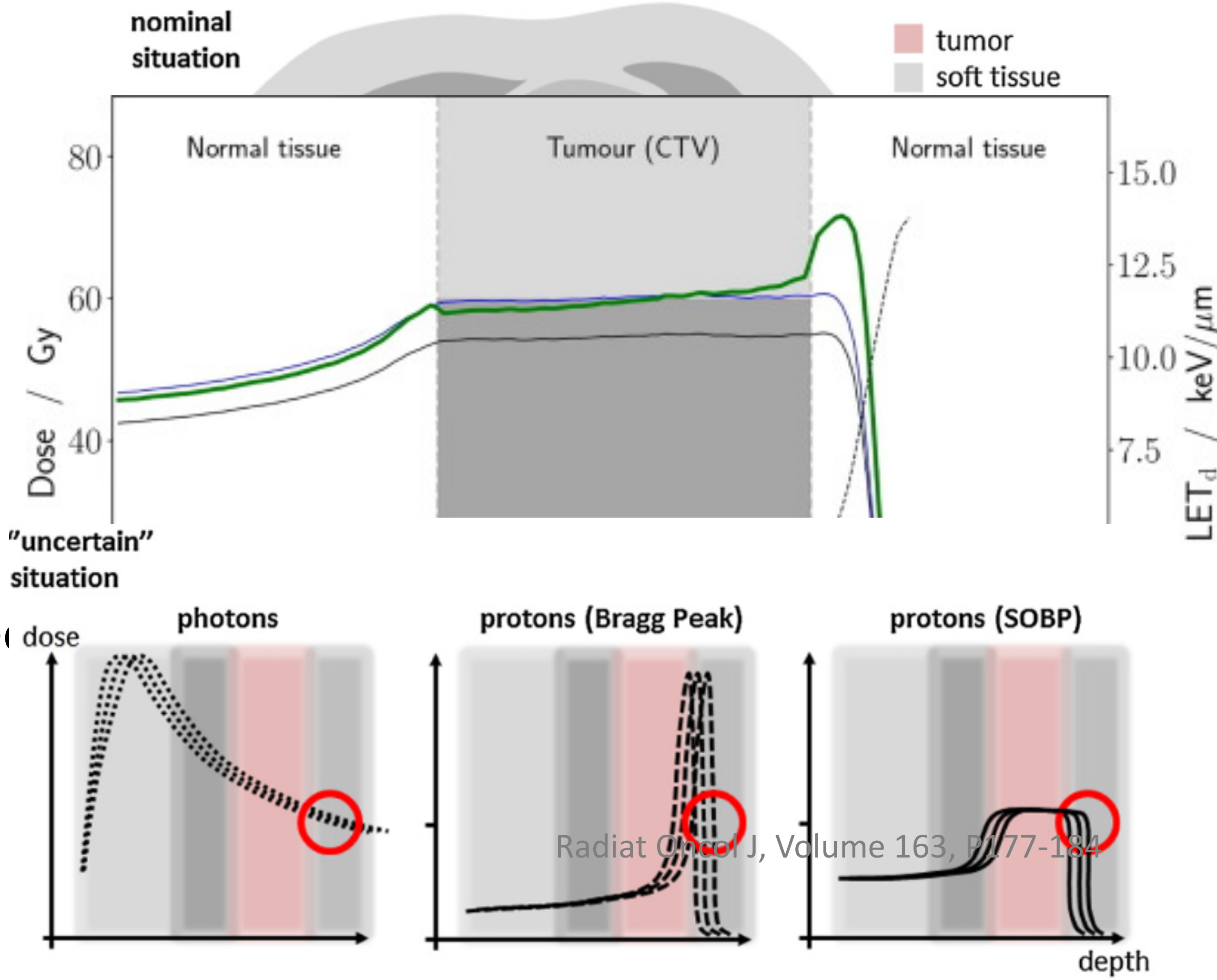

Radiat Oncol J, Volume 163, P177-184

Ion beam therapy uncertainties

- Positioning and anatomical changes
  - ➢ Positioning of the patient as on treatment planning day
  - ➢ Setup errors -> Altered dose
  - ➢ Anatomical changes since the treatment planning day
  - ➢ Anatomical changes -> non-valid treatment plans

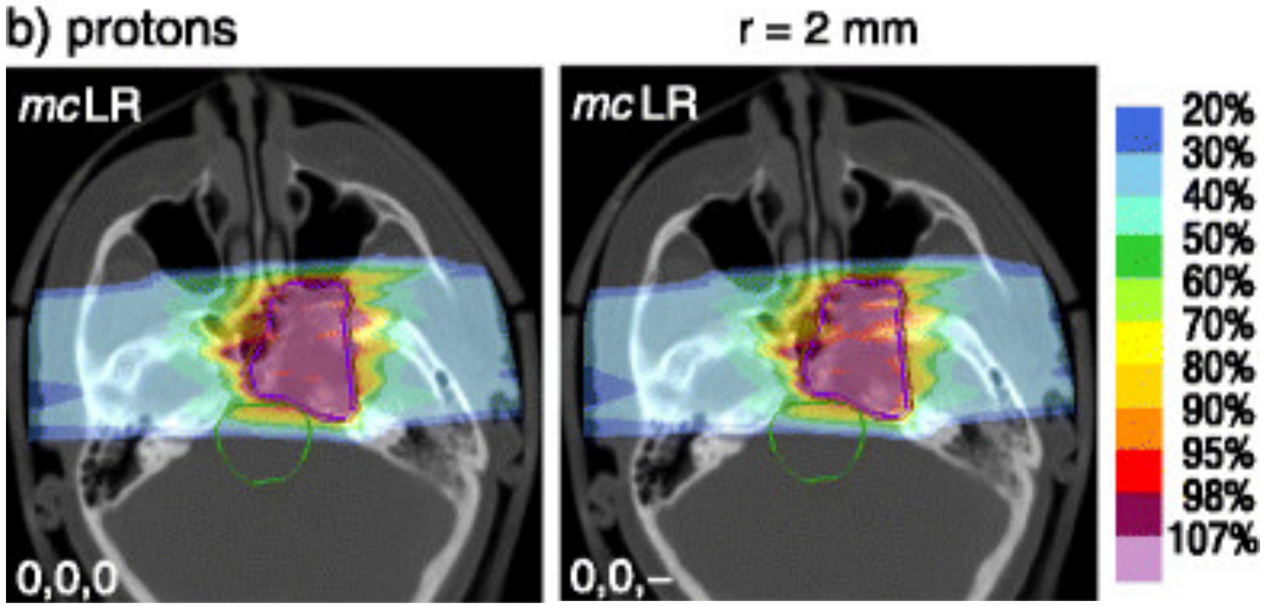

Radiation Oncology. 9. 279. 10.1186/s13014-014-0279-2.

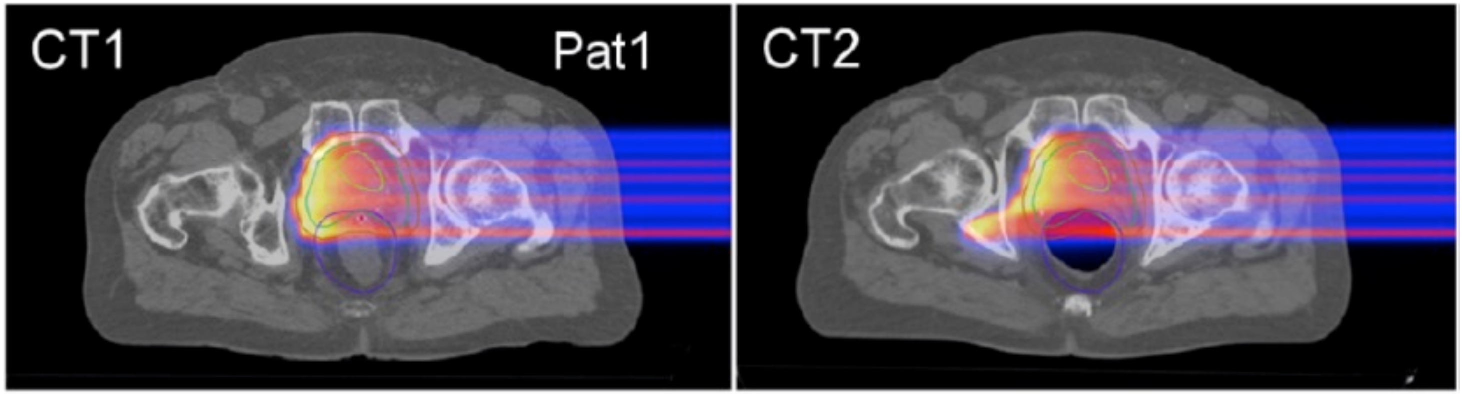

Schmid S., …, Dedes G. Phys Med Biol. 2015 Nov 18;60(24):9329-934

Proton imaging

https://physicsworld.com/a/exploiting-dual-energy-ct-and-directspr-software-to-reduce-range-uncertainty-in-proton-therapy/

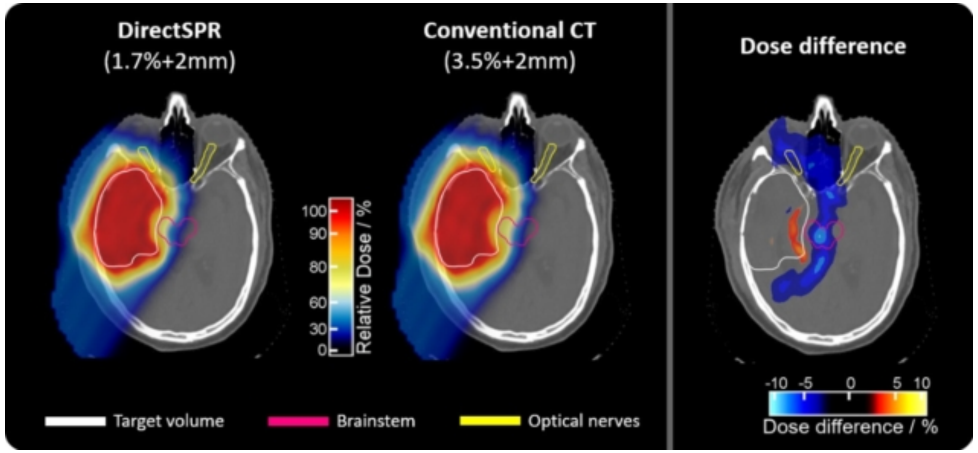

- Treating with protons, imaging with photons

- Proton imaging: direct RSP determination (<1%)

- X-ray imaging:
  - ➢ Measure in each projection the integrated (linear) attenuation coefficient along a line
  - ➢ Reconstruct from the projections the attenuation coefficient map

- Proton imaging:
  - ➢ Measure in each projection the integrated RSP along a line, the water equivalent path length (WEPL)
  - ➢ Reconstruct from the WEPL projections the RSP map

Proton imaging

- Proton’s position, direction and energy
- Position and direction -> proton trajectory
- Energy before and after the object -> WEPL

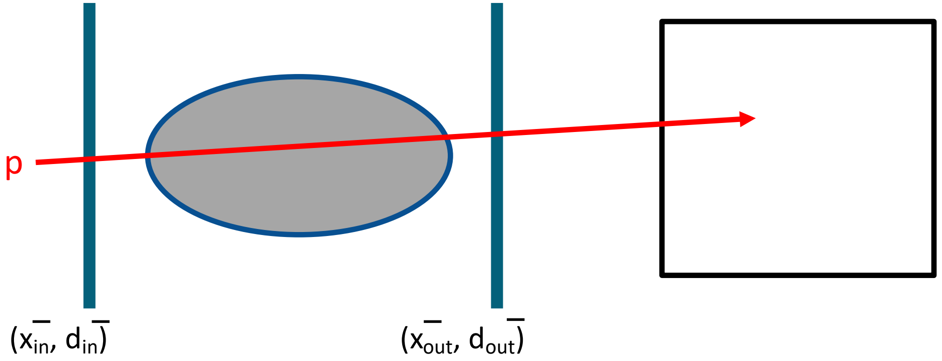

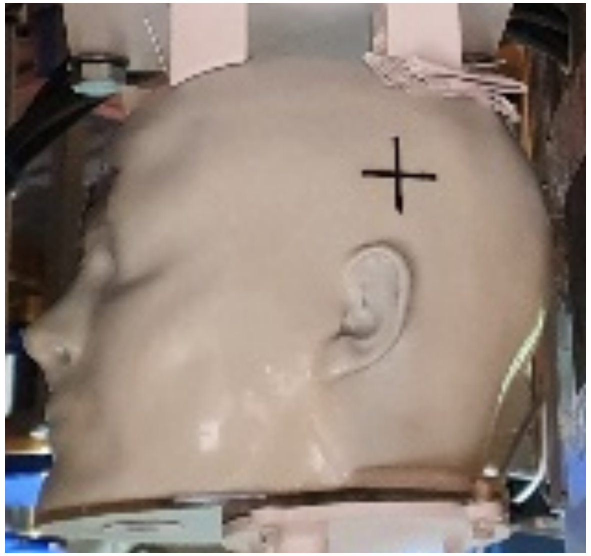

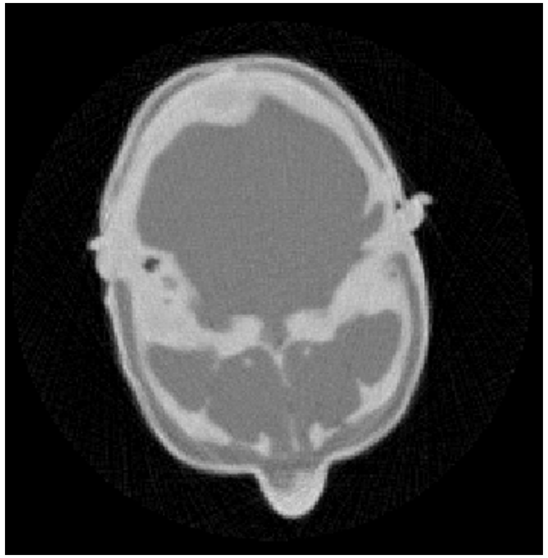

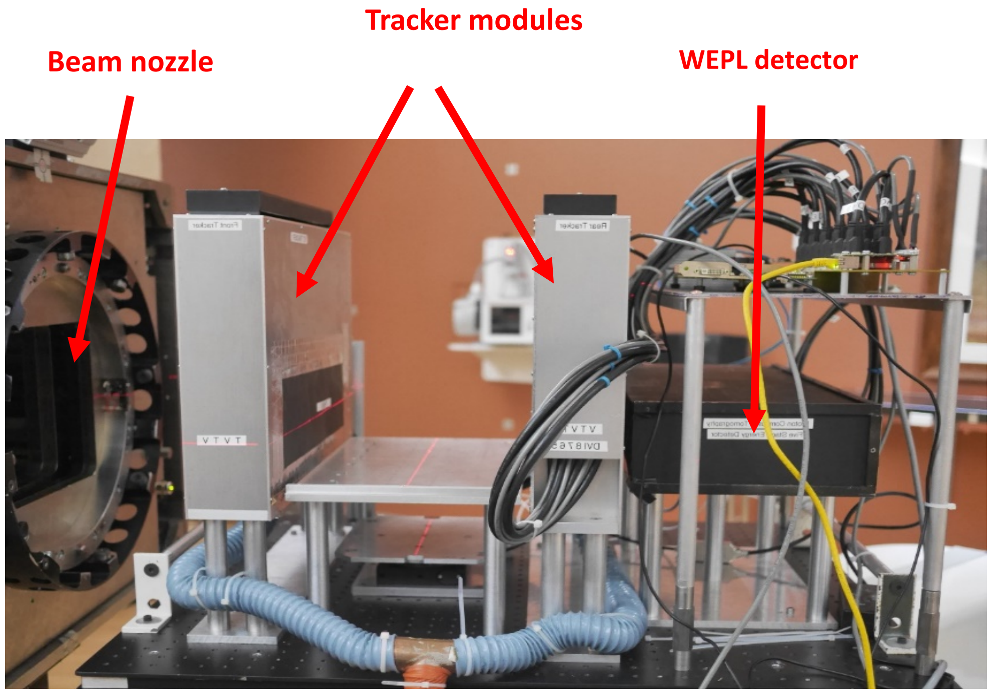

Proton imaging for TP – pCT vs DECT

- Dual energy x-ray CT (DECT): two imaging energies
- Due to μ(ρ,Z,E), better estimation of RSP with du
- First direct experimental proton CT (pCT) vs. DE(

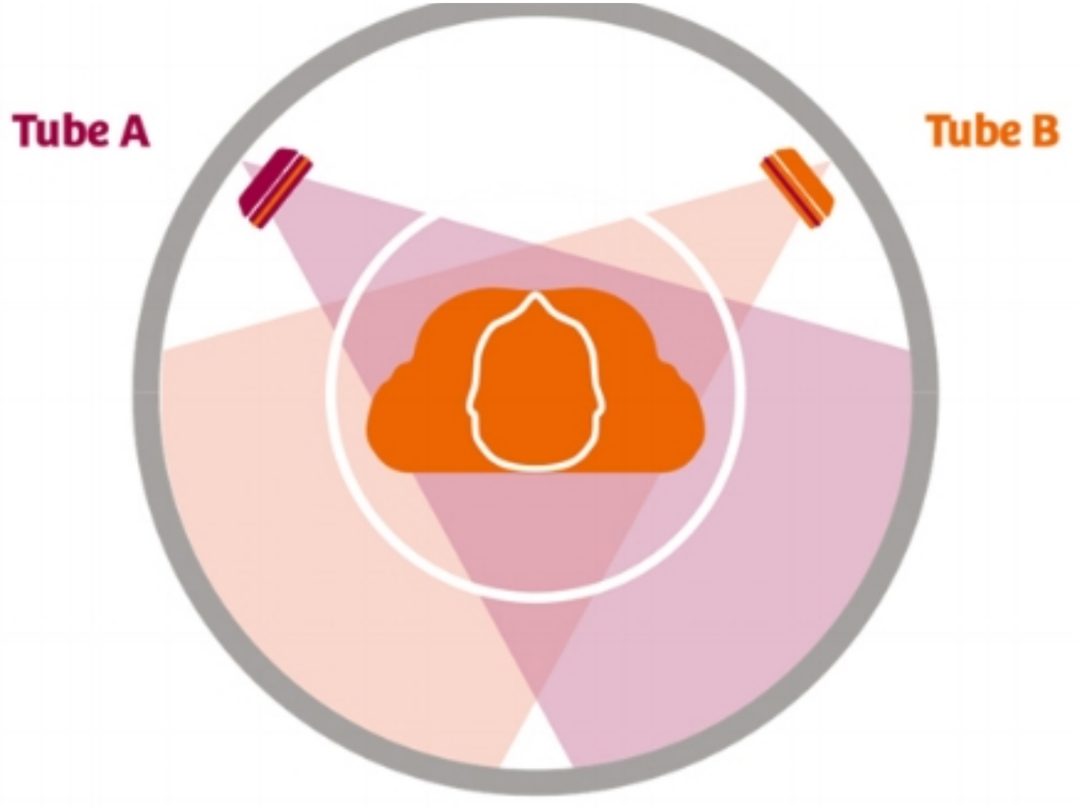

Proton imaging for TP – pCT vs DECT

- Scanned objects:

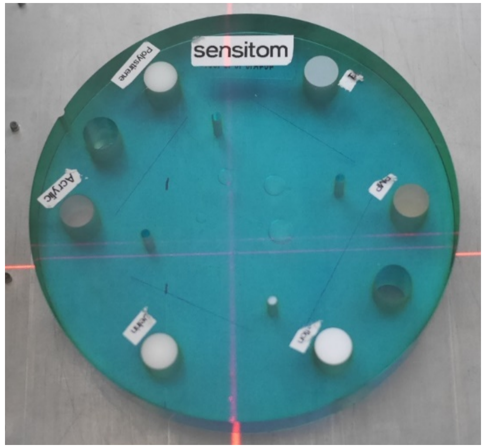

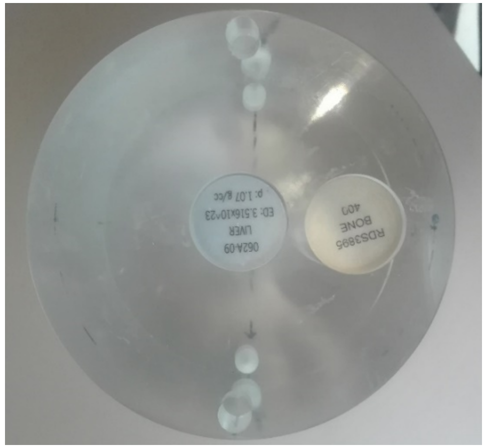

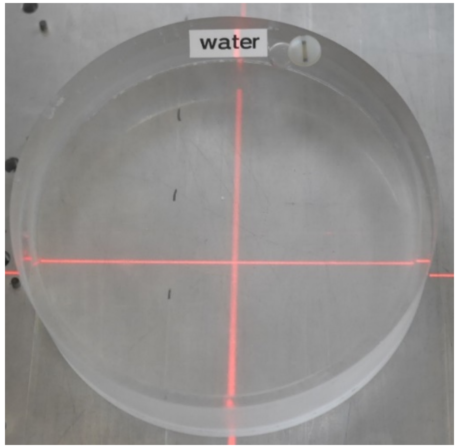

- pCT dose: 1.3 mGy, DECT dose: 35 mGy

- pCT: 6 min, DECT: 14 sec

Proton imaging for TP – pCT vs DECT

- Reconstructed images:

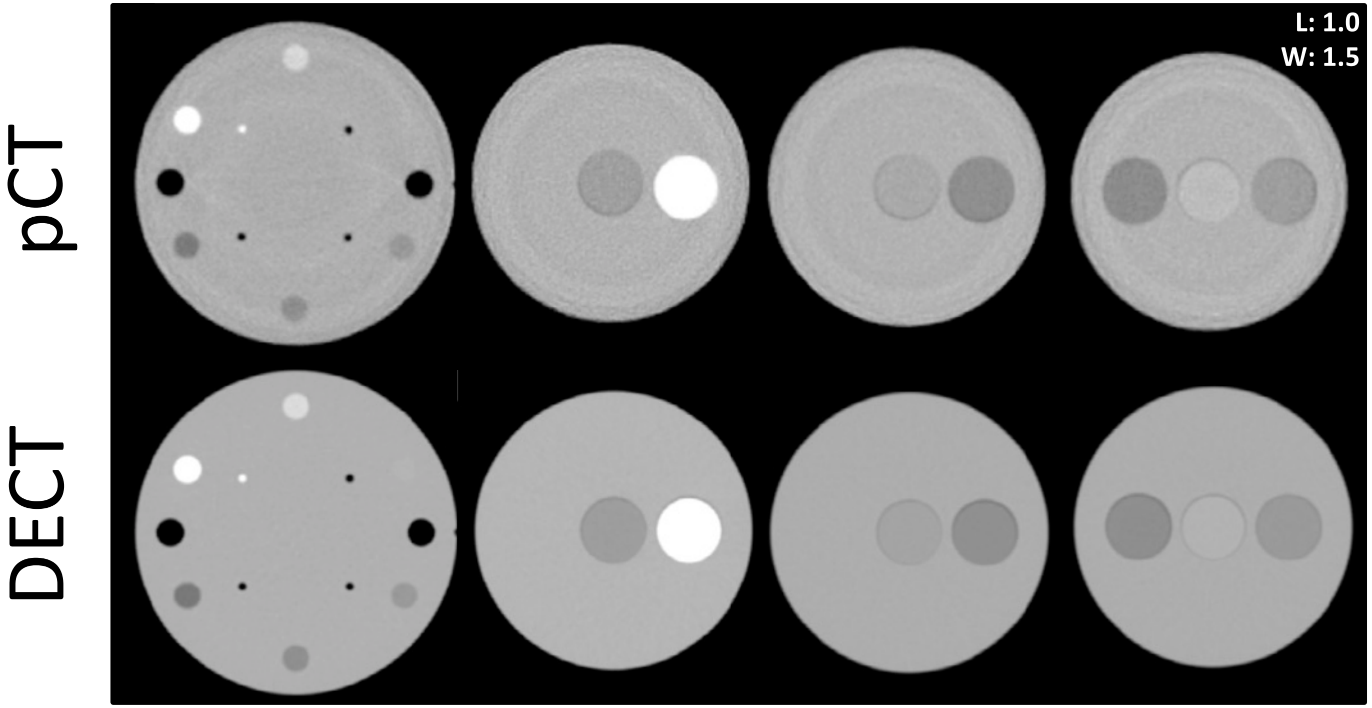

Dedes G. et al. Phys Med Biol. 2019 Aug 14;64(16):16500

- pCT from prototype scanner: ring shaped artifacts

Proton imaging for TP – pCT vs DECT

- Quantification of RSP accuracy:

$$\mathrm{RSP_{acc}} = 100 \cdot \frac{\mathrm{RSP_{mean}} - \mathrm{RSP_{ref}}}{\mathrm{RSP_{ref}}} \quad \%$$

$$\mathrm{MAPE} = \frac{\sum_{i=1}^{n} |\mathrm{RSP}_{\mathrm{acc},i}|}{n}$$

Dedes G. et al. Phys Med Biol. 2019 Aug 14;64(16):16500

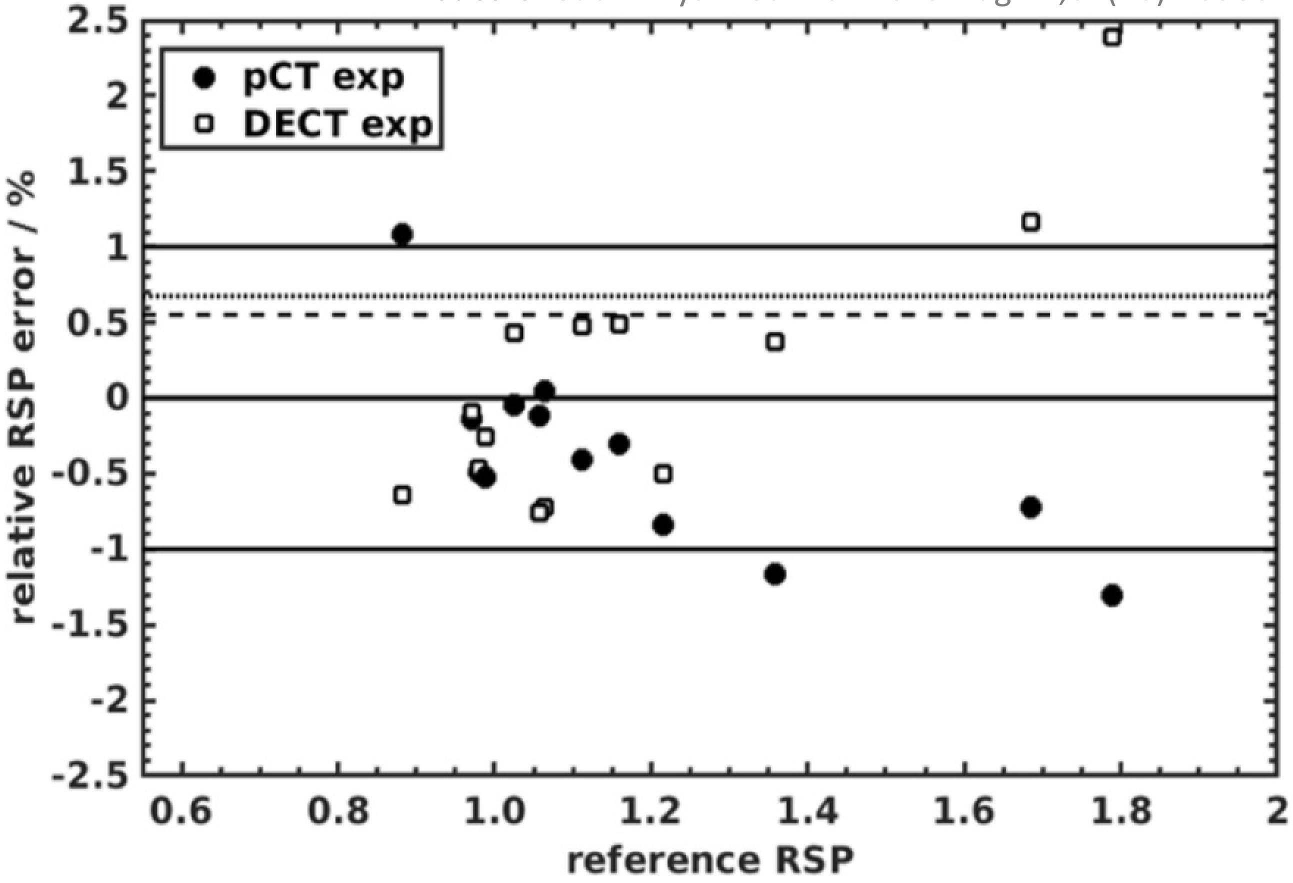

Biological uncertainties

- Increased biological effectiveness at end of range
- Cell survival vs. dose: $S = \exp(-\alpha D - \beta D^2)$
- From photons to protons: $\frac{\alpha_\mathrm{p}}{\alpha_x} := 1 + \frac{q}{(\alpha/\beta)_x} \cdot L$
- Relative biological effectiveness (RBE) to photons: $\mathrm{RBE} = \left.\frac{D_{ref}}{D_{ion}}\right|_{iso}$

$$\mathrm{RBE}\left(\left(\frac{\alpha}{\beta}\right)_x, L, D\right) = -\frac{1}{2D}\left(\frac{\alpha}{\beta}\right)_x + \frac{1}{D} \times \sqrt{\frac{1}{4}\left(\frac{\alpha}{\beta}\right)_x^2 + \left(qL + \left(\frac{\alpha}{\beta}\right)_x\right) D + D^2}$$

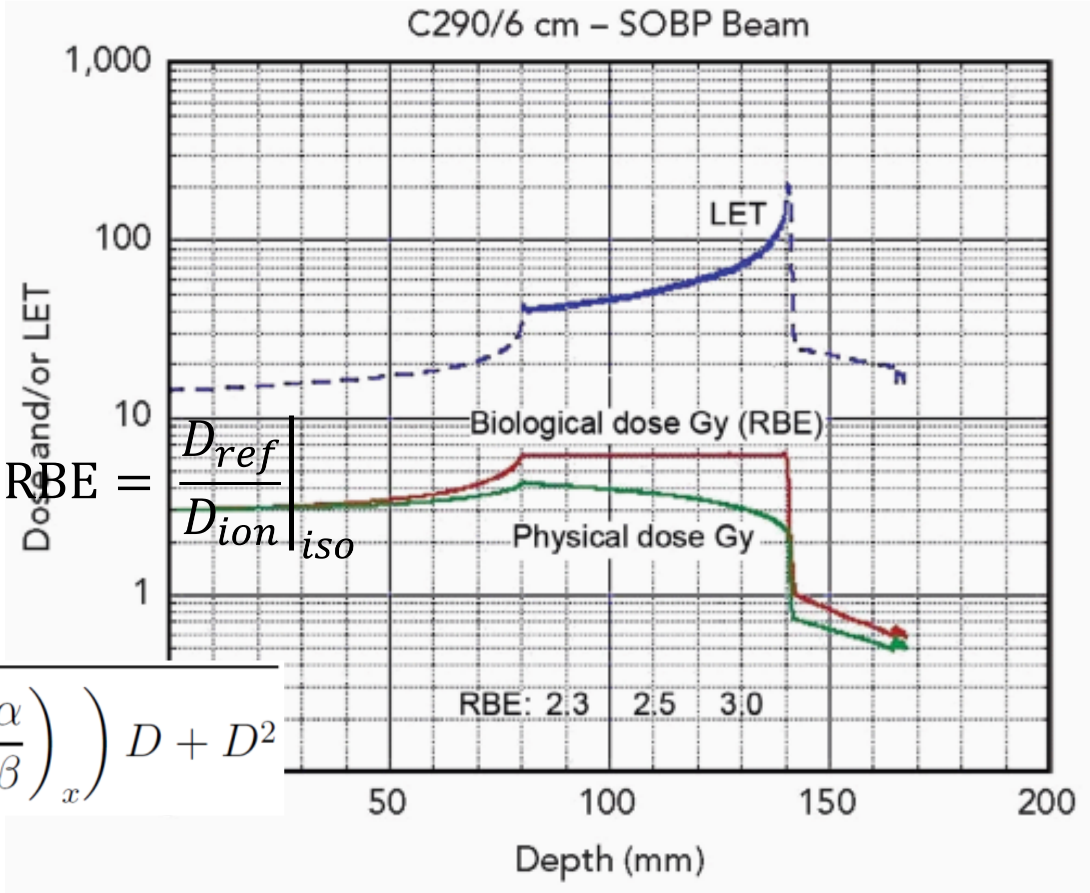

- Protons: almost constant RBE, assumed 1.1

https://radiologykey.com/overview-of-experience-with-heavier-charged-particle-radiotherapy/

Biological uncertainties

- Radiobiological dependencies and uncertainties (dose, LET, tissue type)

Resch A., …, Dedes G. Phys Med. 2017 Apr;36:91-102

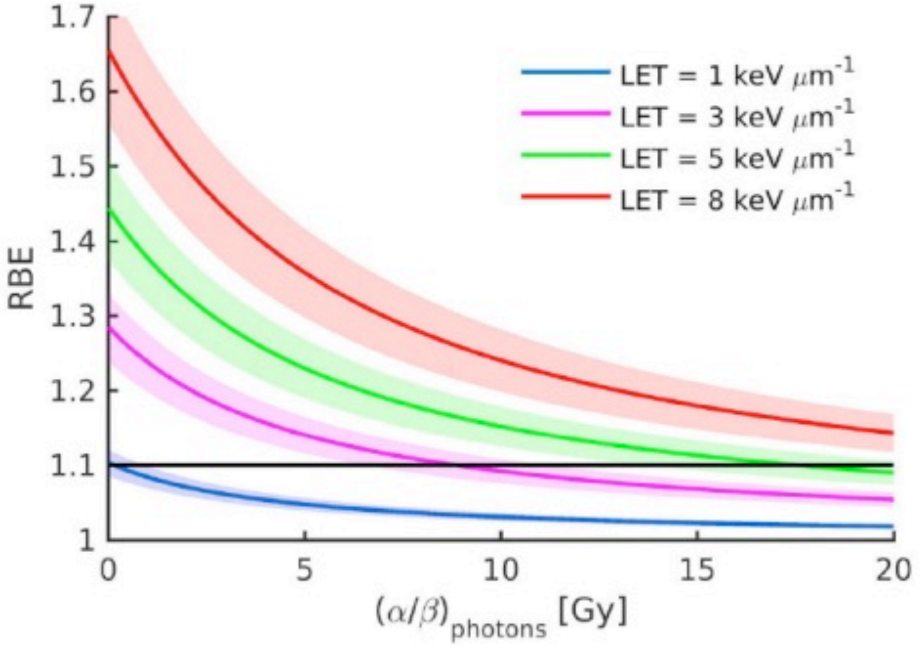

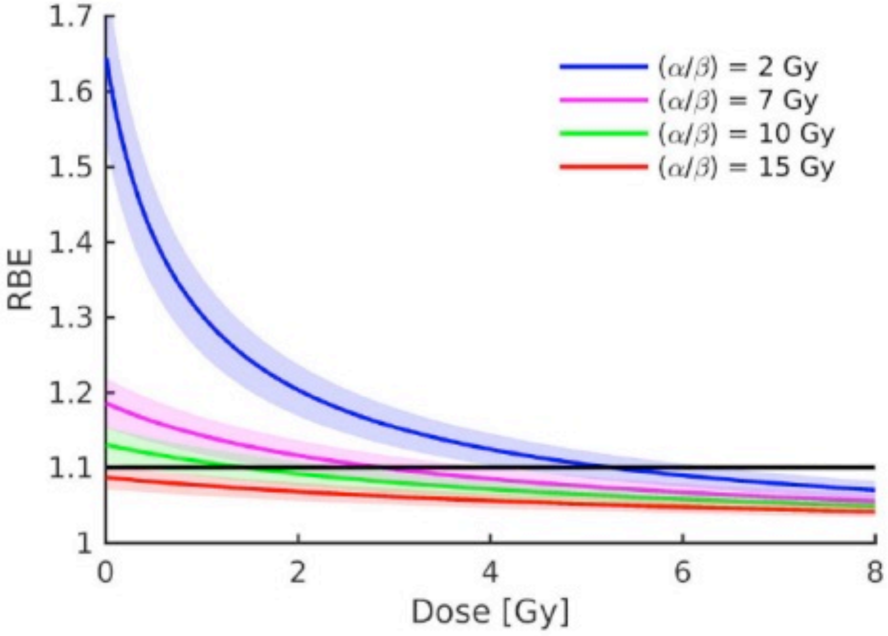

- Uncertainties stem from data based modeling

Biological uncertainties

- RBE=1.1 vs variable RBE treatment plans

- Still different when modelling uncertainties included?

RBE = 1.1

Variable RBE

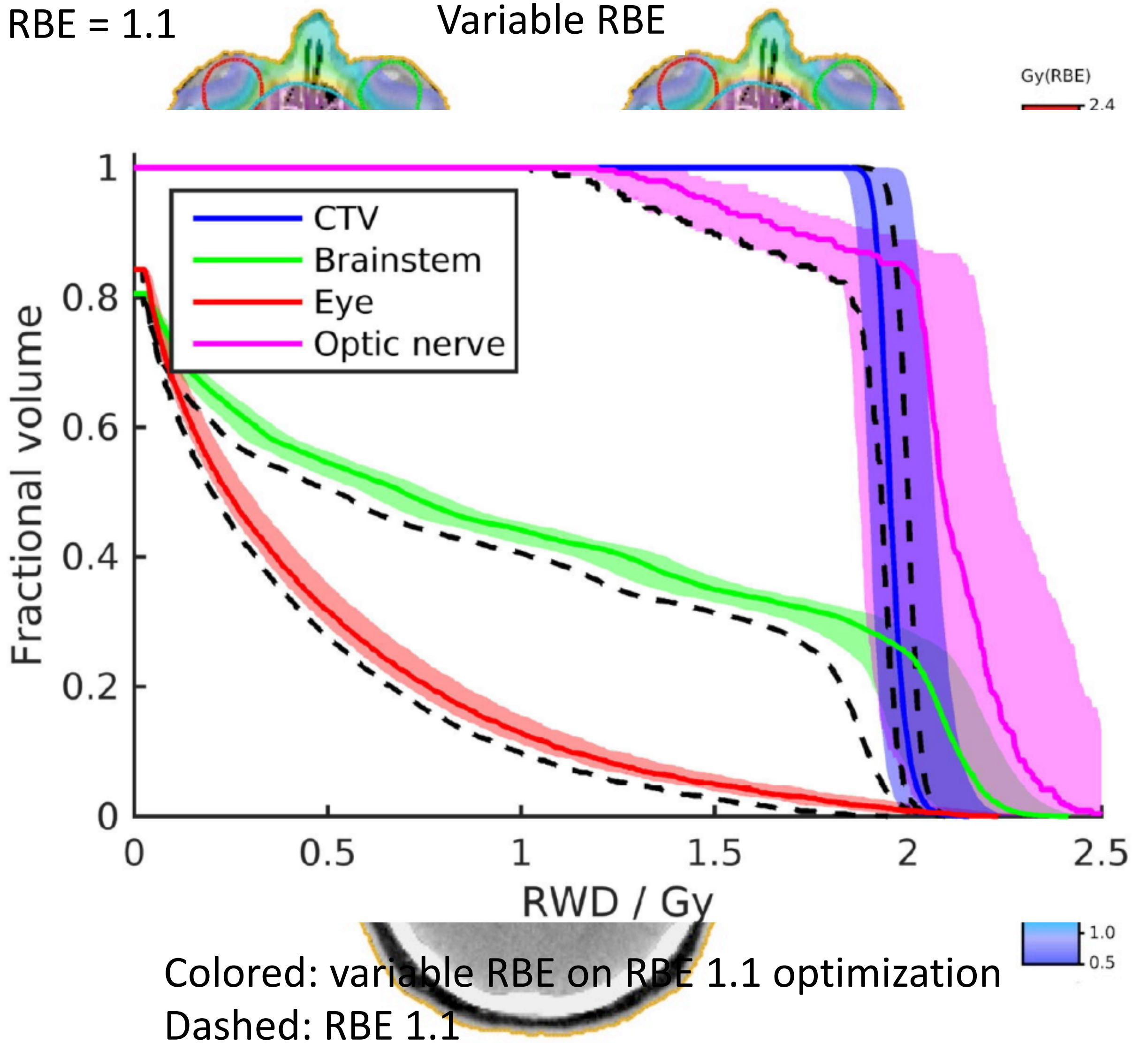

Colored: variable RBE on RBE 1.1 optimization
Dashed: RBE 1.1

Resch A., …, Dedes G. Phys Med. 2017 Apr;36:91-102

Biological uncertainties

- Optimal plans: variable RBE and model uncertainties included

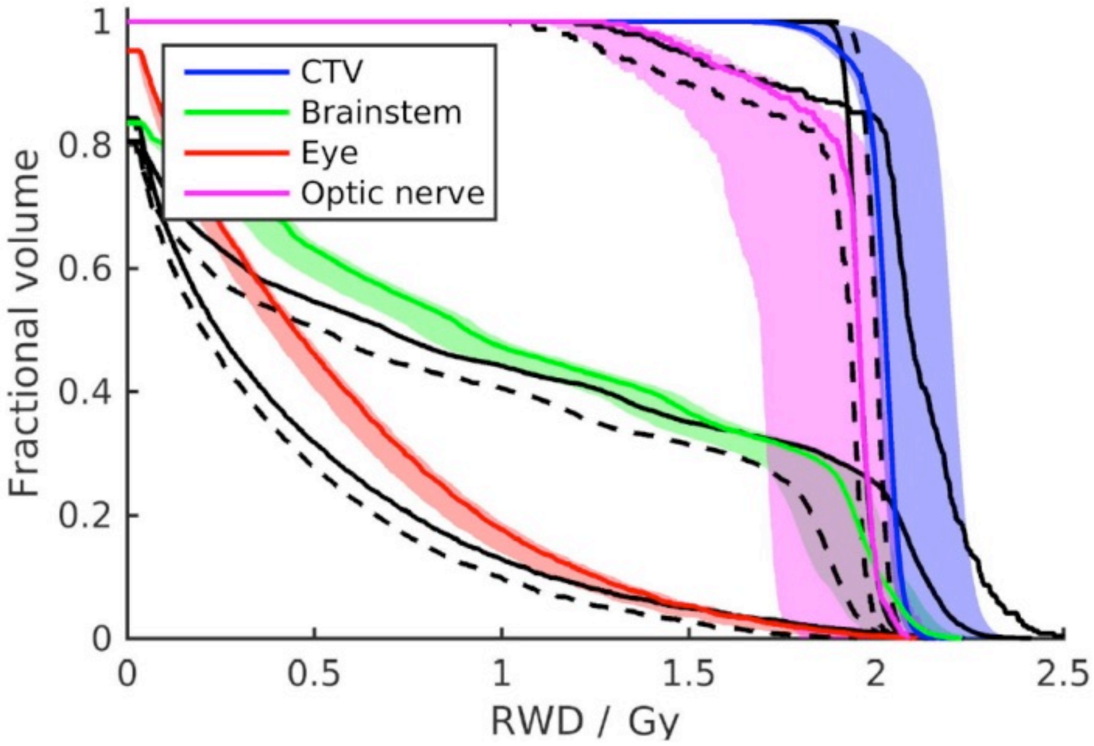

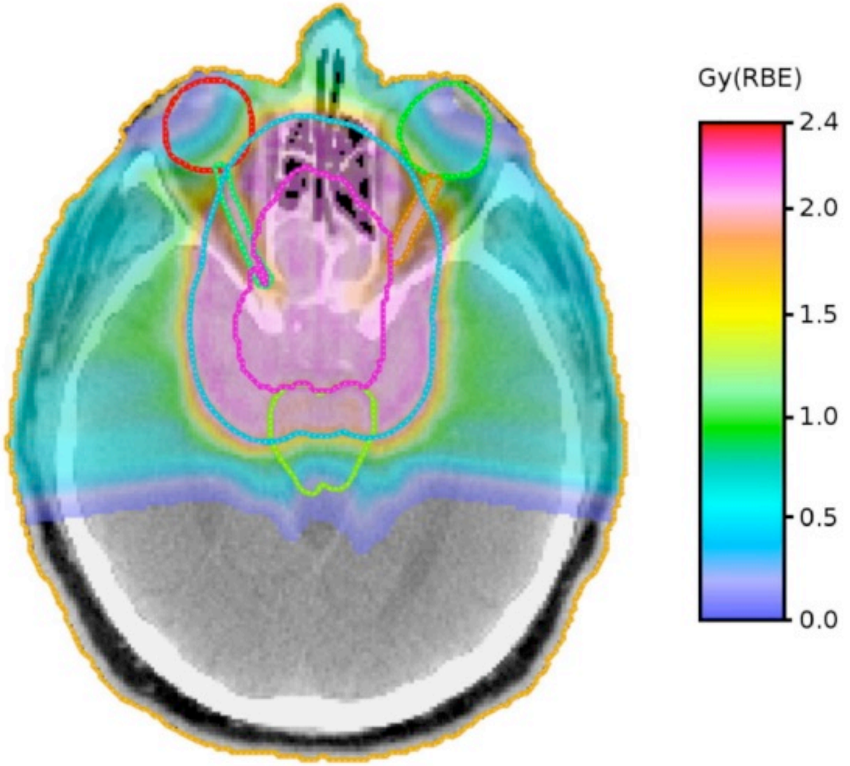

Resch A., …, Dedes G. Phys Med. 2017 Apr;36:91-102

Colored: biological effect optimization
Dashed: RBE 1.1 optimization
Solid: variable RBE on RBE 1.1 optimization

Proton imaging for plan adaptation - general

- Patient treatment in ~30 sessions (fractions)
- Image guidance prior each session desirable
- Imaging dose from ~30 pCT/cone beam CT (CBCT) similar to low dose bath from therapy
- Although low (hundreds of mGy), can contribute to second cancer risk
- Reduce dose to healthy tissue/retain image quality?

Proton imaging for plan adaptation – FMpCT

- Constant imaging fluence:
  - Constant dose
  - Spatially fixed image quality

- Optimized imaging fluence:
  - Retain image quality in a region of interest (ROI)
  - Minimize dose to other regions

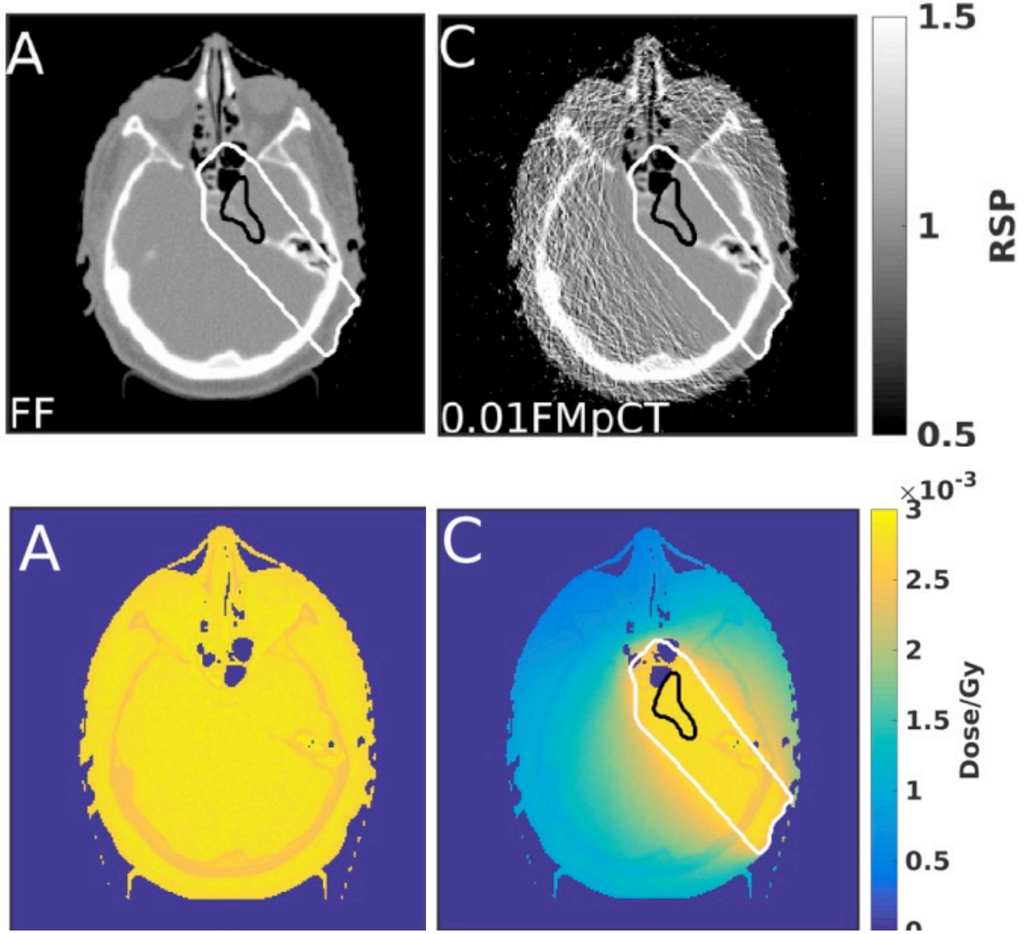

Dedes G., et al. Phys Med Biol. 2017 Jul 12;62(15):6026-604

Proton imaging for plan adaptation – FMpCT

- Basic implementation:
    - ➢ Clinical facilities: pencil beam (PB) scanning
    - ➢ Exploit clinical narrow proton beams
    - ➢ Determine fluence depending on intersection with ROI
    - ➢ Fluence modulated pCT (FMpCT)
- Disadvantage: non-prescribed image quality

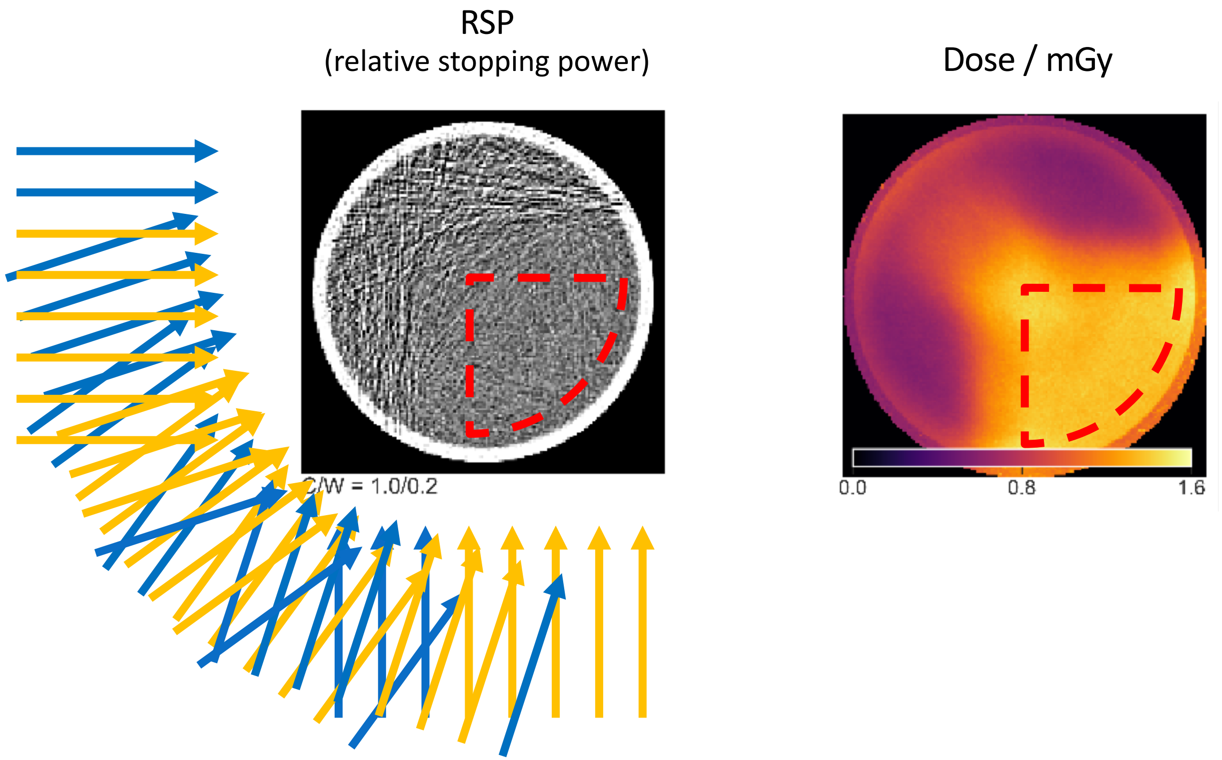

Dickmann J., …, Dedes G.. Med Phys. 2020 Apr;47(4):1895-190

Proton imaging for plan adaptation – FMpCT

- Simulated results on patient anatomies
- Dose reduction to healthy tissues:
  - 35 – 55%
- Dependent on ROI size/shape
- Need to understand noise formation and control it

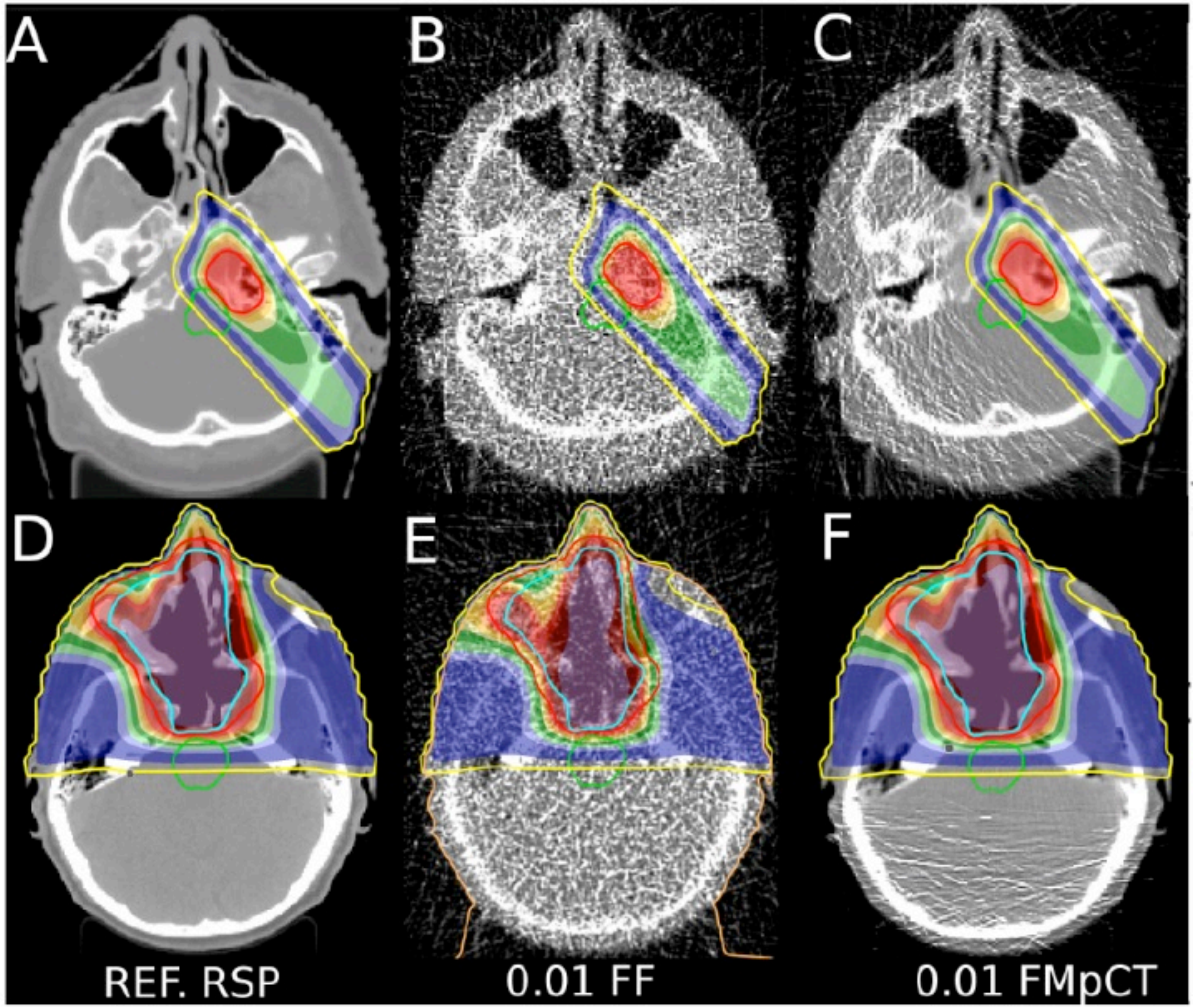

Dedes G., et al. Phys Med Biol. 2017 Jul 12;62(15):6026-604

Proton imaging – image reconstruction

- Filtered backprojection:

$$f(x,y) = \frac{\pi}{N_p} \sum_{n=1}^{N_p} h_{\gamma_n}(x\cos(\gamma_n) + y\sin(\gamma_n))$$

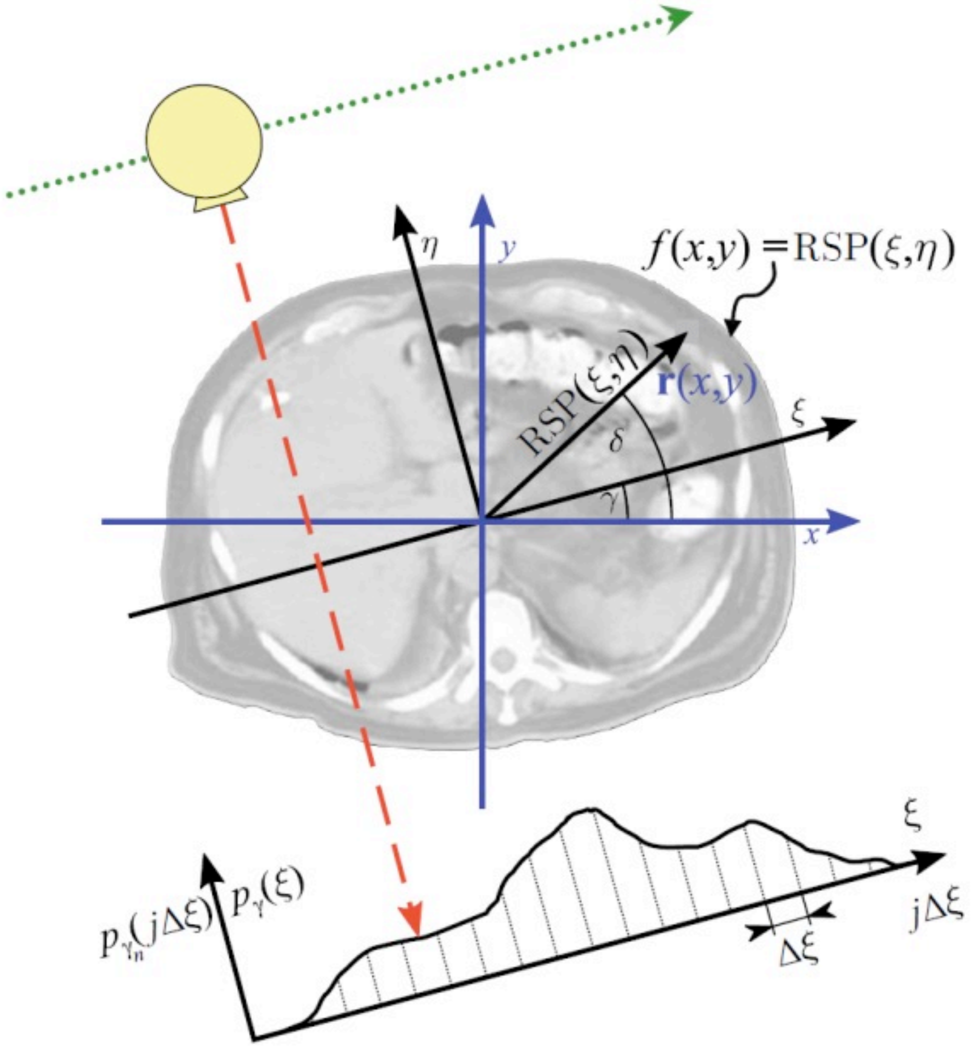

Rädler M., …, Dedes G. Phys Med Biol. 2018 Oct 24;63(21):21500

Proton imaging – noise theory

- Variance on the projection: $$\sigma^2_{\gamma_n}(j\Delta\xi) = \frac{\sigma^2_{\mathrm{WEPL},\gamma_n}(j\Delta\xi)}{N_{\gamma_n}(j\Delta\xi)}$$

- WEPL variance: $$\sigma^2_{\mathrm{WEPL}} = \left(\frac{\partial \mathrm{WEPL}\left(\overline{E}_{\mathrm{out}}\right)}{\partial E}\right)^2 \cdot \sigma^2_{E_{\mathrm{out}}} = \frac{\sigma^2_{E_{\mathrm{out}}}}{S^2_{\mathrm{W}}\left(\overline{E}_{\mathrm{out}}\right)}$$

- Final projection variance: $$\sigma^2_{\gamma_n}(j\Delta\xi) = \frac{\sigma^2_{E_{\mathrm{out}},\gamma_n}(j\Delta\xi)}{N_{\gamma_n}(j\Delta\xi)\cdot S^2_{\mathrm{W}}\left(\overline{E}_{\mathrm{out},\gamma_n}(j\Delta\xi)\right)}$$

- FBP noise reconstruction: $$\mathrm{Var}\left[f(x_p, y_p)\right] = f_{\mathrm{interp},\mu}\left(\frac{\pi}{N_p}\Delta\xi\right)^2 \sum_{n=1}^{N_p} V_{\gamma_n}(j\Delta\xi)$$

Proton imaging – FMpCT noise validation

- Experimental and simulated validation of pCT noise theory:

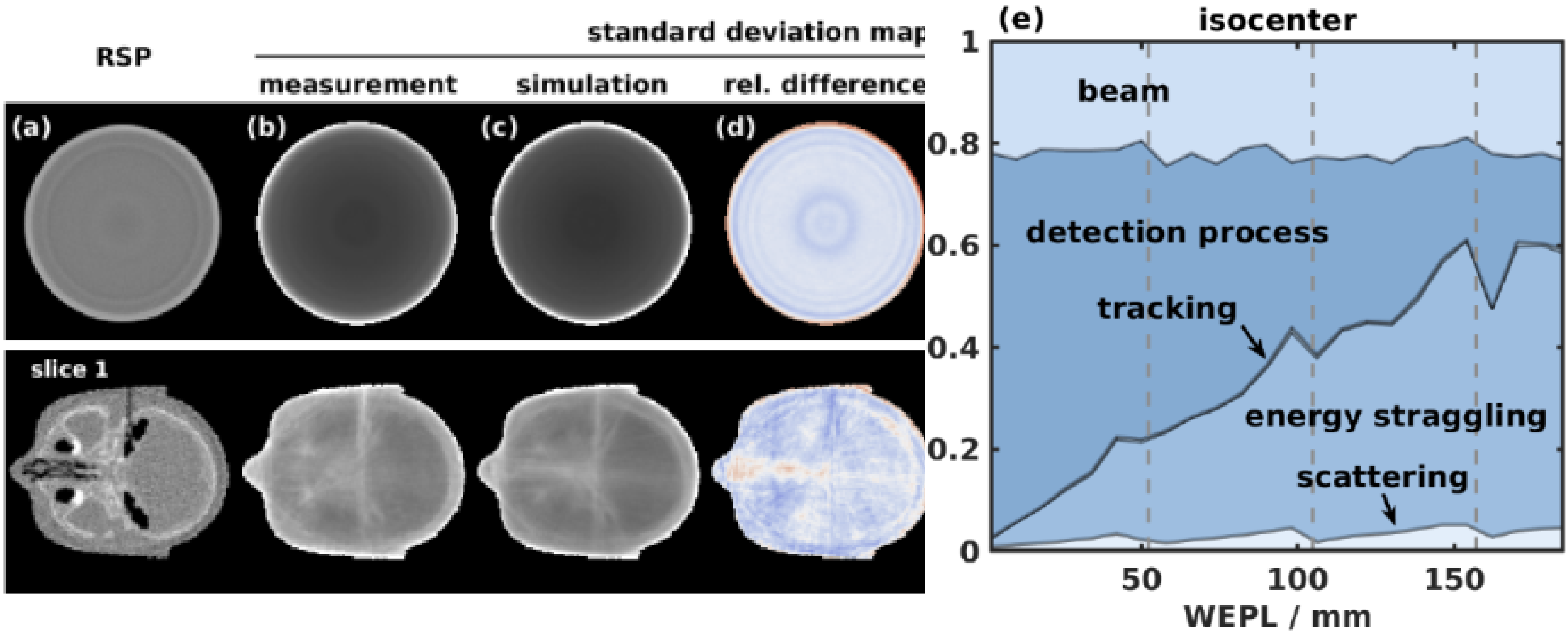

- Noise
  - Be
  - En
  - En
  - Sc

Dickmann J., …, Dedes G. Phys Med Biol. 2018 Oct 30;63(21):215025

Proton imaging – FMpCT optimization

- Using pixel: $\sigma^2_{\gamma_n}(j\Delta\xi) = \dfrac{\sigma^2_{E_{\mathrm{out}},\gamma_n}(j\Delta\xi)}{N_{\gamma_n}(j\Delta\xi) \cdot S^2_{\mathrm{W}}(\overline{E}_{\mathrm{out},\gamma_n}(j\Delta\xi))}$

- Noise target / fluence pattern prescription

- Iterative fluence optimization algorithm

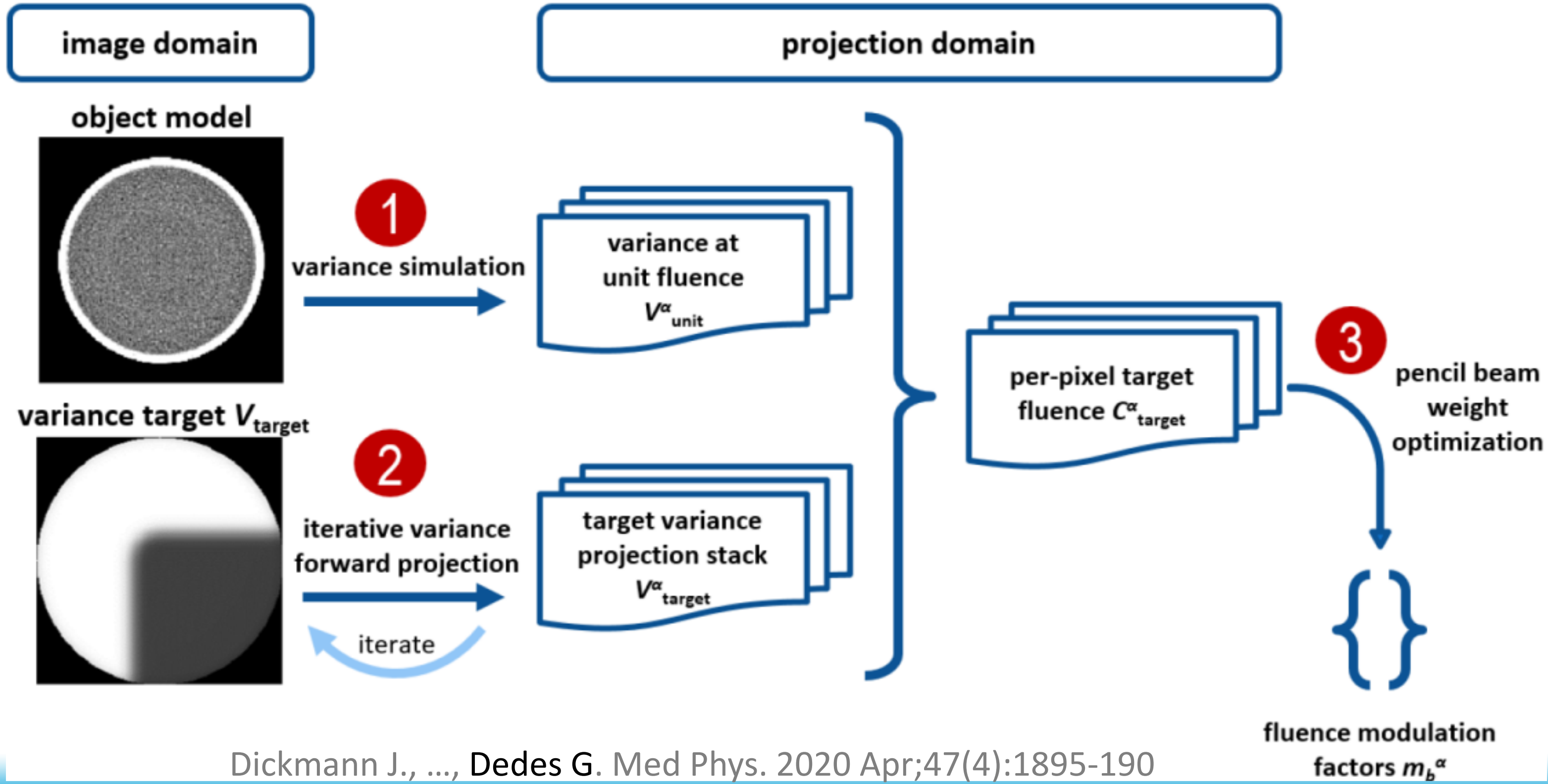

Dickmann J., …, Dedes G. Med Phys. 2020 Apr;47(4):1895-190

Proton imaging – FMpCT optimization

- Optimized fluences applied to simulated acquisitions

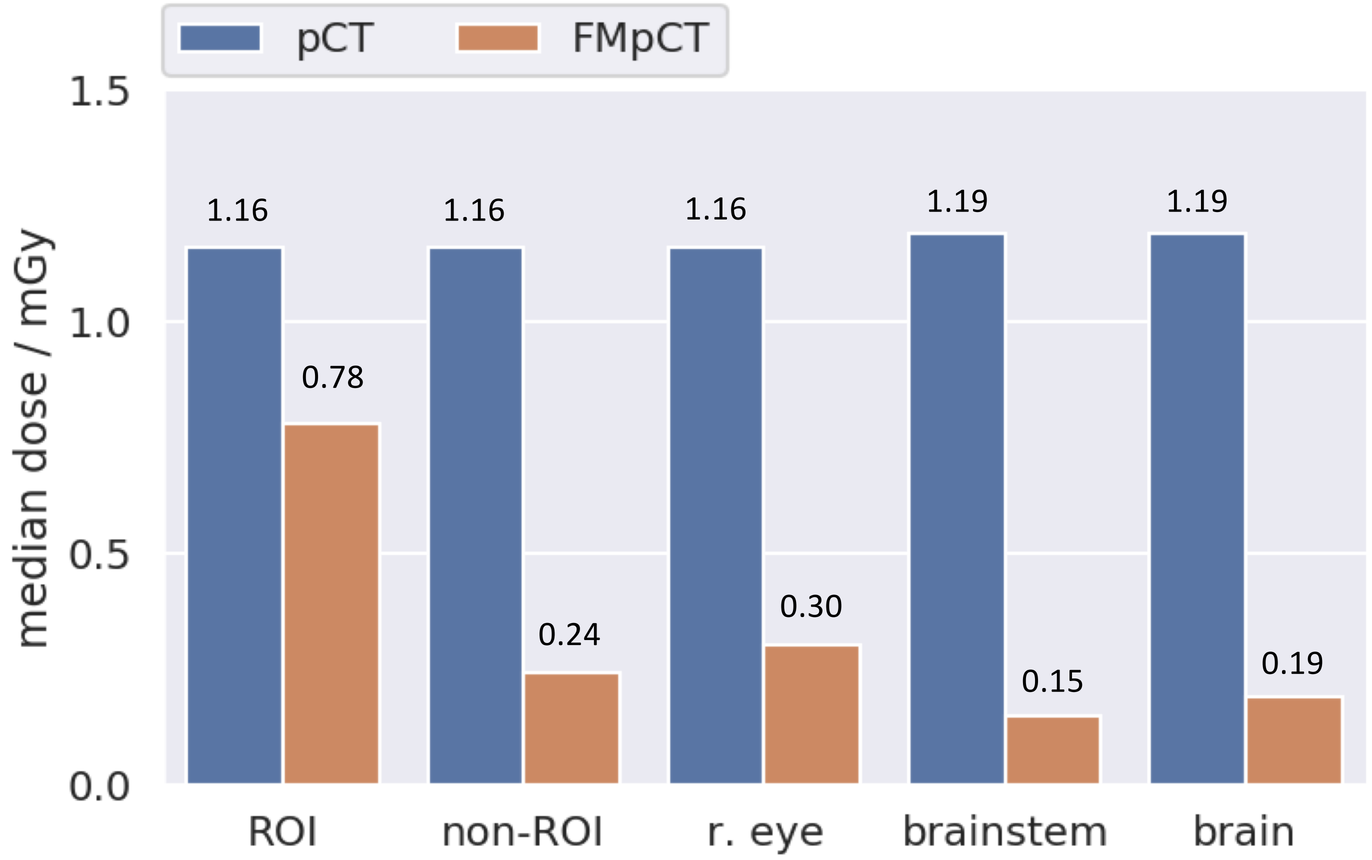

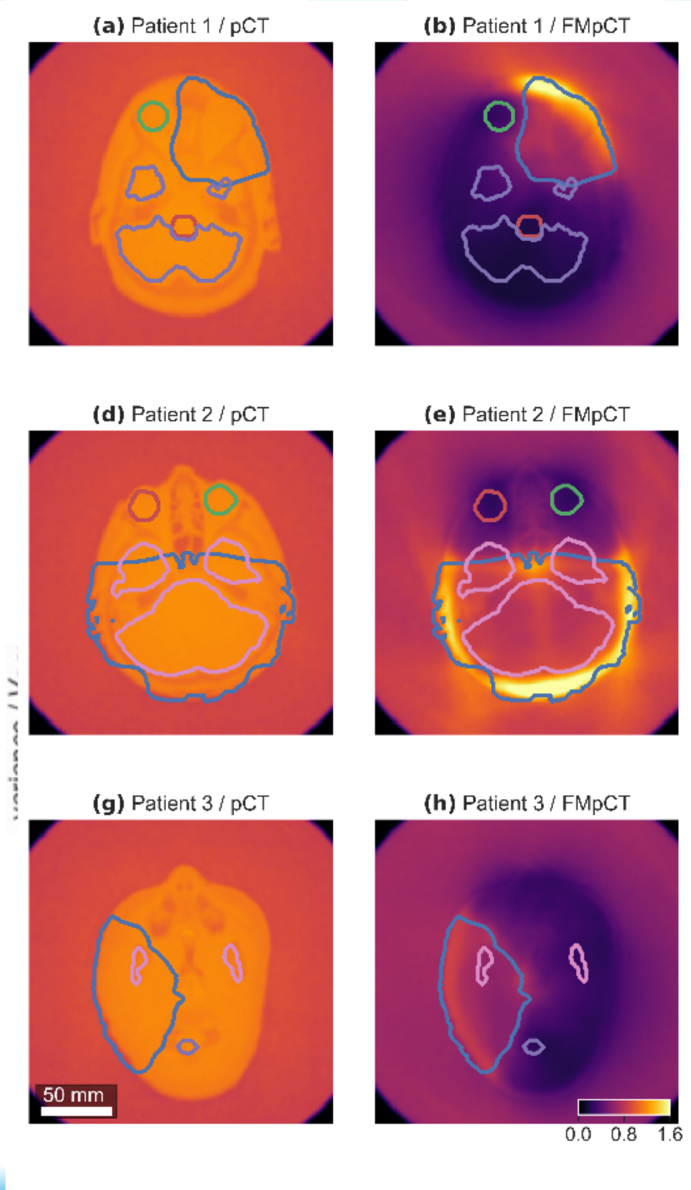

Dickmann J., …, Dedes G. Med Phys. 2020 Apr;47(4):1895-190

Proton imaging – FMpCT optimization

- Experimental implementation of optimized FMpCT

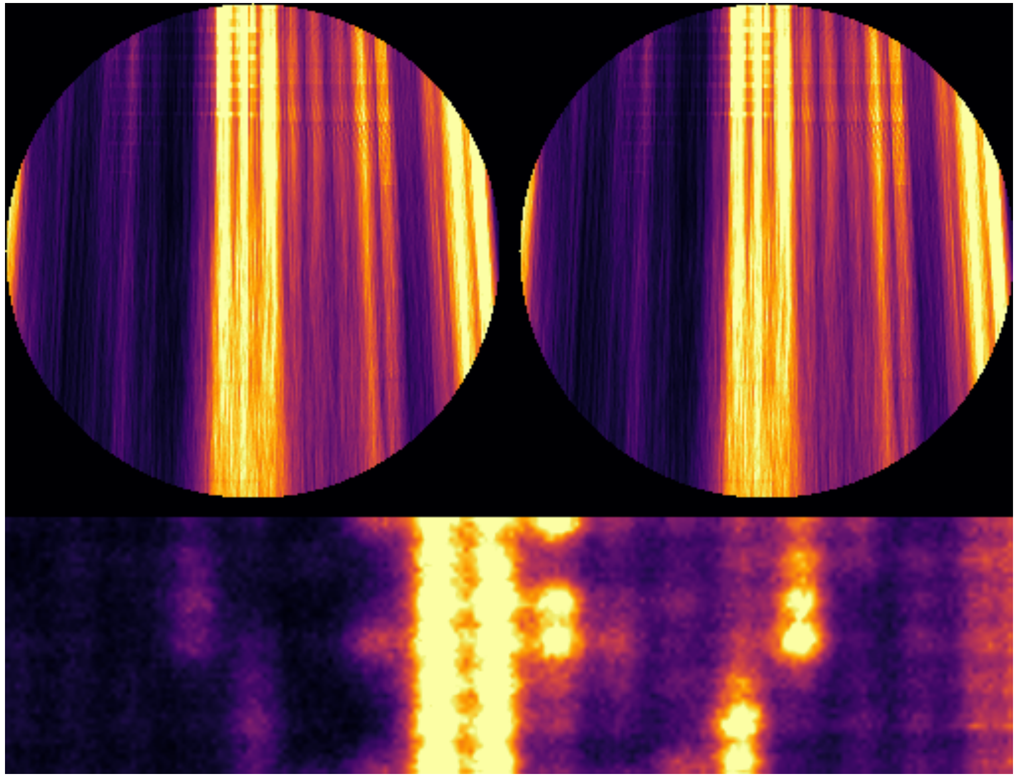

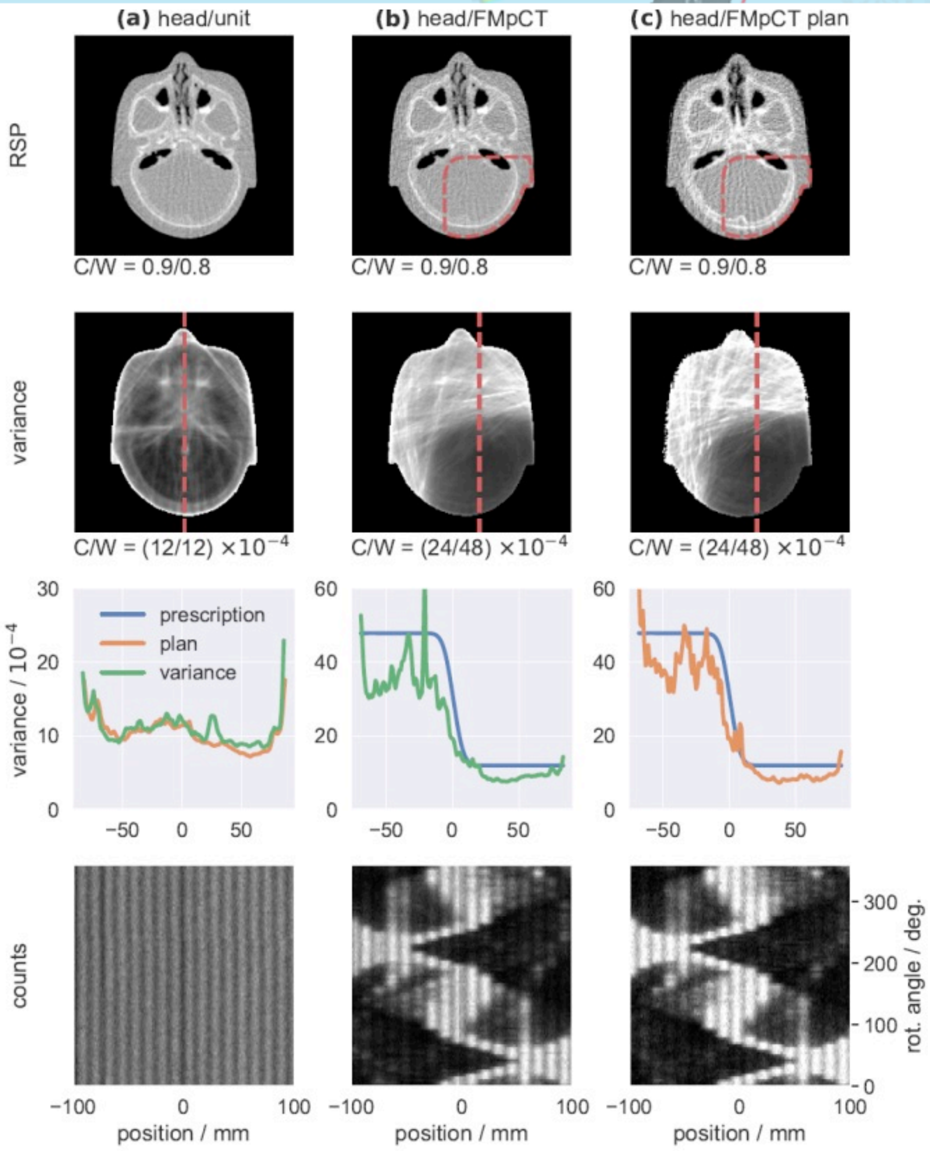

Dickmann J., …, Dedes G. Phys Med Biol. 2020 Sep 25;65(19):19500

Ion beam range monitoring – general

- The ion beam stops in the patient

- How to monitor the Bragg peak position?
  - ➢ By means of secondary emission
  - ➢ Origin: beam induced nuclear interactions
  - ➢ Or thermoacoustic

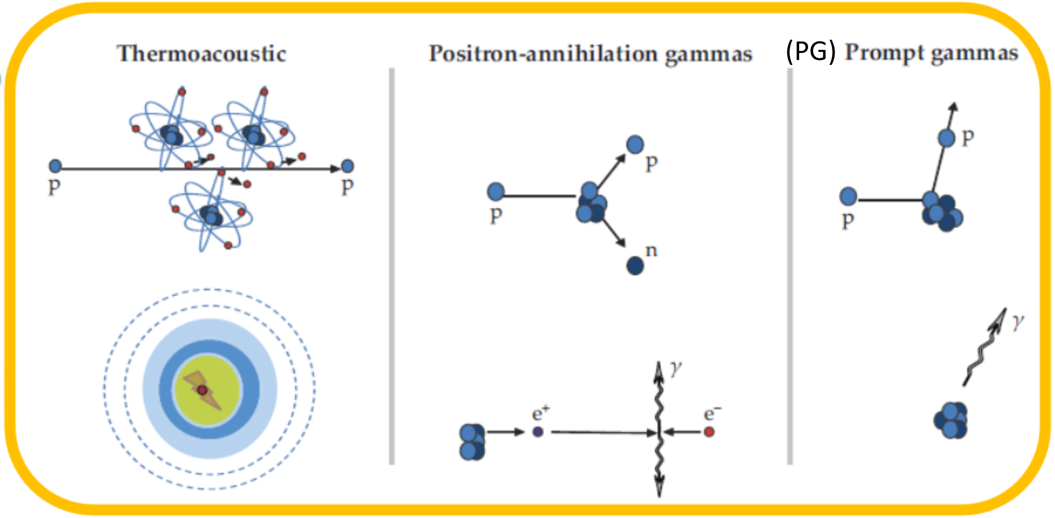

Physics Today 68(10), 28 (2015)

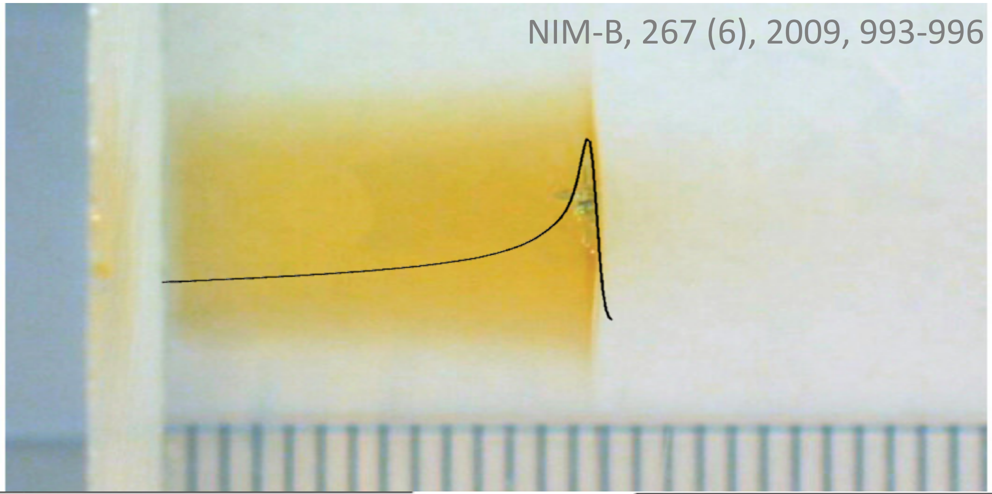

NIM-B, 267 (6), 2009, 993-996

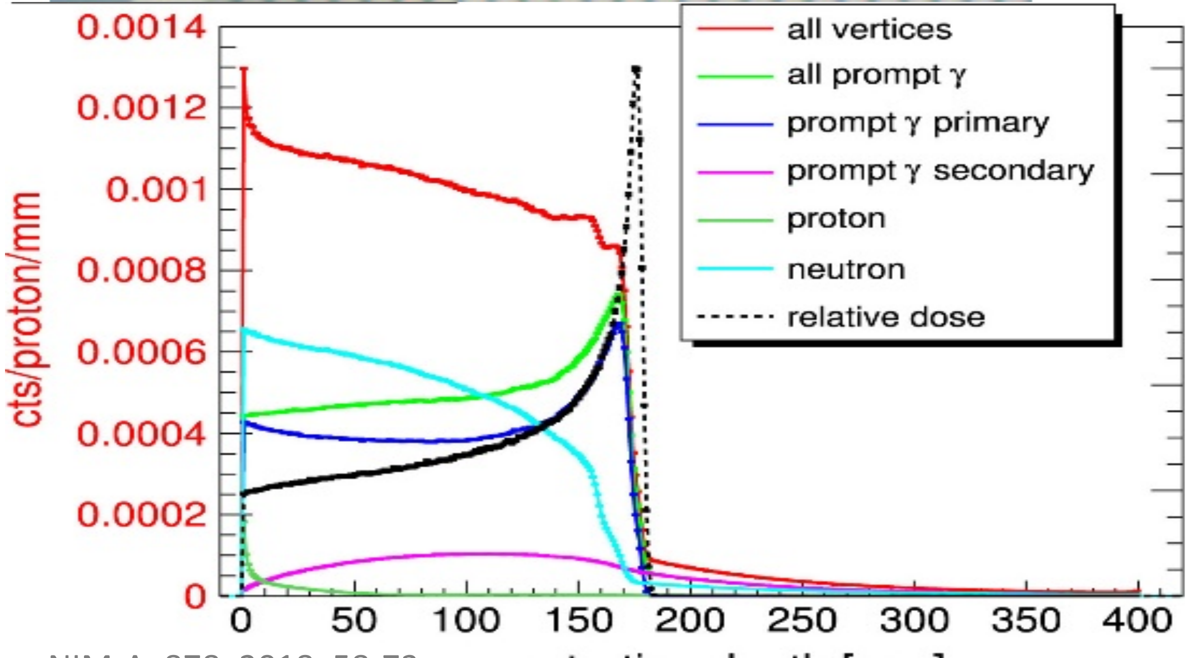

NIM-A, 878, 2018, 58-73

Ion beam range monitoring – general

- Workflow:
  - ➢ Calculate dose in treatment planning system
  - ➢ Calculate monitoring observable
  - ➢ Deliver dose
  - ➢ Measure monitoring observable
  - ➢ Compare measured and calculated observable

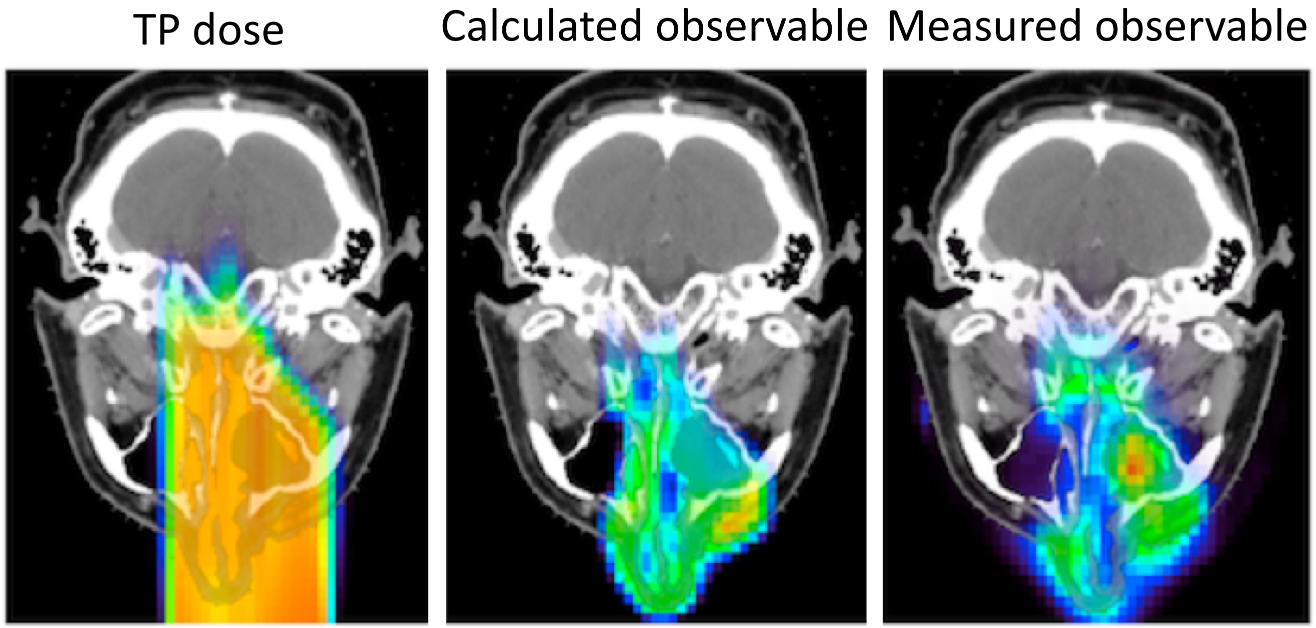

Int. J. Radiat. Oncol. Biol. Phys, 86(1), 2013, 183-189

Prompt-gamma range monitoring

- PG range monitoring in patient anatomies

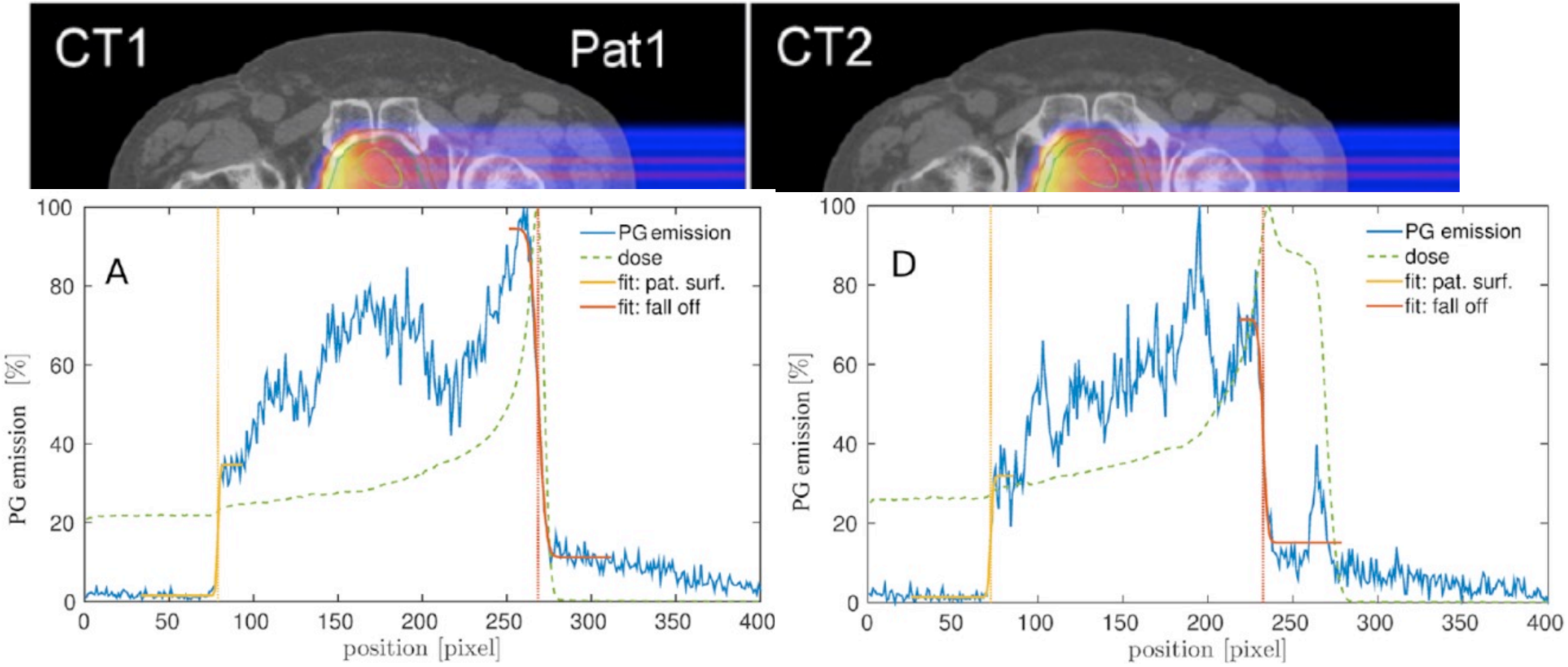

Schmid S., …, Dedes G. Phys Med Biol. 2015 Nov 18;60(24):9329-934

Prompt-gamma range monitoring

- Feasible PG monitoring methodology
- Performance in patient anatomies:
  - 95% of all beams within ±2 mm
  - Median: < 1mm
  - Discarded 10% of 1738 spots

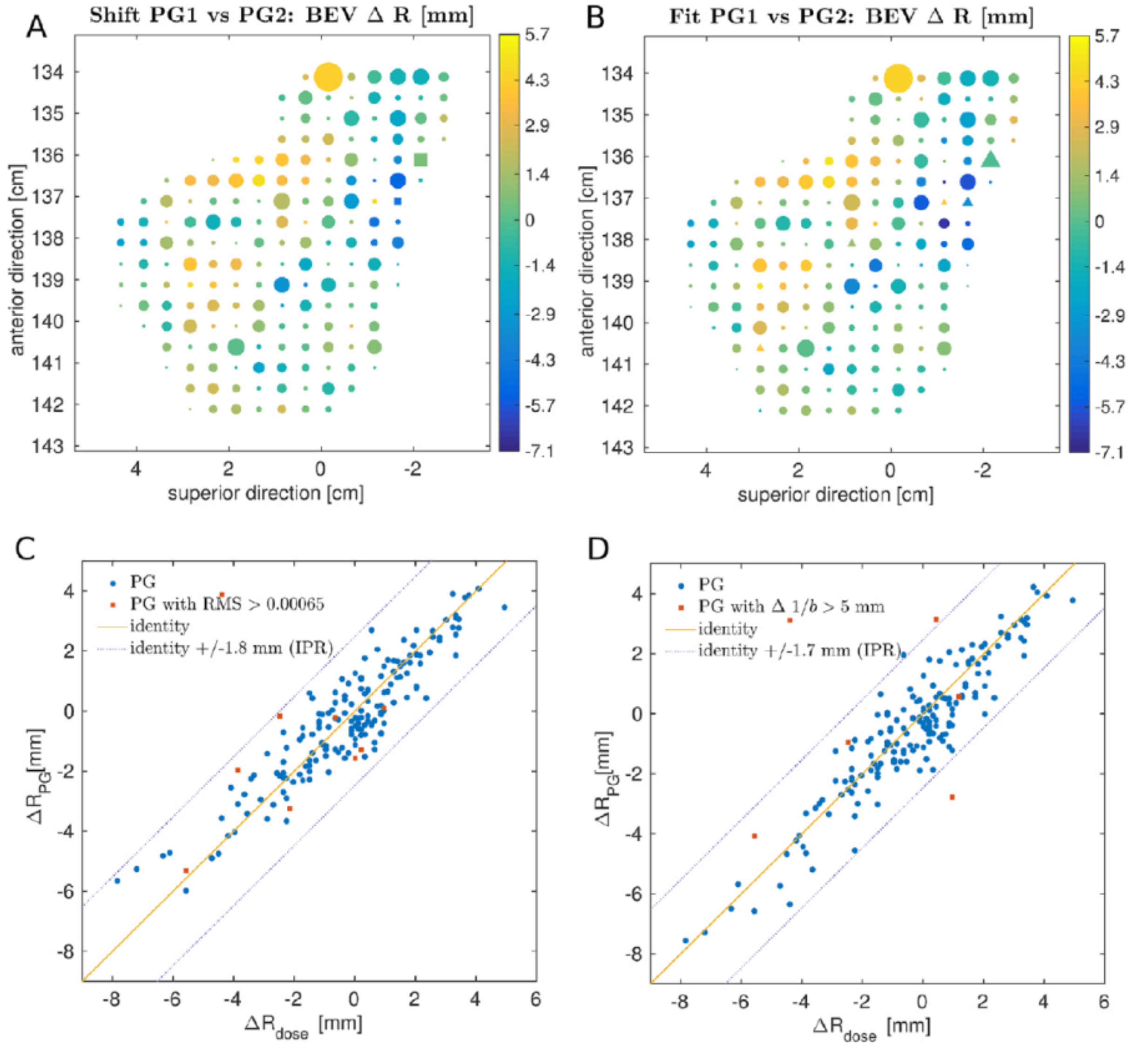

Schmid S., …, Dedes G. Phys Med Biol. 2015 Nov 18;60(24):9329-934

Conclusions

- Proton therapy: “sharp” clinical tool, sensitive to uncertainties
- Imaging, biology, accelerator science, math can reduce these uncertainties
- Three aspects presented:
  - ➢ Proton imaging as a promising imaging tool for proton therapy
  - ➢ Radiobiology as a tool for better understanding proton therapy effectiveness
  - ➢ Range monitoring of protons beams as a clinically feasible method

https://ionimaging2022.sciencesconf.org/

WELCOME TO THE THIRD ION IMAGING WORKSHOP 2022

The ion imaging workshop 2022 will take place in Munich, Germany. It is the third edition after the workshops in 2018 and 2019.

Date: October 13-14, 2022

Venue: LMU Munich, Germany

Important dates:

Registration is now open.

Registration fee is 180 Euro including lunches, coffee breaks, and the social dinner.

Registration deadline: September 1, 2022.

Abstract submission deadline: ~~July 15, 2022~~, extended to July 27, 2022.

If you want to stay up-to-date about events around ion imaging, **sign up for the** ion imaging researchers mailing list.

LUDWIG-
MAXIMILIANS-
UNIVERSITÄT
MÜNCHEN

Thank you

LUDWIG-
MAXIMILIANS-
UNIVERSITÄT
MÜNCHEN

Backup slides

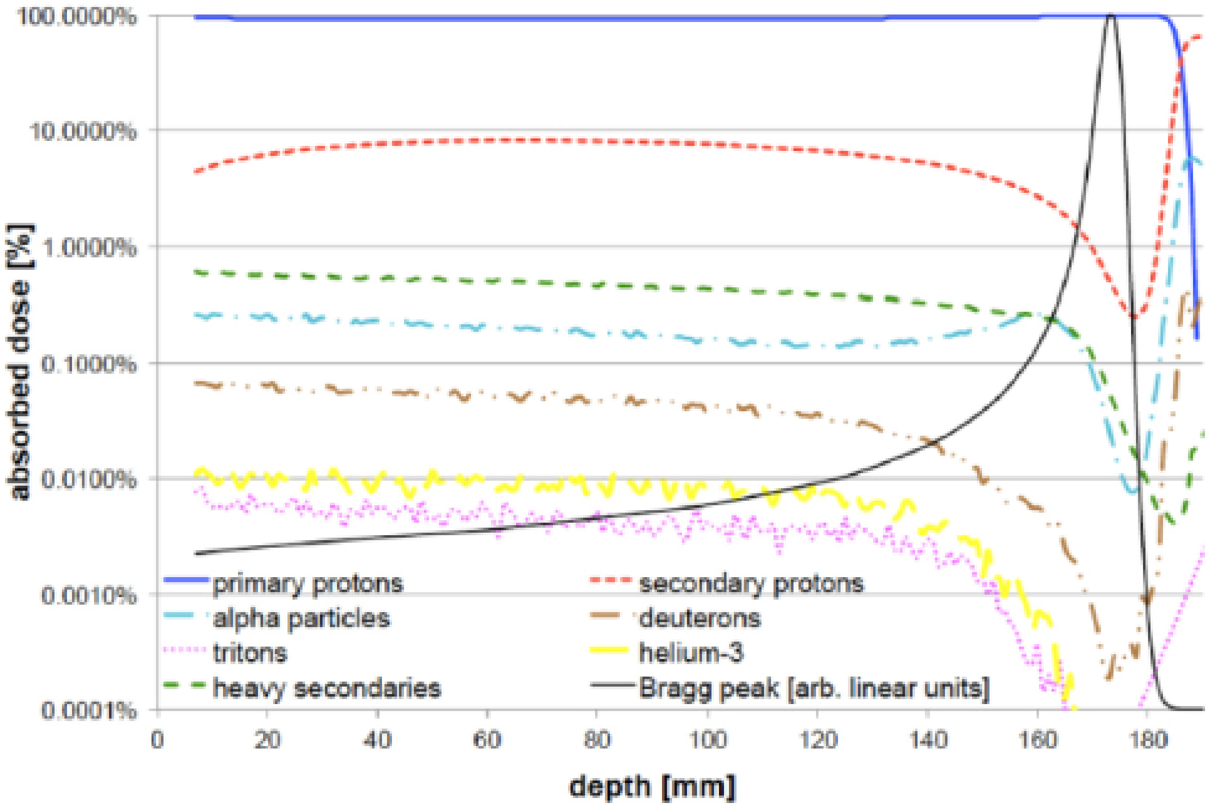
100.0000%
10.0000%
1.0000%
0.1000%
0.0100%
0.0010%
0.0001%
absorbed dose [%]
primary protons
secondary protons
alpha particles
deuterons
tritons
helium-3
heavy secondaries
Bragg peak [arb. linear units]
0
20
40
60
80
100
120
140
160
180
depth [mm]

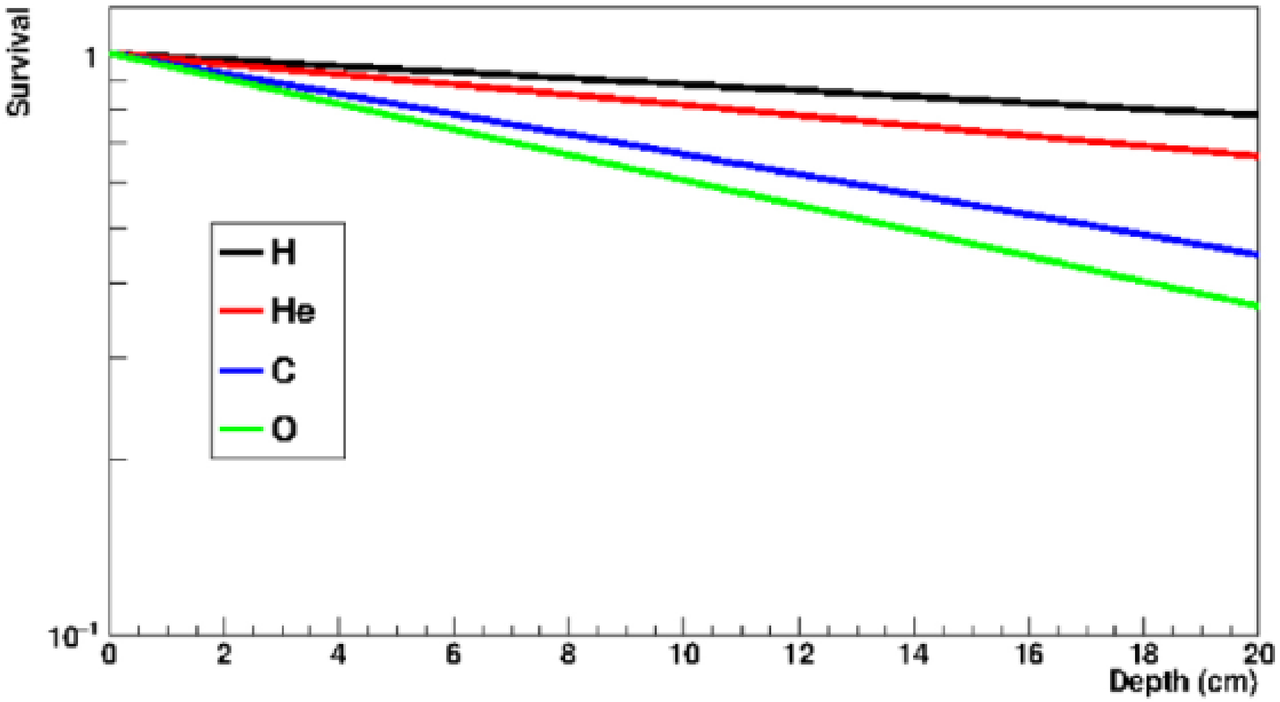
Survival
1
10^-1
H
He
C
O
0
2
4
6
8
10
12
14
16
18
20
Depth (cm)

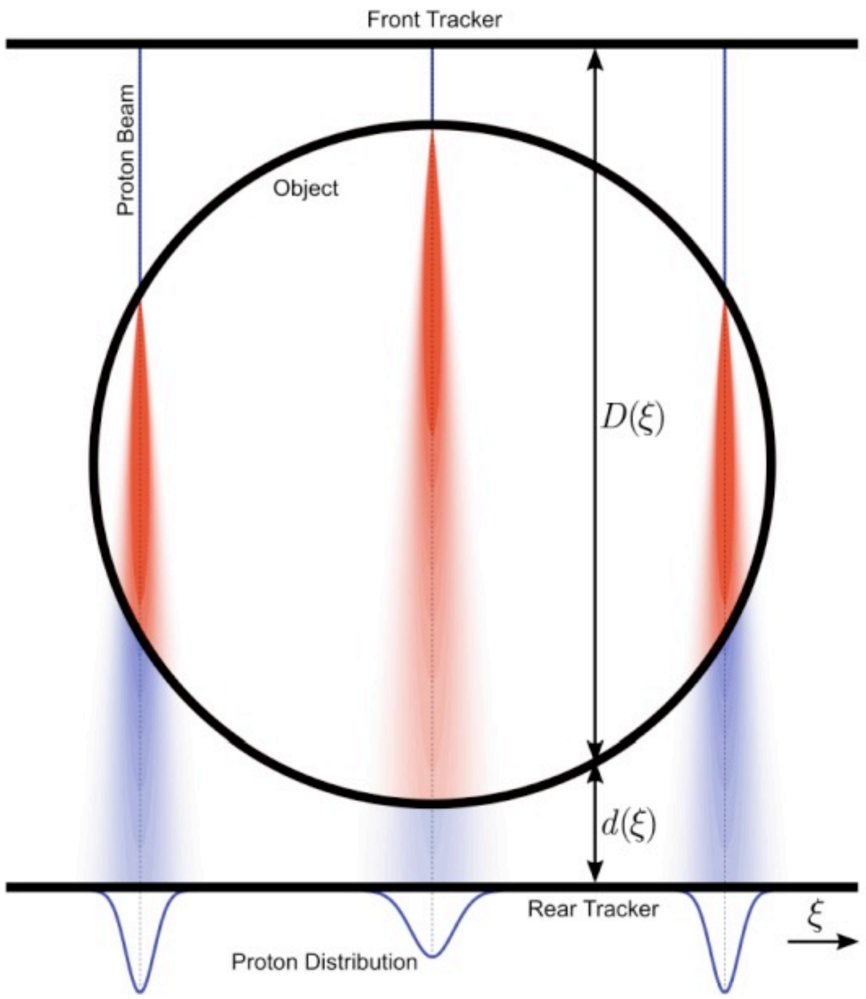
Front Tracker
Proton Beam
Object
$D(\xi)$
$d(\xi)$
Rear Tracker
ξ
Proton Distribution

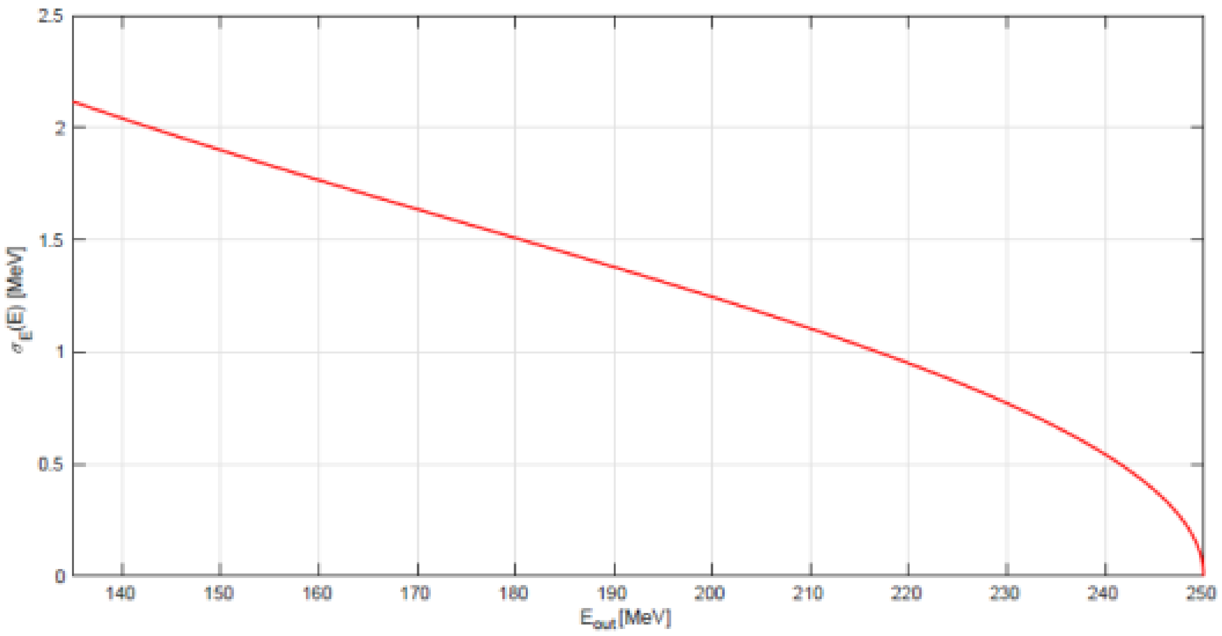
$\sigma_E(E)$ [MeV]
E_{out} [MeV]
2.5
2
1.5
1
0.5
0
140
150
160
170
180
190
200
210
220
230
240
250

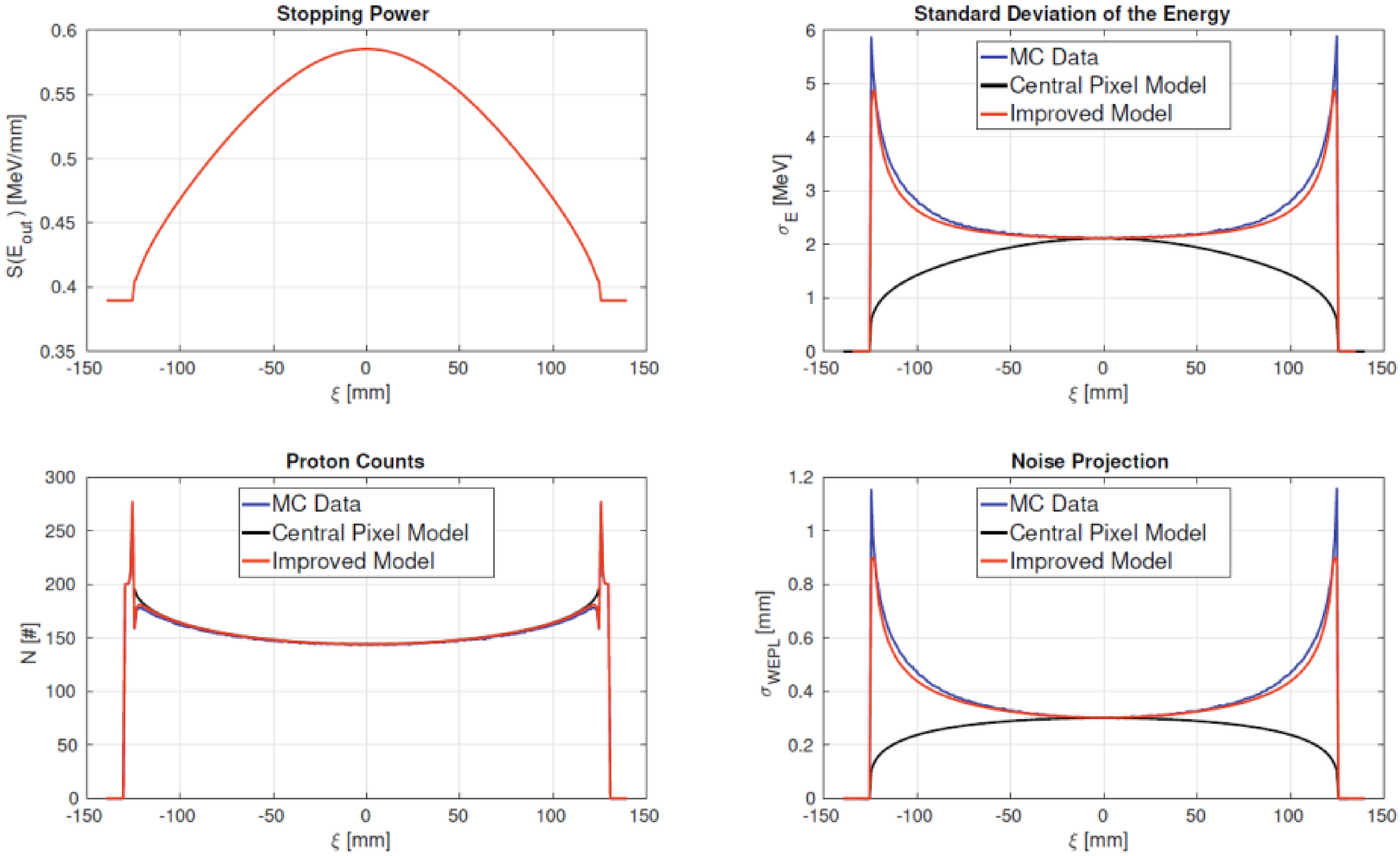

Stopping Power
S(E_out) [MeV/mm]
ξ [mm]
Standard Deviation of the Energy
σ_E [MeV]
ξ [mm]
MC Data
Central Pixel Model
Improved Model
Proton Counts
N [#]
ξ [mm]
MC Data
Central Pixel Model
Improved Model
Noise Projection
σ_WEPL [mm]
ξ [mm]
MC Data
Central Pixel Model
Improved Model

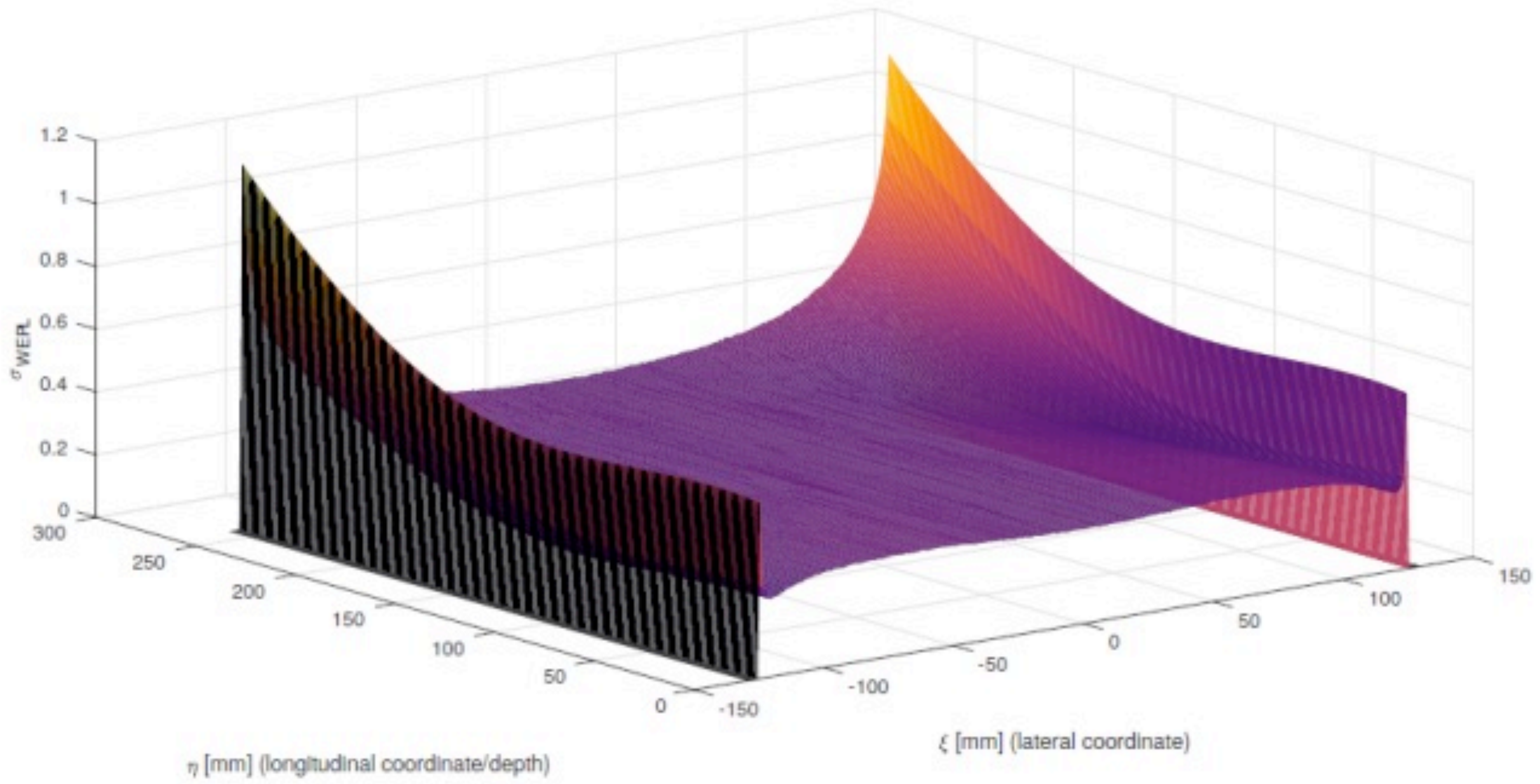

σ WER
η [mm] (longitudinal coordinate/depth)
ξ [mm] (lateral coordinate)

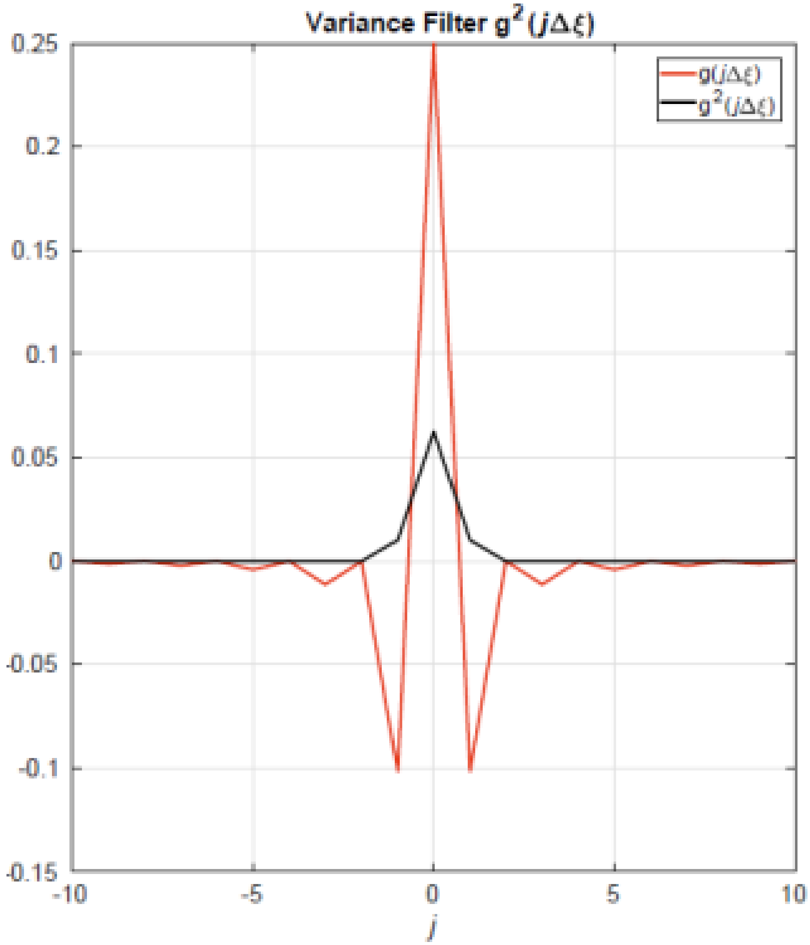

1D INTERPOLATION FOR REAR TRACKER BINNING

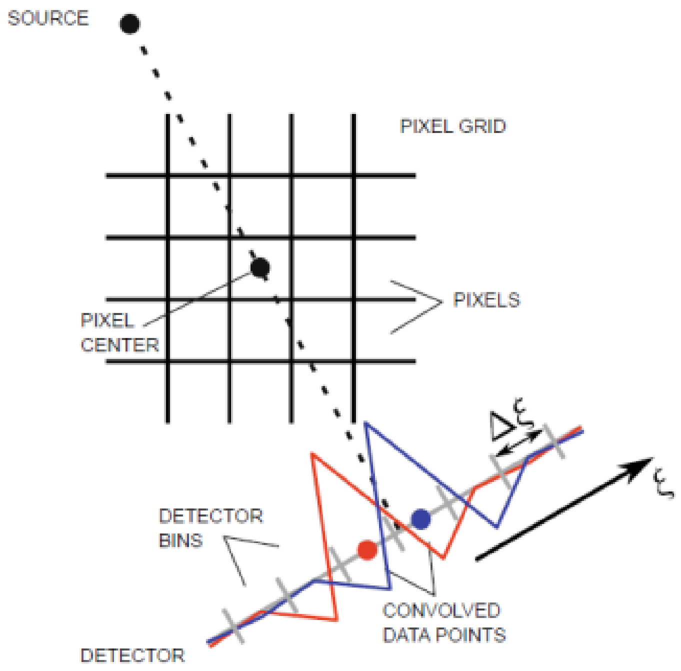

- $h_{\gamma_n}(j\Delta\xi)$
- $h_{\gamma_n}((j+1)\,\Delta\xi)$

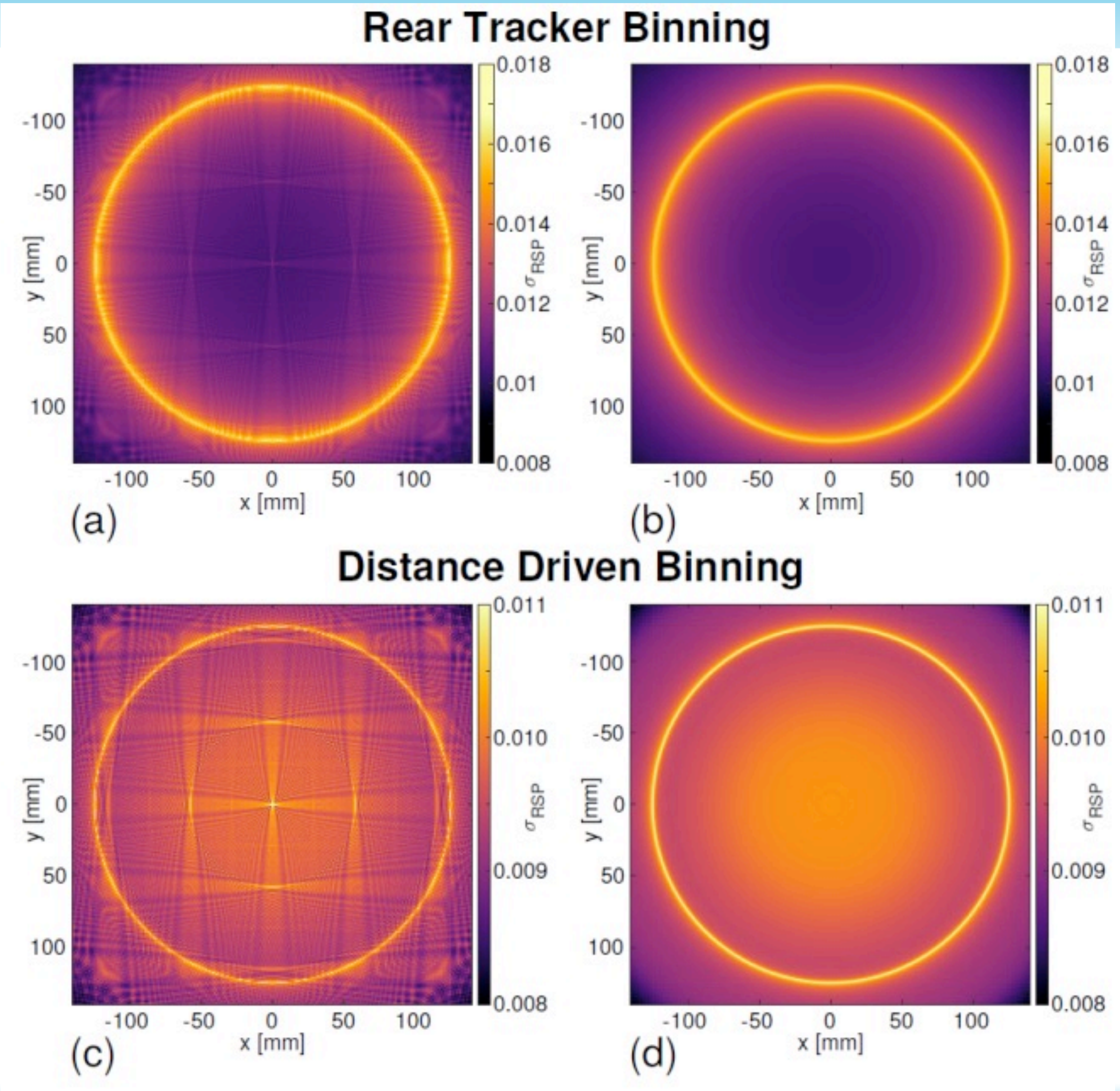
Rear Tracker Binning
Distance Driven Binning
(a)
(b)
(c)
(d)
x [mm]
y [mm]
σ_{RSP}
-100
-50
0
50
100
0.018
0.016
0.014
0.012
0.01
0.008
0.011
0.010
0.009

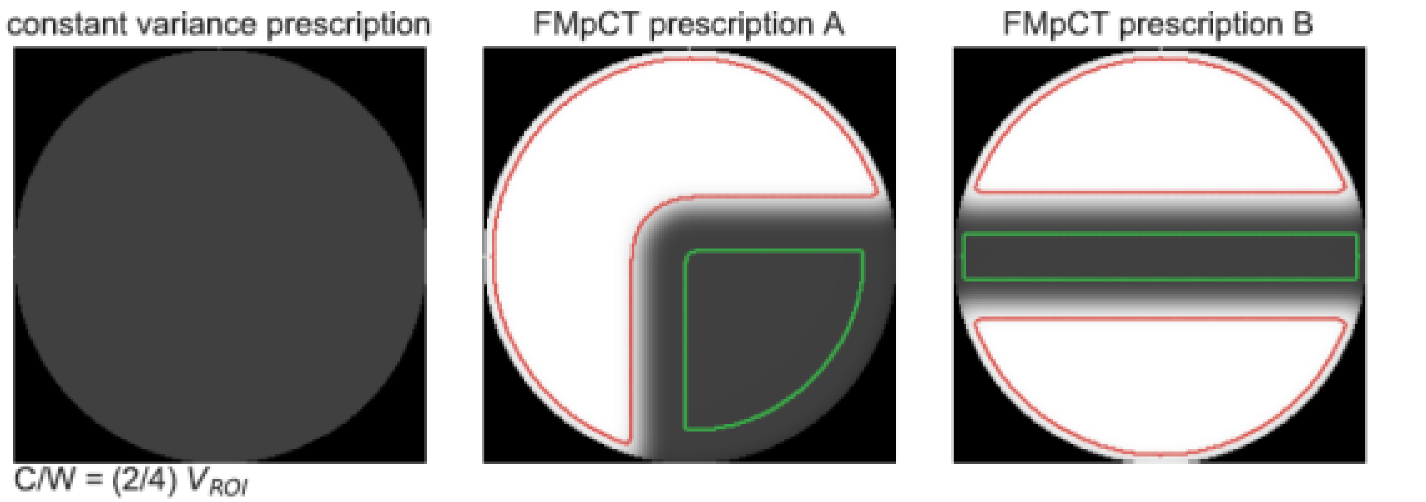
constant variance prescription
FMpCT prescription A
FMpCT prescription B
C/W = (2/4) V_ROI

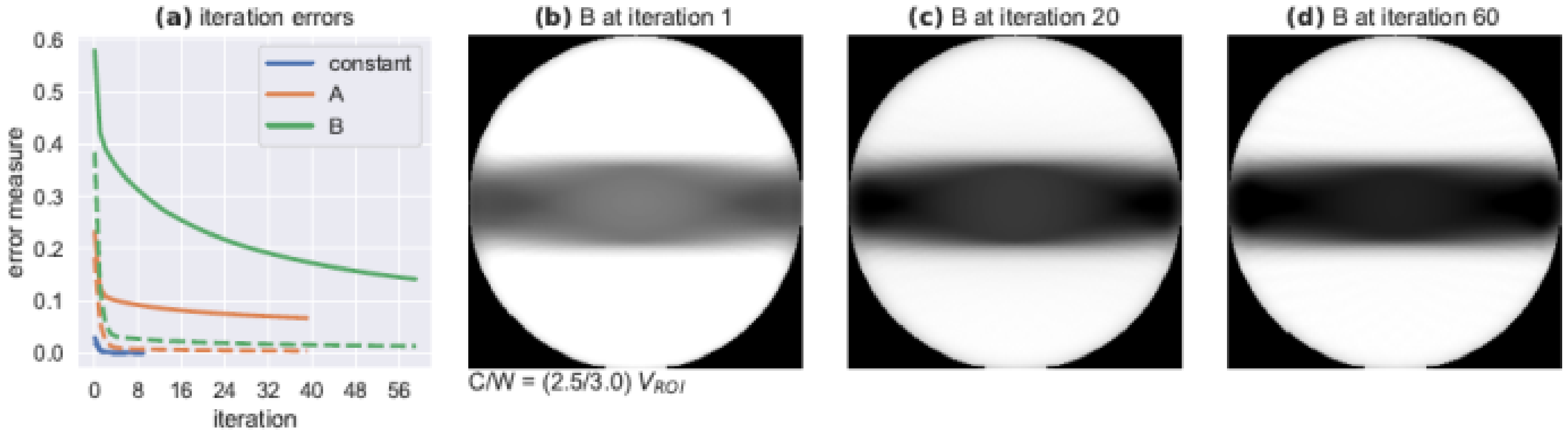
(a) iteration errors
(b) B at iteration 1
(c) B at iteration 20
(d) B at iteration 60
error measure
iteration
constant
A
B
0.0
0.1
0.2
0.3
0.4
0.5
0.6
0
8
16
24
32
40
48
56
C/W = (2.5/3.0) V_ROI

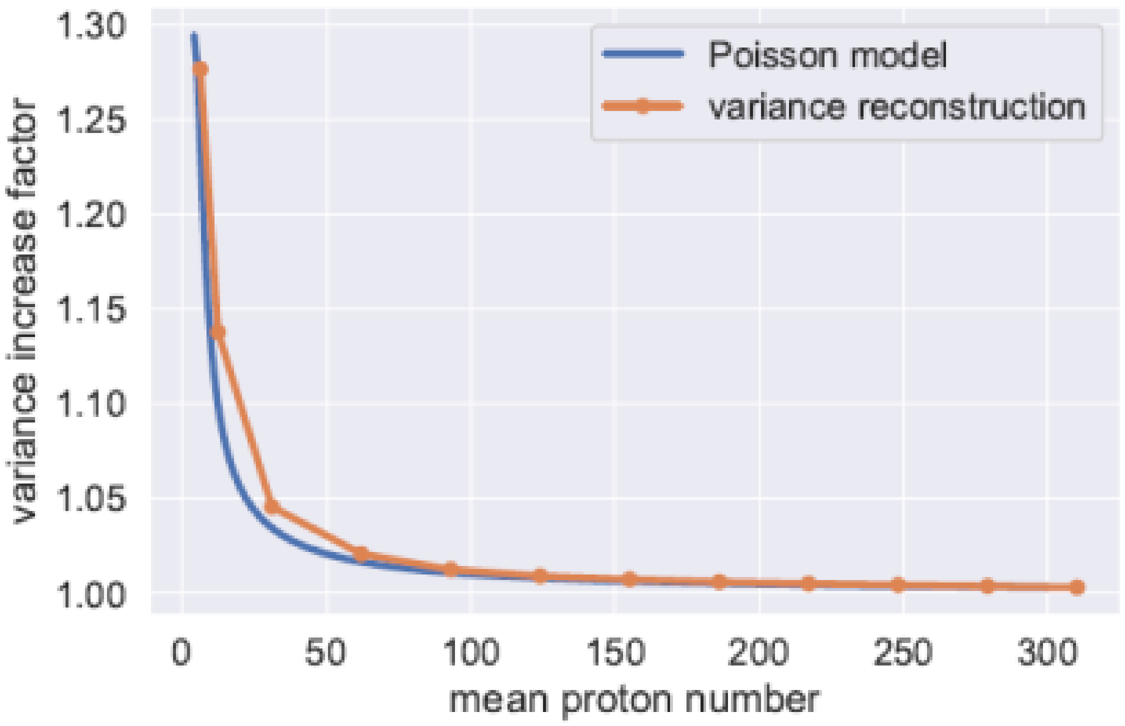
1.30
1.25
1.20
1.15
1.10
1.05
1.00
variance increase factor
0
50
100
150
200
250
300
mean proton number
Poisson model
variance reconstruction

$$D_w = \frac{\rho_m}{\rho_w} \frac{S_w}{S_m} D_m,$$

$$L_i = \frac{\sum_{n=1}^{N} \sum_{s=1}^{S_n} \frac{\varepsilon_{sn}^2}{l_{sn}}}{\sum_{n=1}^{N} \sum_{s=1}^{S_n} \varepsilon_{sn}}$$

$$x = r\cos\theta$$

$$y = r\sin\theta$$

$$\frac{\partial(x,y)}{\partial(r,\theta)} = \begin{bmatrix} \cos\theta & -r\sin\theta \\ \sin\theta & r\cos\theta \end{bmatrix}$$

$$\text{Jacobian} = \det \frac{\partial(x,y)}{\partial(r,\theta)} = r$$

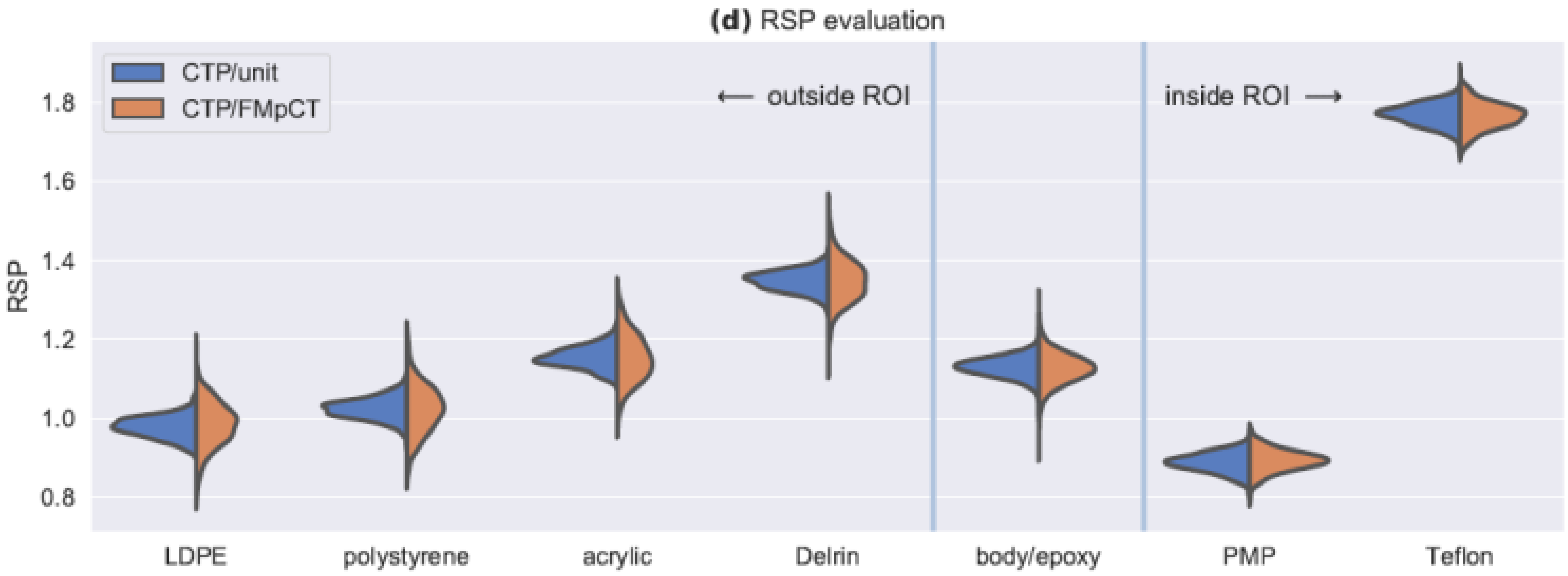
(d) RSP evaluation
CTP/unit
CTP/FMpCT
← outside ROI
inside ROI →
RSP
1.8
1.6
1.4
1.2
1.0
0.8
LDPE
polystyrene
acrylic
Delrin
body/epoxy
PMP
Teflon

RSP artifacts

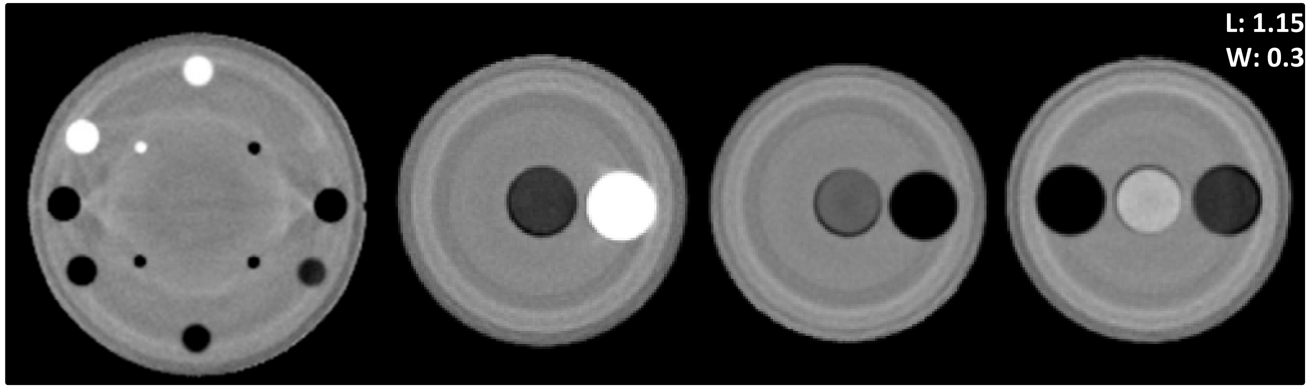

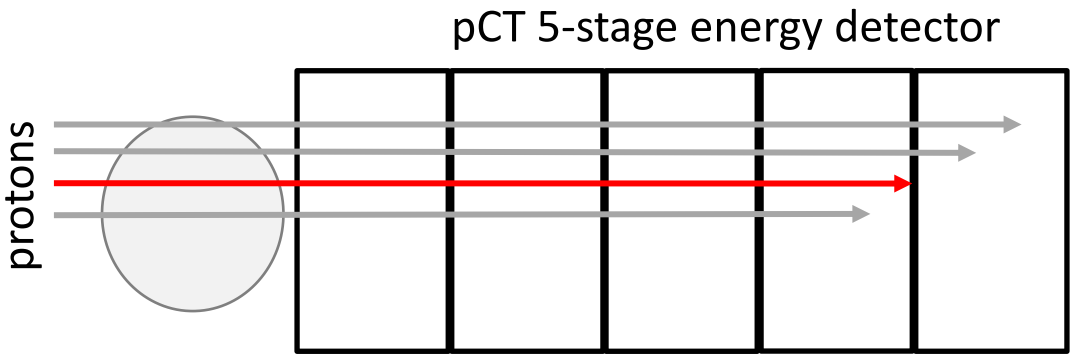

- Protons stopping near stage interfaces yield less accurate information
- In homogeneous cylindrical objects this results in ring artifacts

- Calculating for each voxel, the fraction of protons stopping near stage interfaces

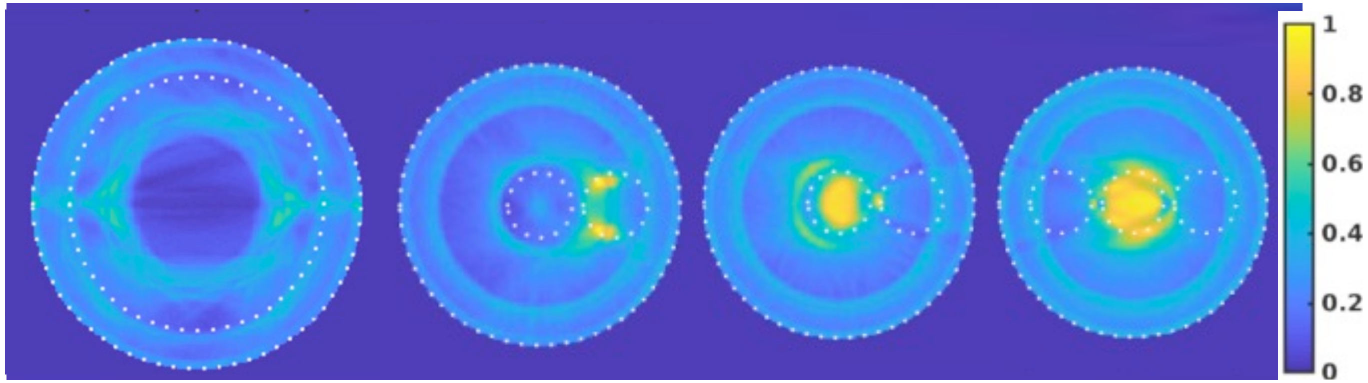

pCT calibration

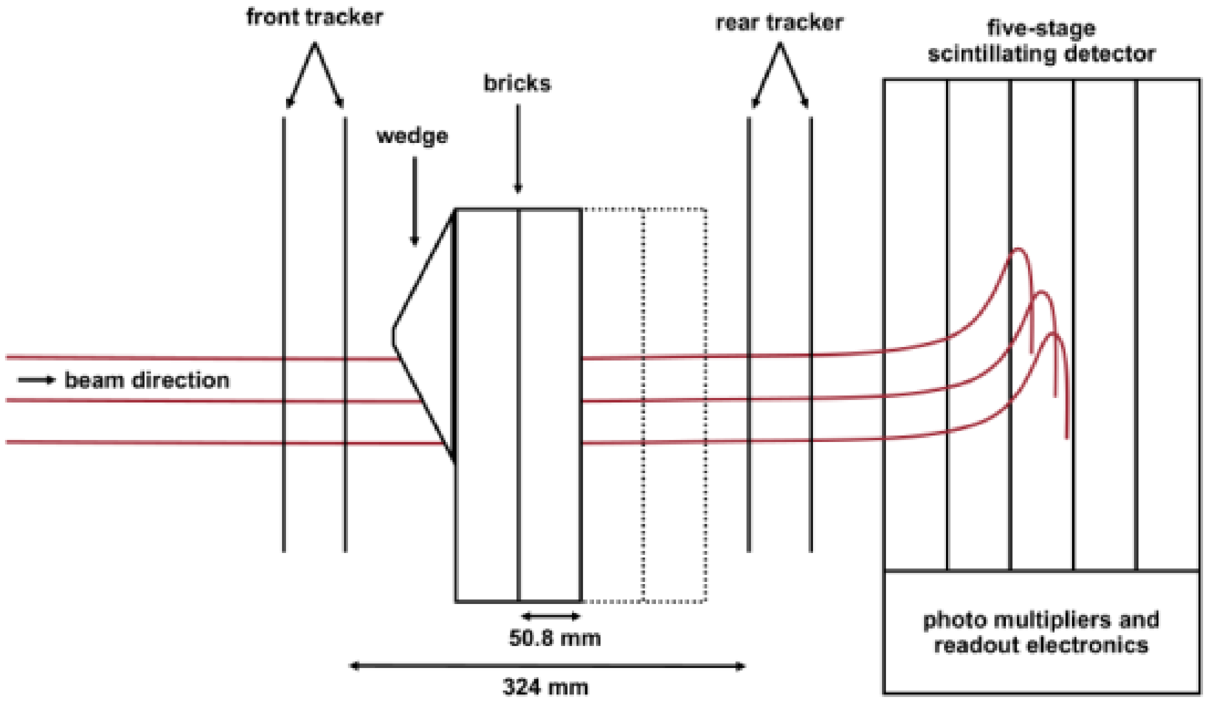

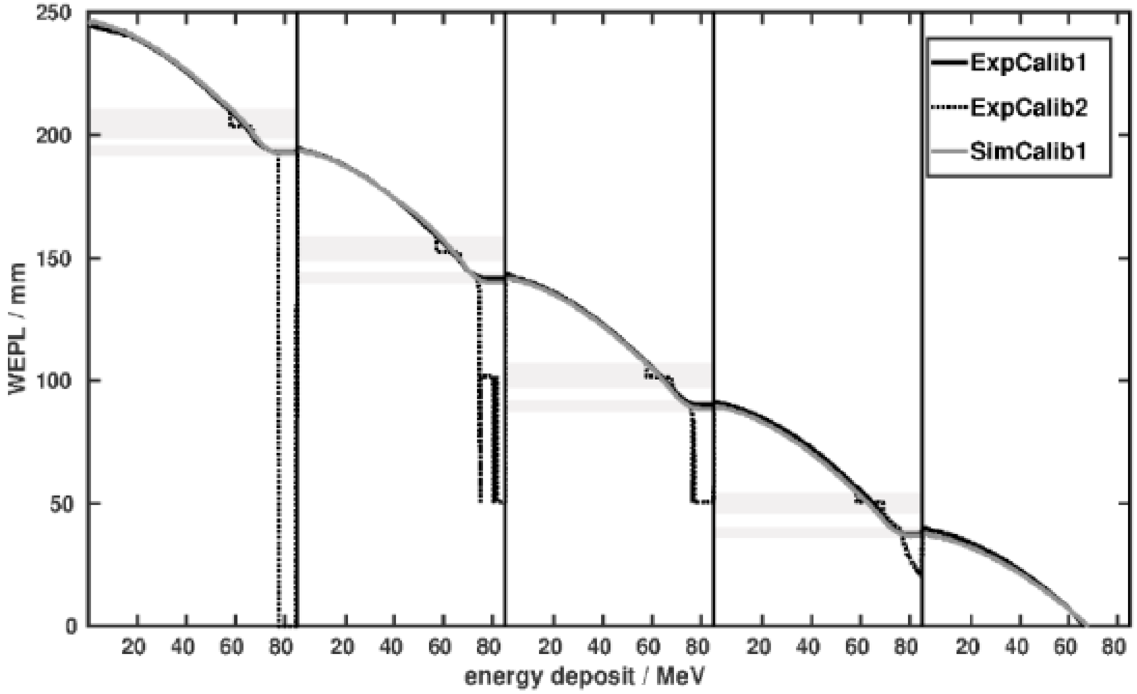

Method (continued)

- The full workflow: Dickmann *et al. Phys Med.* 2021 Jun;86:57-65

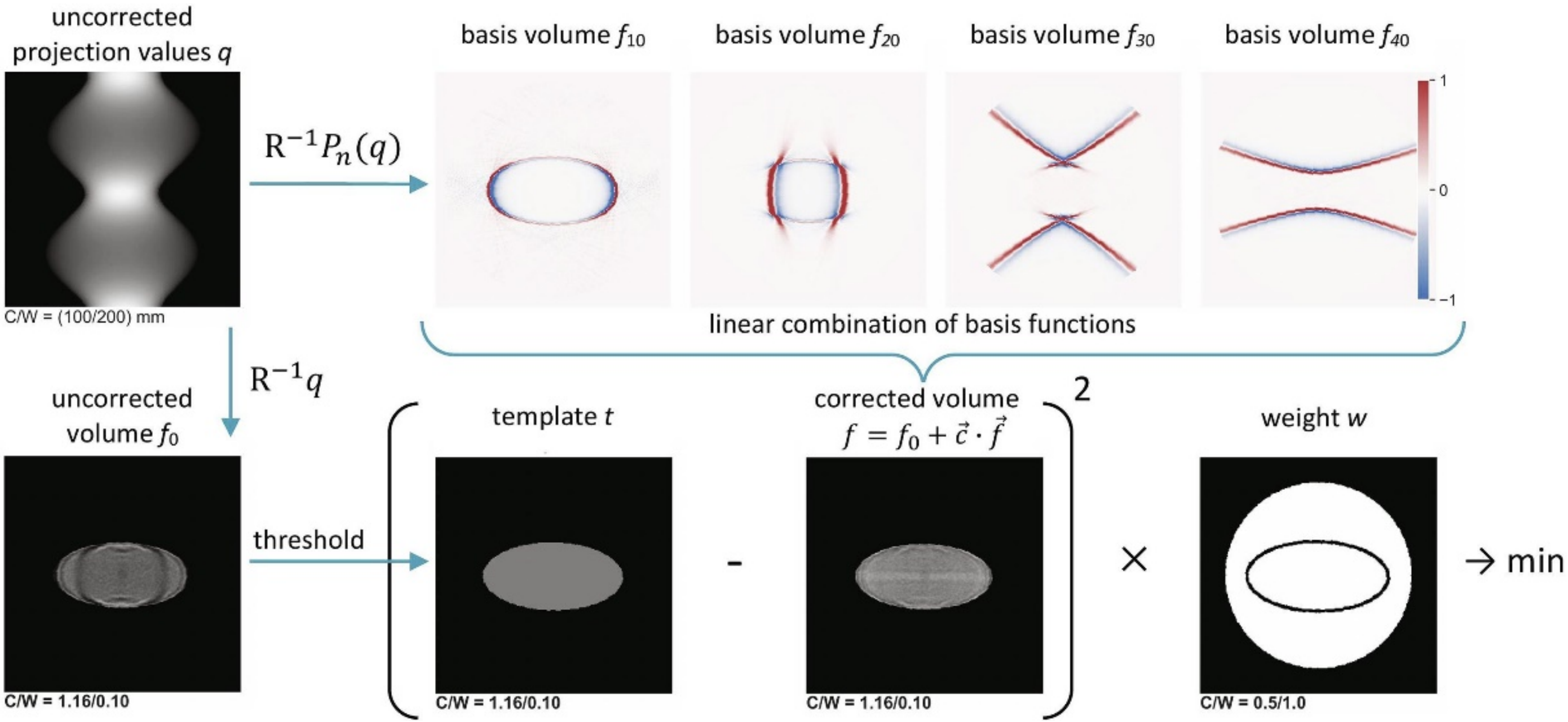

EMpCT

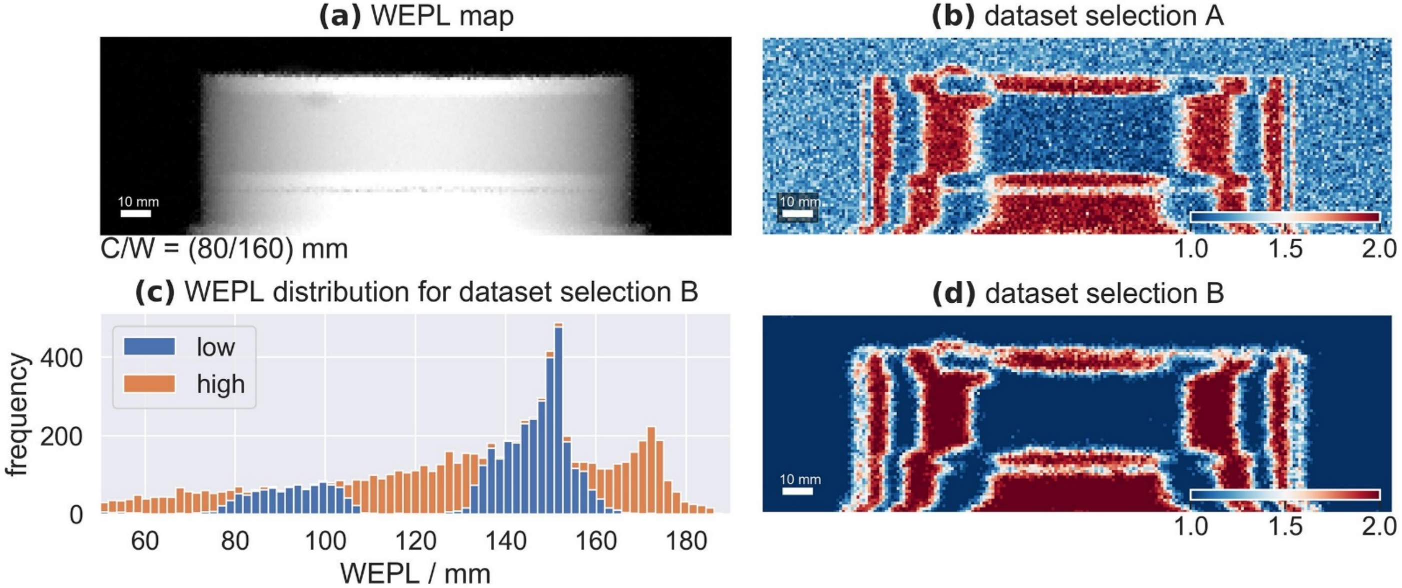
(a) WEPL map
10 mm
C/W = (80/160) mm
(b) dataset selection A
10 mm
1.0 1.5 2.0
(c) WEPL distribution for dataset selection B
low
high
frequency
400
200
0
60 80 100 120 140 160 180
WEPL / mm
(d) dataset selection B
10 mm
1.0 1.5 2.0

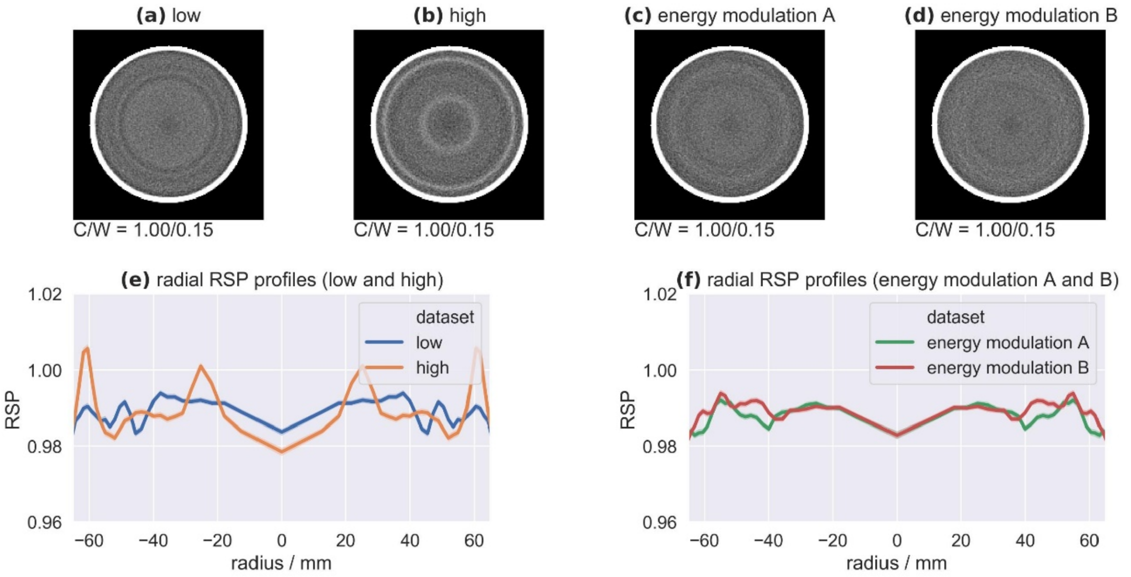
(a) low
(b) high
(c) energy modulation A
(d) energy modulation B
C/W = 1.00/0.15
C/W = 1.00/0.15
C/W = 1.00/0.15
C/W = 1.00/0.15
(e) radial RSP profiles (low and high)
dataset
low
high
RSP
1.02
1.00
0.98
0.96
−60 −40 −20 0 20 40 60
radius / mm
(f) radial RSP profiles (energy modulation A and B)
dataset
energy modulation A
energy modulation B
RSP
1.02
1.00
0.98
0.96
−60 −40 −20 0 20 40 60
radius / mm

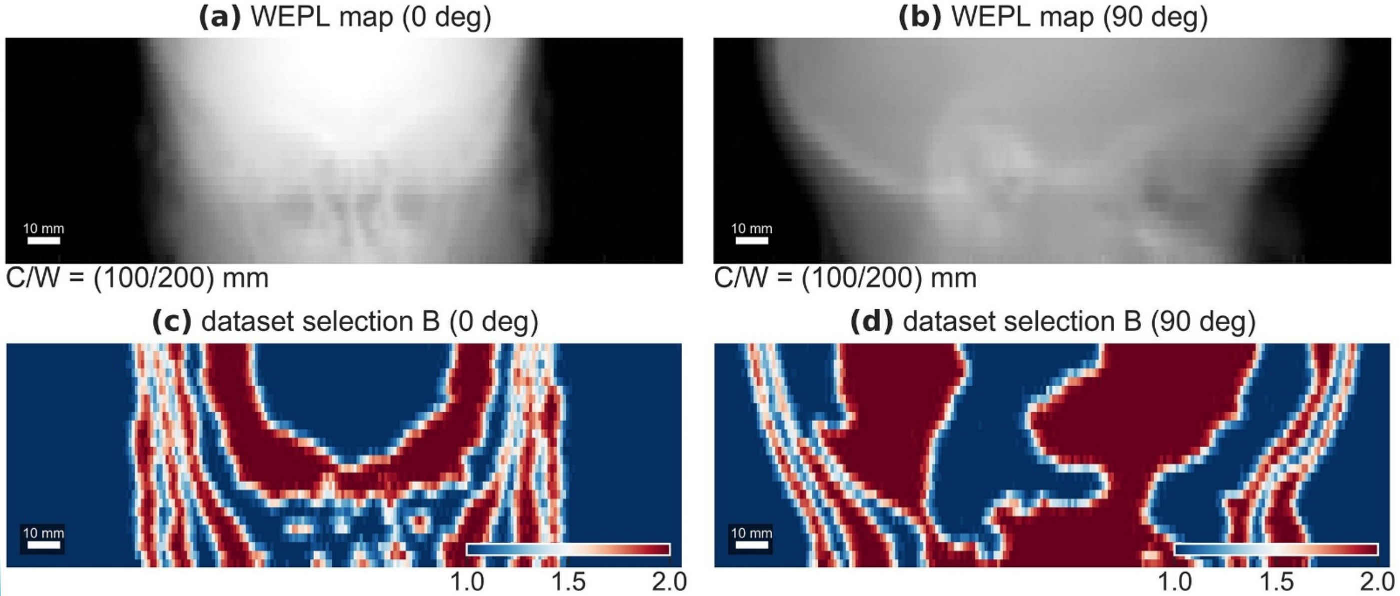
(a) WEPL map (0 deg)
10 mm
C/W = (100/200) mm
(b) WEPL map (90 deg)
10 mm
C/W = (100/200) mm
(c) dataset selection B (0 deg)
10 mm
1.0 1.5 2.0
(d) dataset selection B (90 deg)
10 mm
1.0 1.5 2.0

Prototype pCT scanner

- Validated MC simulation platform, used in this study

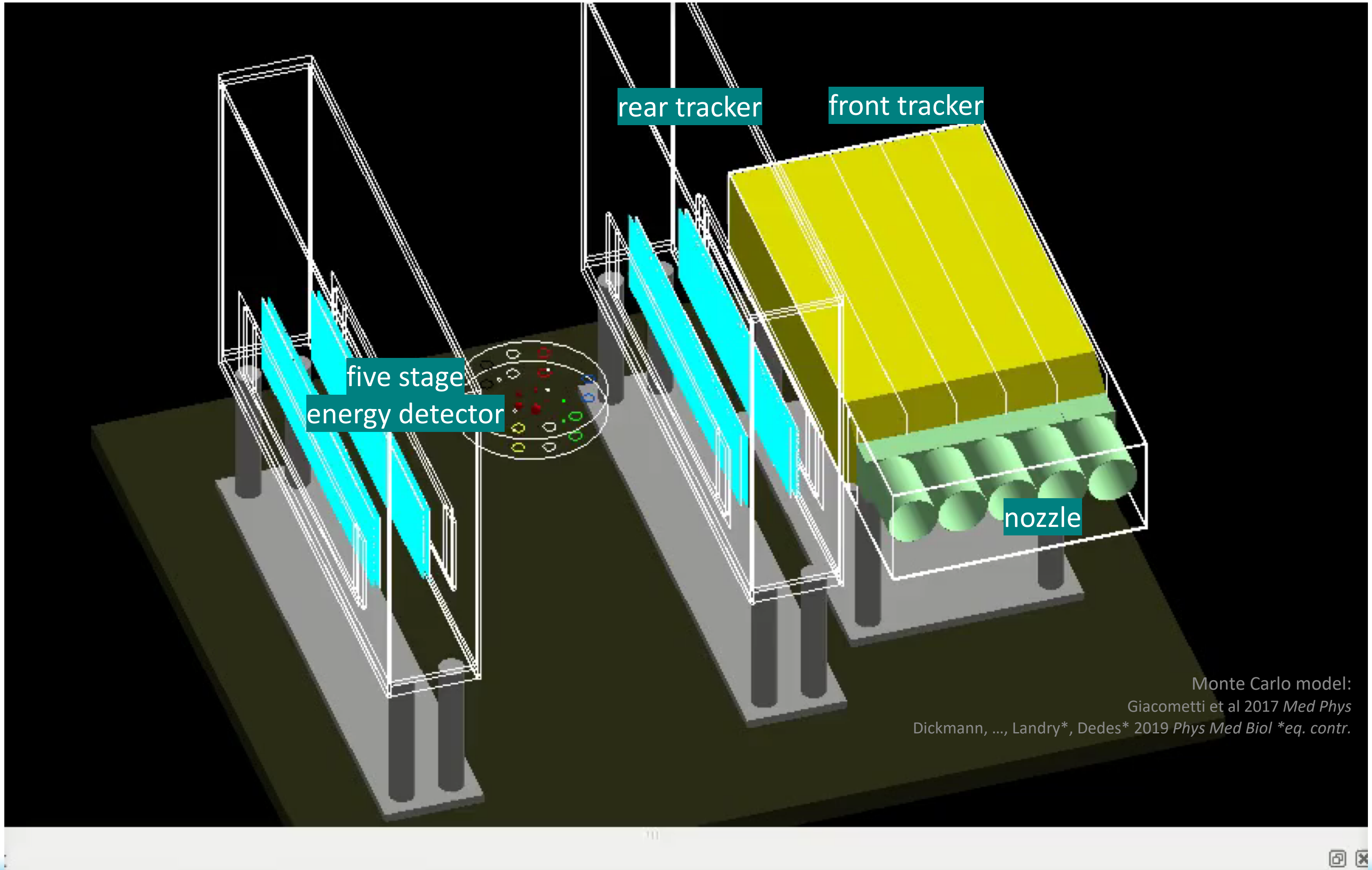

Joint optimization

- Dose and variance optimization

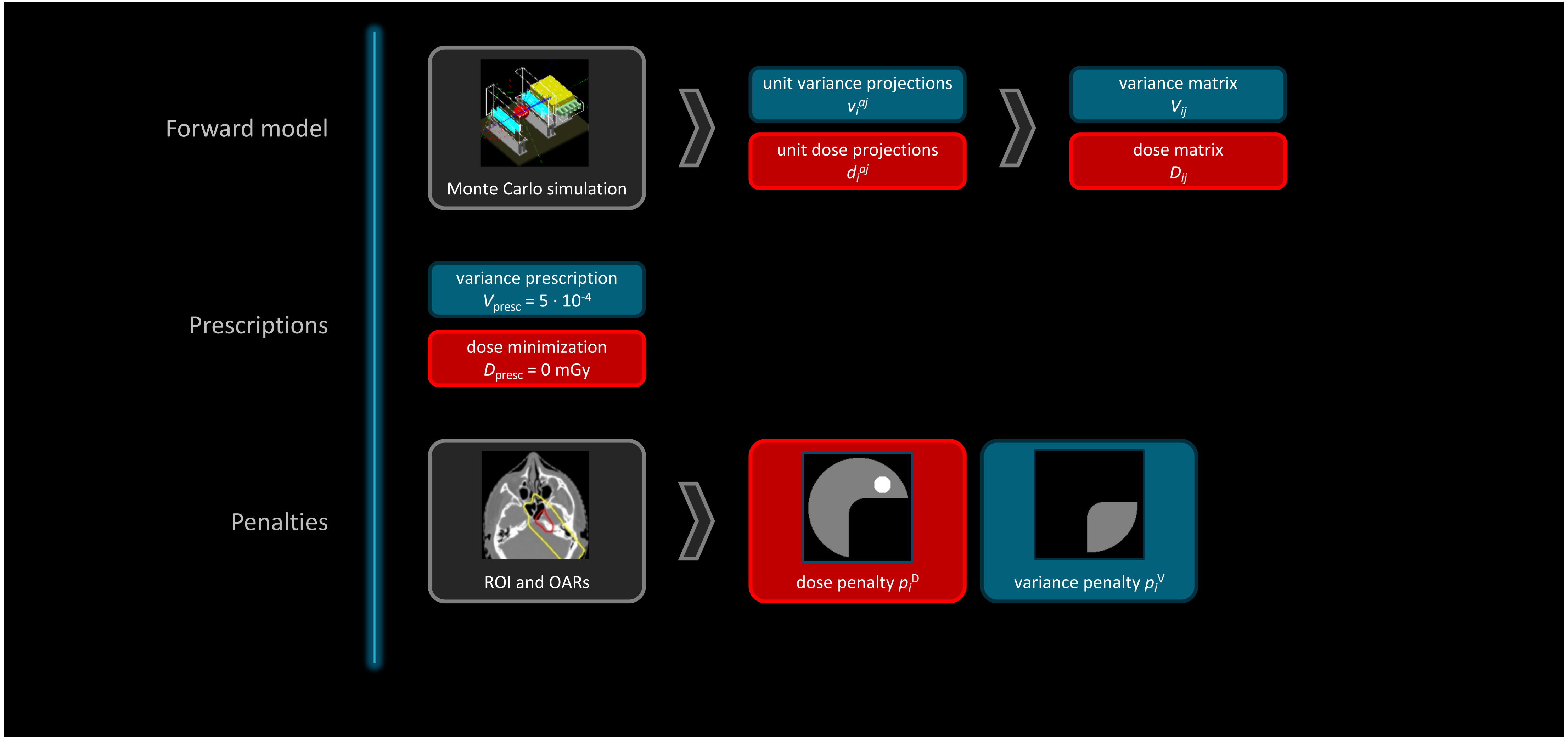

Joint optimization

- Bixel-based approach

variance matrix V_{ij}

dose matrix D_{ij}

x

weight vector w_j

Limited memory Broyden Fletcher Goldfarb Shannon minimizer
s.t. $0.05 < w_j < 10$

$\left(\begin{array}{c} \text{current variance } V_i \\ \text{current dose } D_i \end{array} - \begin{array}{c} \text{variance prescription } V_{presc} = 5 \cdot 10^{-4} \\ \text{dose minimization } D_{presc} = 0 \text{ mGy} \end{array} \right)^2$ x

variance penalty p_i^V

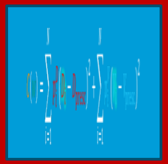

dose penalty p_i^D

= cost function $C(w)$

gradient $\partial/\partial w_j\, C(w)$

$$C(w) = \sum_{i=1}^{N} p_i^D \left(D_i - D_{presc}\right)^2 + \sum_{i=1}^{N} p_i^V \left(V_i - V_{presc}\right)^2$$

$$\frac{\partial}{\partial w_j} C(w) = 2\sum_{i=1}^{N} p_i^D \left(D_i - D_{presc}\right) D_{ik} - 2\sum_{i=1}^{N} p_i^V \left(V_i - V_{presc}\right) \frac{V_{ik}}{w_j^2}$$

Dickmann, ..., Dedes, Landry 2021 *Phys Med Biol*

FMpCT in treatment planning

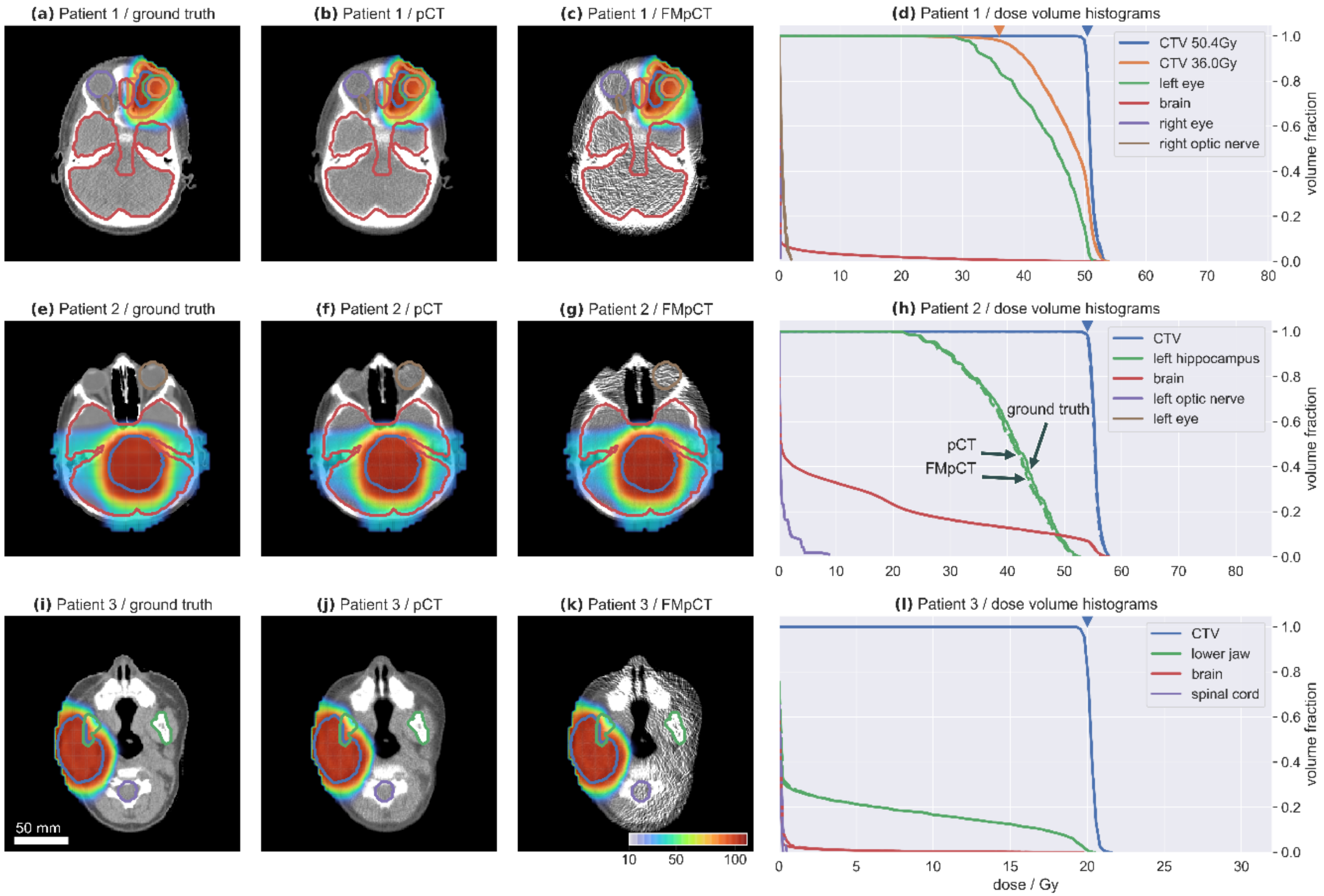

- three **pediatric cases** treated with IMRT selected
- **proton treatment plans** generated on the basis of the IMRT dose distributions using **ground truth RSP**
- **ground truth RSP** from the patient model in the pCT MC **simulation** with **full detector modelling**
- **treatment dose recalculated** on pCT and FMpCT images

Imaging dose

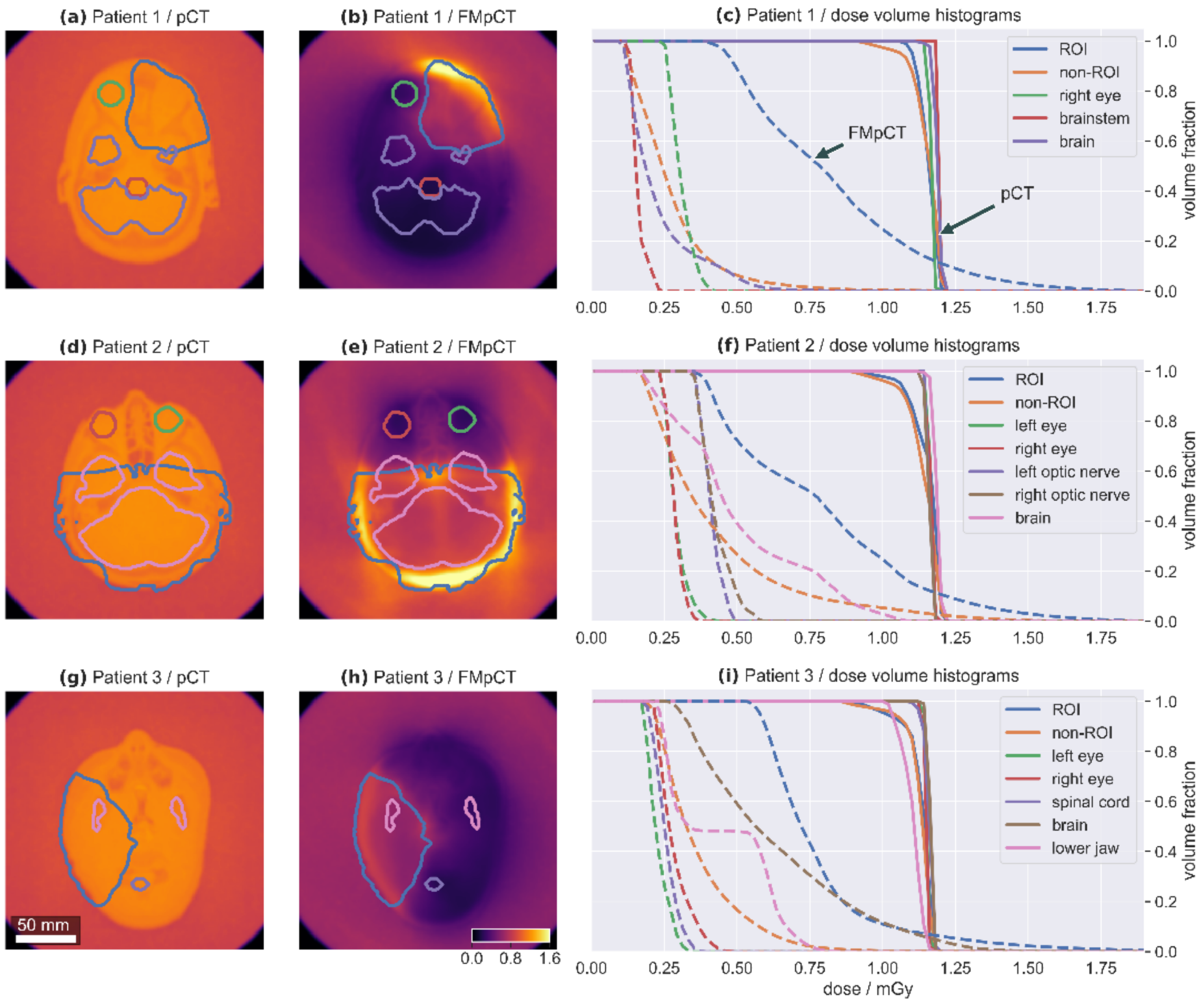

- **DVH** for **imaging** dose
- Important **dose reduction** for all **out-of-ROI areas**
- **Dose** can be slightly increased **in-ROI** where **treatment dose** is also **high**
- **OAR dose** can be **pushed down**

Summary

- **Inverse planning** approach yields optimal fluence distributions
- FMpCT allows **substantial imaging dose savings** while preserving dose calculation accuracy
  - **80%** outside the ROI
  - **87%** in some OARs
- Results expected to be **applicable** to **real world** due to fully realistic simulations
- Previous work showed **imaging plans** are **deliverable**

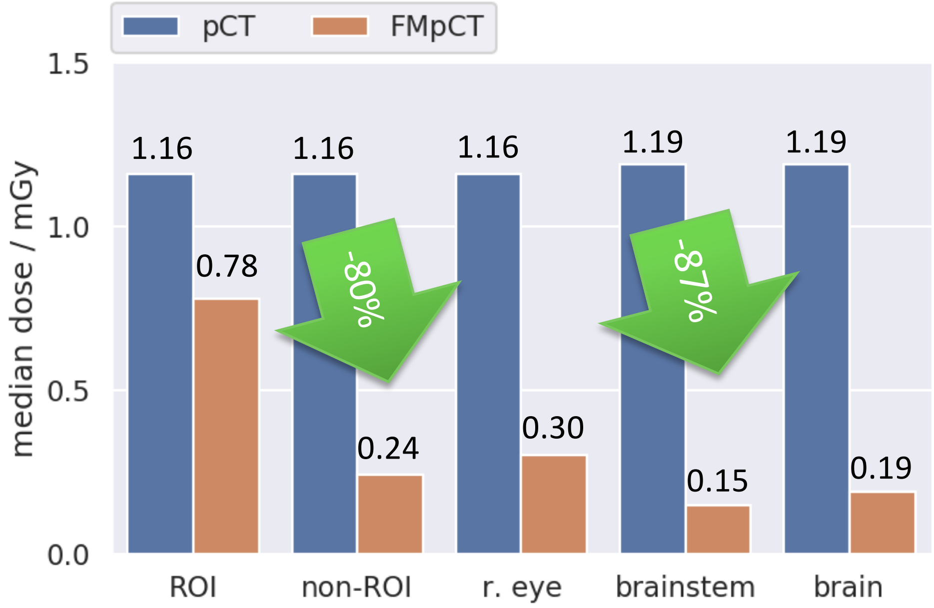

Full details:

Physics in Medicine & Biology

IPEM Institute of Physics and Engineering in Medicine

PAPER

Fluence-modulated proton CT optimized with patient-specific dose and variance objectives for proton dose calculation

J Dickmann[1], F Kamp[2,*], M Hillbrand[3], S Corradini[2], C Belka[2,4], R W Schulte[5], K Parodi[1], G Dedes[1] and G Landry[1,2]

[1] Department of Medical Physics, Fakultät für Physik, Ludwig-Maximilians-Universität München (LMU Munich), D-85748 Garching bei München, Germany
[2] Department of Radiation Oncology, University Hospital, LMU Munich, D-81377 Munich, Germany
[3] Institut für Radio–Onkologie, Kantonsspital Graubünden, CH-7000 Chur, Switzerland
[4] German Cancer Consortium (DKTK), D-81377 Munich, Germany
[5] Division of Biomedical Engineering Sciences, Loma Linda University, Loma Linda, CA 92354, United States of America
[*] Currently at Department of Radiation Oncology and Cyberknife Center, University Hospital of Cologne, D-50937 Cologne, Germany.

E-mail: guillaume.landry@med.uni-muenchen.de

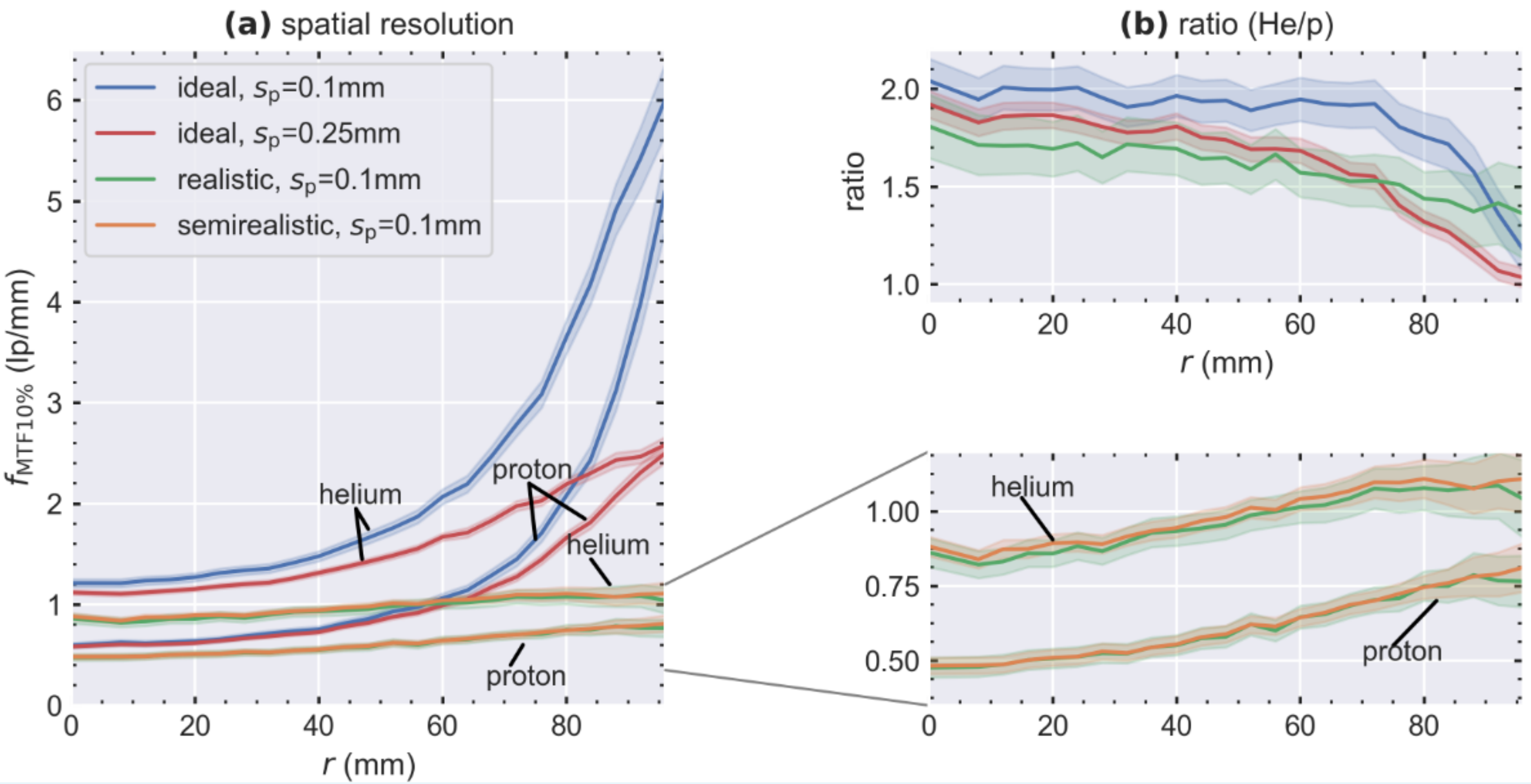

(a) spatial resolution
(b) ratio (He/p)
ideal, s_p=0.1mm
ideal, s_p=0.25mm
realistic, s_p=0.1mm
semirealistic, s_p=0.1mm
$f_{MTF10\%}$ (lp/mm)
ratio
r (mm)
helium
proton

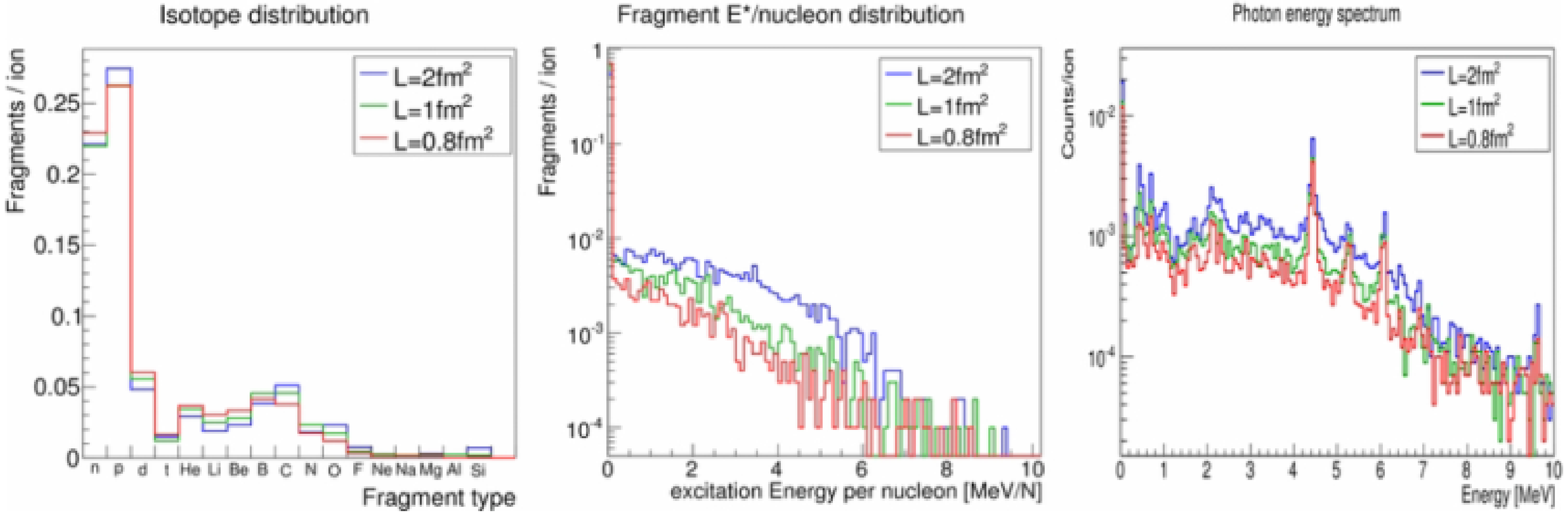
Isotope distribution
Fragments / ion
L=2fm²
L=1fm²
L=0.8fm²
n p d t He Li Be B C N O F Ne Na Mg Al Si
Fragment type
Fragment E*/nucleon distribution
excitation Energy per nucleon [MeV/N]
Photon energy spectrum
Counts/ion
Energy [MeV]

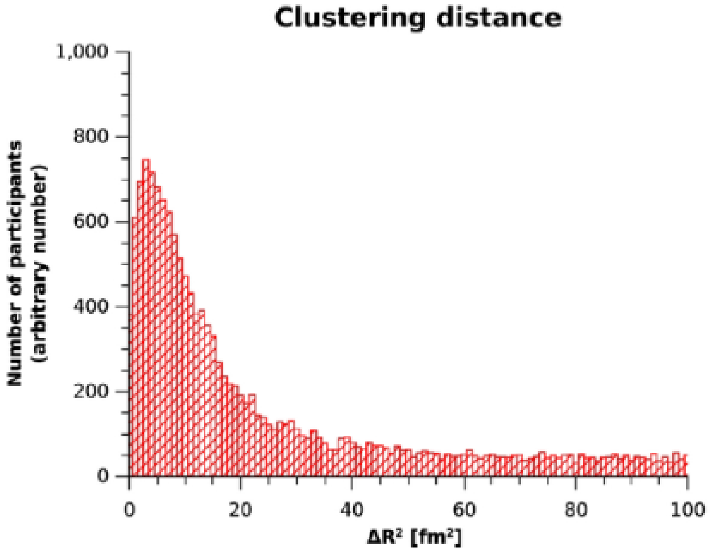
Clustering distance
Number of participants (arbitrary number)
ΔR² [fm²]

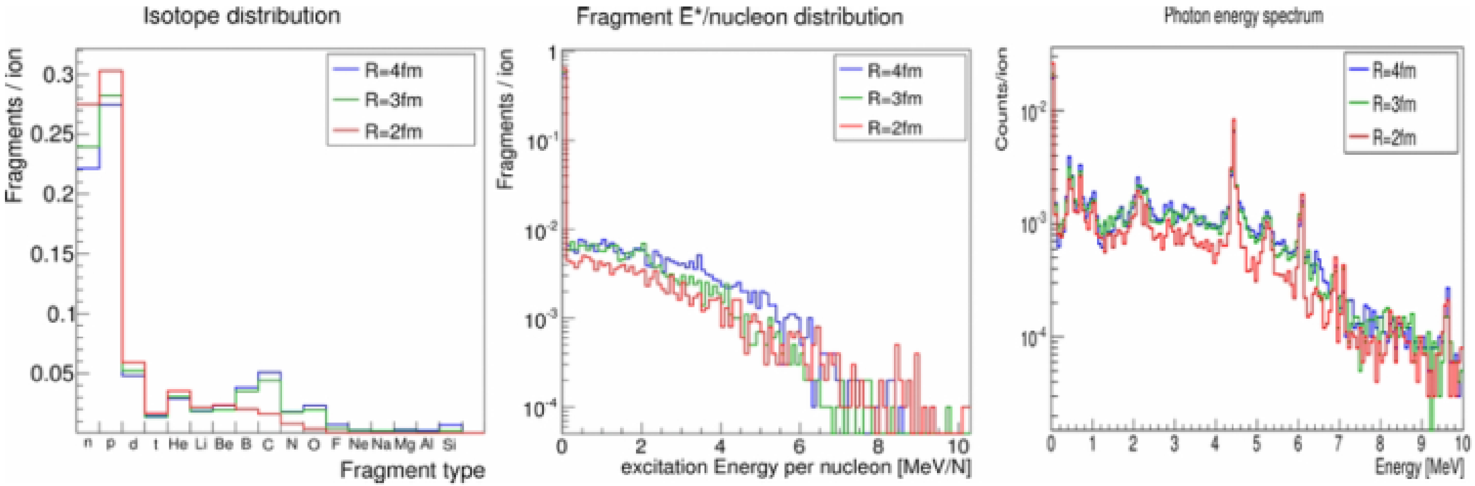
Isotope distribution
Fragments / ion
R=4fm
R=3fm
R=2fm
n p d t He Li Be B C N O F Ne Na Mg Al Si
Fragment type
Fragment E*/nucleon distribution
excitation Energy per nucleon [MeV/N]
Photon energy spectrum
Counts/ion
Energy [MeV]

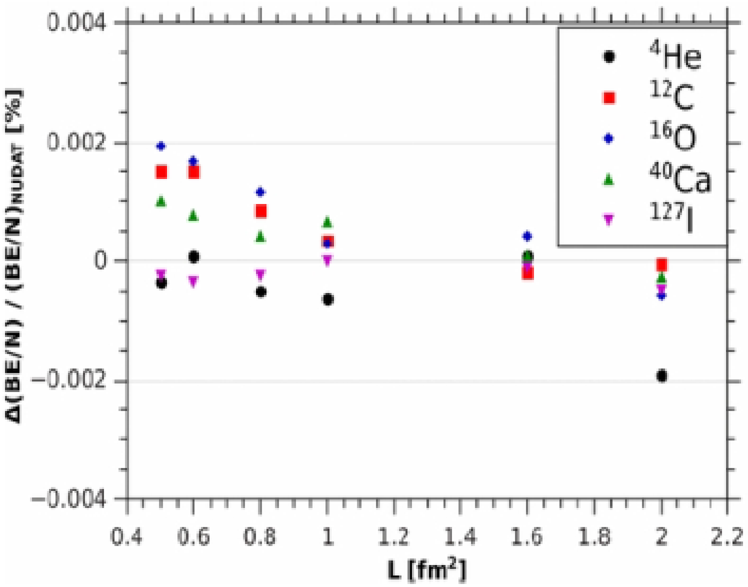
Δ(BE/N) / (BE/N)NUDAT [%]
L [fm²]
⁴He
¹²C
¹⁶O
⁴⁰Ca
¹²⁷I

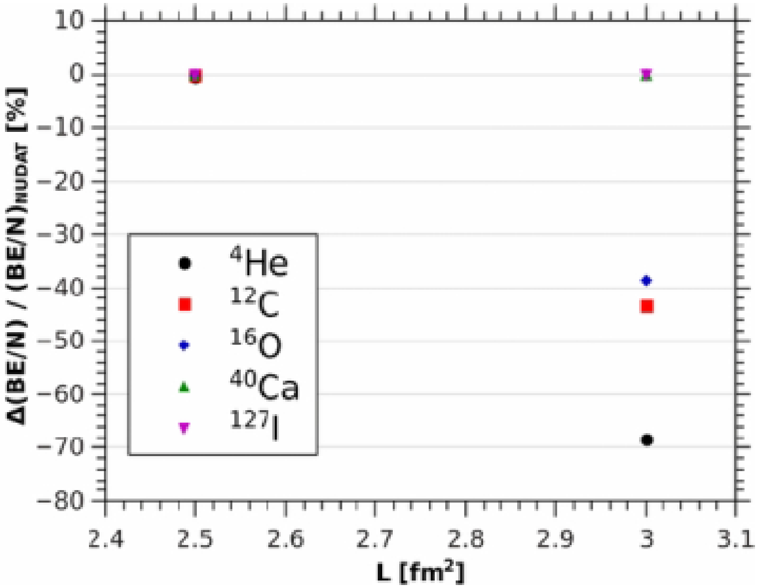
Δ(BE/N) / (BE/N)NUDAT [%]
L [fm²]
⁴He
¹²C
¹⁶O
⁴⁰Ca
¹²⁷I

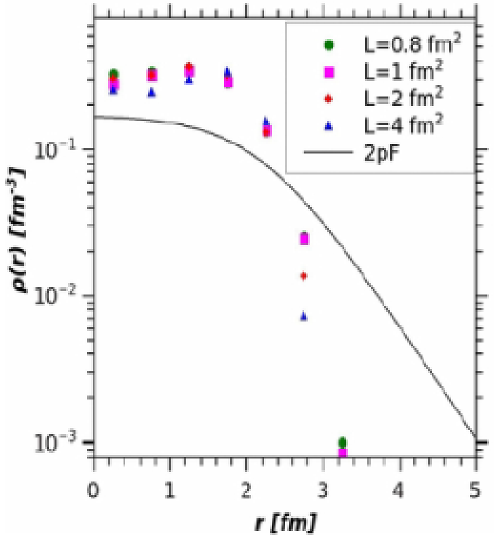
ρ(r) [fm⁻³]
r [fm]
L=0.8 fm²
L=1 fm²
L=2 fm²
L=4 fm²
2pF

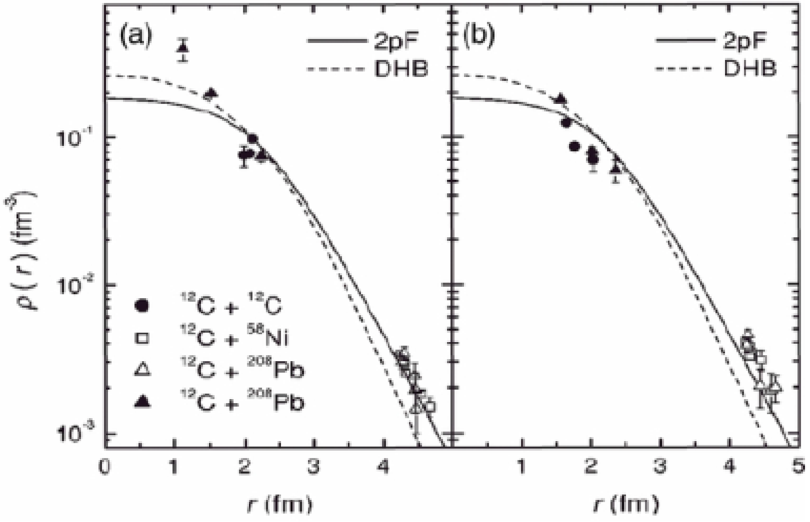
(a)
(b)
2pF
DHB
ρ (r) (fm⁻³)
r (fm)
¹²C + ¹²C
¹²C + ⁵⁸Ni
¹²C + ²⁰⁸Pb
¹²C + ²⁰⁸Pb

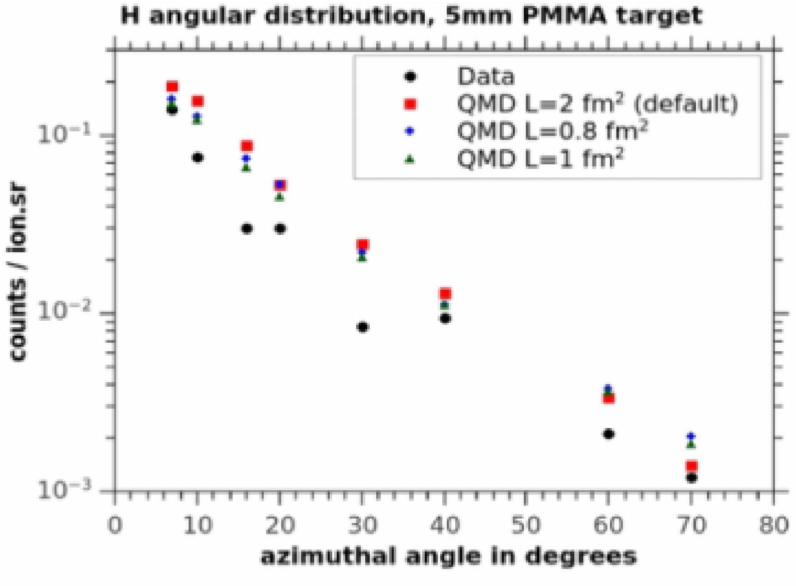
H angular distribution, 5mm PMMA target
Data
QMD L=2 fm² (default)
QMD L=0.8 fm²
QMD L=1 fm²
counts / ion.sr
azimuthal angle in degrees

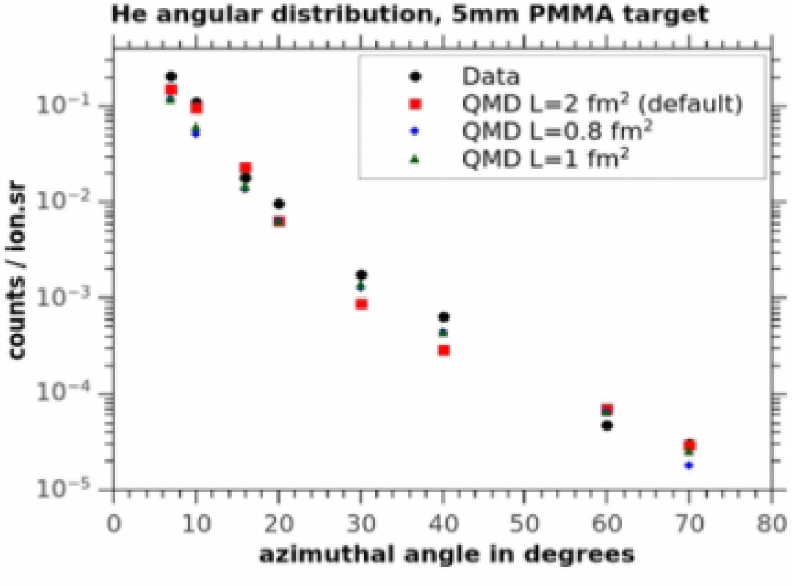
He angular distribution, 5mm PMMA target
Data
QMD L=2 fm² (default)
QMD L=0.8 fm²
QMD L=1 fm²
counts / ion.sr
azimuthal angle in degrees

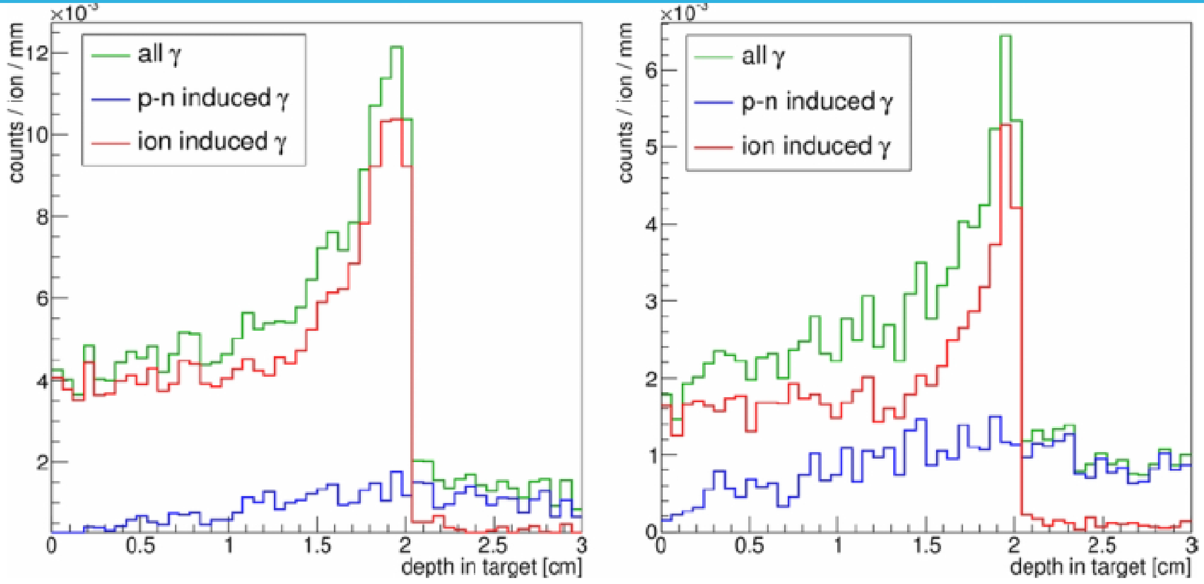

Figure 11.13: 95 MeV/u ^{12}C simulated prompt–gamma emission in a PMMA target, for $L = 2\,\mathrm{fm}^2$ (left) and $L = 0.8\,\mathrm{fm}^2$ (right). The total emission profile as well as the contributions from ion induced (QMD) and p/n induced (BIC) reactions are shown.

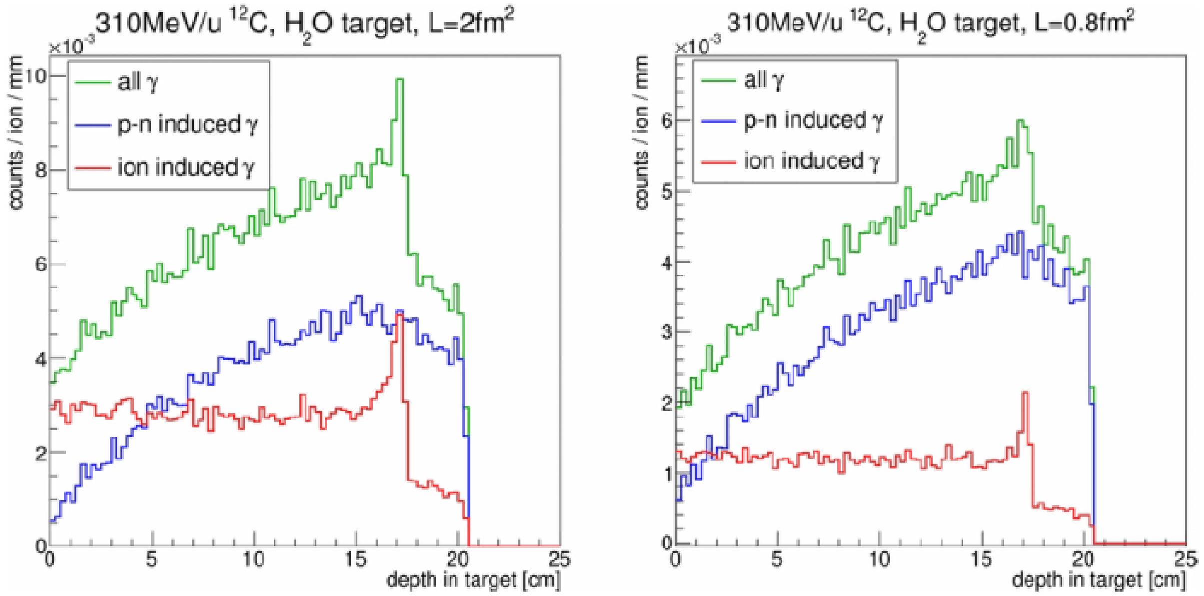

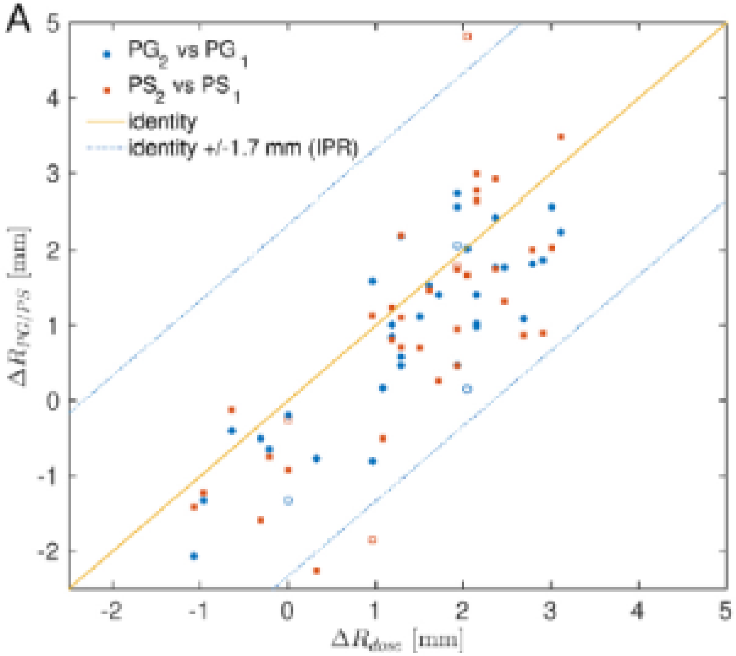
A
PG2 vs PG1
PS2 vs PS1
identity
identity +/-1.7 mm (IPR)
ΔR PG/PS [mm]
ΔR dose [mm]

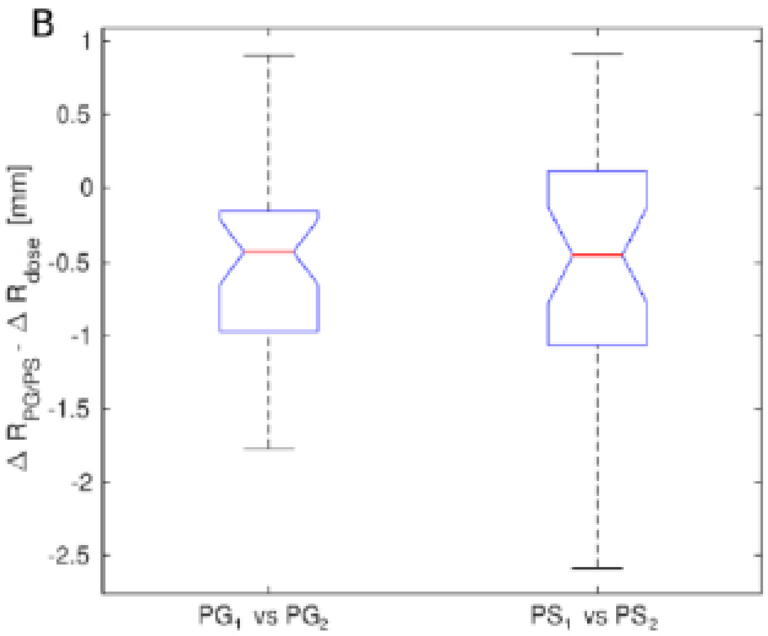
B
Δ R PG/PS - Δ R dose [mm]
PG1 vs PG2
PS1 vs PS2

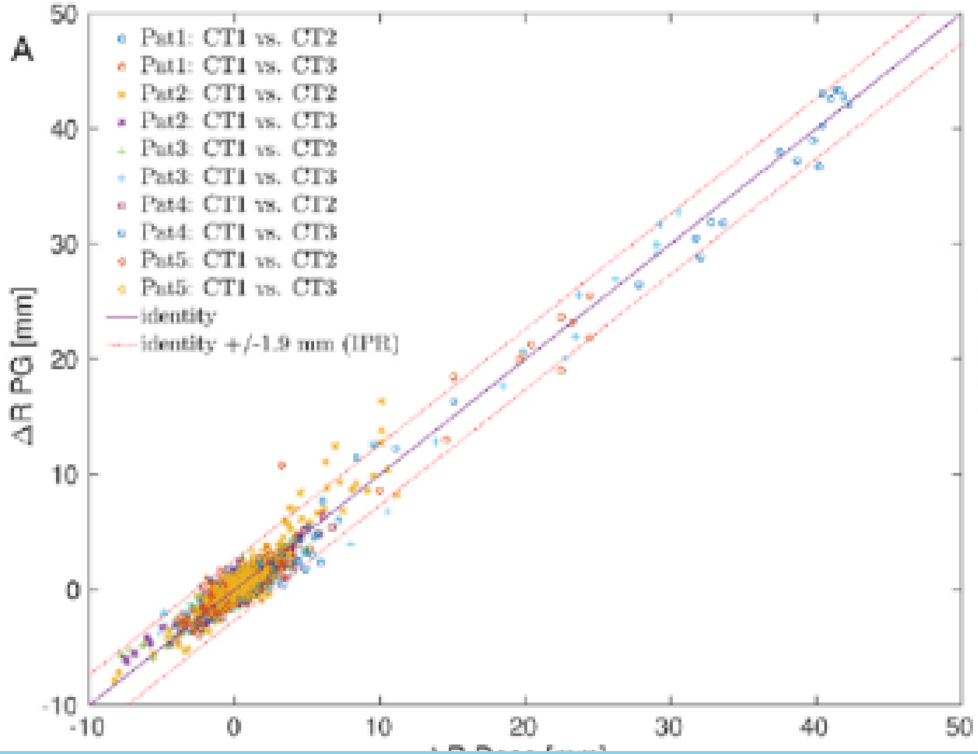
A
Pat1: CT1 vs. CT2
Pat1: CT1 vs. CT3
Pat2: CT1 vs. CT2
Pat2: CT1 vs. CT3
Pat3: CT1 vs. CT2
Pat3: CT1 vs. CT3
Pat4: CT1 vs. CT2
Pat4: CT1 vs. CT3
Pat5: CT1 vs. CT2
Pat5: CT1 vs. CT3
identity
identity +/-1.9 mm (IPR)
ΔR PG [mm]

LUDWIG-
MAXIMILIANS-
UNIVERSITÄT
MÜNCHEN